UNIVERSITY OF LEEDS

This is a repository copy of *Complexities in interpreting chironomid-based temperature reconstructions over the Holocene from a lake in Western Ireland*.

White Rose Research Online URL for this paper:
http://eprints.whiterose.ac.uk/150486/

Version: Accepted Version

Article:
McKeown, MM, Caseldine, CJ, Thompson, G et al. (5 more authors) (2019) Complexities in interpreting chironomid-based temperature reconstructions over the Holocene from a lake in Western Ireland. Quaternary Science Reviews, 222. ARTN: 105908. ISSN 0277-3791

https://doi.org/10.1016/j.quascirev.2019.105908

© 2019 Elsevier Ltd. Licensed under the Creative Commons Attribution-NonCommercial-NoDerivatives 4.0 International License (http://creativecommons.org/licenses/by-nc-nd/4.0/).

Reuse
This article is distributed under the terms of the Creative Commons Attribution-NonCommercial-NoDerivs (CC BY-NC-ND) licence. This licence only allows you to download this work and share it with others as long as you credit the authors, but you can't change the article in any way or use it commercially. More information and the full terms of the licence here: https://creativecommons.org/licenses/

Takedown
If you consider content in White Rose Research Online to be in breach of UK law, please notify us by emailing eprints@whiterose.ac.uk including the URL of the record and the reason for the withdrawal request.

White Rose
university consortium
Universities of Leeds, Sheffield & York

eprints@whiterose.ac.uk
https://eprints.whiterose.ac.uk/

Highlights:

- There is a connection between chironomid functional traits, expressed through feeding guilds, and simulated annual air temperature
- The chironomid July air temperature transfer function from Lough Nakeeroge is not solely reconstructing air temperature from than mid- to late Holocene, but is being driven by a complicated range of influencing variables
- Several important Holocene climate phases and events can be identified from the Irish palaeoclimate records
- There is a clear contradiction between the proxy records and climate model hindcasts over the mid- to late Holocene, which supports the hypothesis that the North Atlantic may be responsible for the Holocene climate 'conundrum'

Complexities in interpreting chironomid-based temperature reconstructions over the Holocene from a lake in Western Ireland

Michelle M. McKeown*[1,2], Chris J. Caseldine[3], Gareth Thompson[4], Graeme T. Swindles[5,6], Ruza F. Ivanovic[7], Thomas P. Roland[4], Paul J. Valdes[8], Aaron P. Potito[2]

[1]Manaaki Whenua – Landcare Research, 54 Gerald Street, Lincoln, New Zealand

[2]Palaeoenvironmental Research Unit, School of Geography and Archaeology, National University of Ireland Galway, Galway, Ireland

[3]Centre for Geography, Environment and Society, Penryn Campus, University of Exeter, Penryn, UK

[4]Department of Geography, College of Life and Environmental Sciences, Amory Building, University of Exeter, Exeter, UK

[5]School of Geography, University of Leeds, Leeds, UK

[6]Ottawa-Carleton Geoscience Centre, Department of Earth Sciences, Carleton University, Ottawa, Ontario, Canada

[7]School of Earth and Environment, University of Leeds, Leeds, UK

[8]School of Geographical Sciences, University of Bristol, Bristol, UK

***Corresponding author**

Michelle McKeown, Manaaki Whenua—Landcare Research, 54 Gerald Street, Lincoln 7608, New Zealand.

mckeownm@landcareresearch.co.nz

Abstract:

Investigation of Holocene climate variability remains challenging. This is largely due to chronological uncertainties and complexities associated with proxies and their relationship with climatic drivers. Pertinent questions still exist regarding the Holocene climate in Ireland, particularly in the early Holocene. We present a mean July air temperature reconstruction based on fossil chironomidae (non-biting midge flies), along with an assessment of chironomid functional traits from five guilds (based on their feeding habits) from Lough Nakeeroge, a small glacial lake in western Ireland. These records span the early to late Holocene (c. 10,000 - 1500 cal. yr BP). The chironomid record is supplemented with pollen data to determine landscape vegetation dynamics, and compared to climate model simulations of the same period. As reliable models are essential for robust analysis of long-term climate change, we critically assess the value of the chironomid transfer function and explore the use of chironomid functional traits to infer past climate variability. While this study demonstrates the complexities of chironomid-based temperature reconstruction in Irish lakes, it endeavours to i) disentangle a complicated Holocene climate history through the exploration of other long-term Holocene records from the island; and ii) improve our understanding of environmental responses to climate variability in Ireland. The findings of this study suggest that the interpretation of chironomid-based temperature transfer functions can be challenging. However, our results demonstrate the influence of climate on the functioning of lake ecosystems over the Holocene, with the promising performance of the collector-filterer feeding guild as a palaeothermometer.

Keywords

Holocene, Palaeoclimatology, Palaeolimnology, Ireland, Chironomidae, Functional Traits, Pollen, Climate Models

1. Introduction

It is now well recognised that the climate of the Holocene, the last ~ 11,500 cal. yr BP, has been far from stable (Marcott et al., 2013; Marsicek et al., 2018). Broadly speaking, the Holocene climate is widely considered to have transitioned from the cooler Younger Dryas to a warmer climate between 11,500 and 7000 cal. yr BP, followed by a warm middle Holocene with higher humidity between c. 8000 to 7000 cal. yr BP and c. 6000 to 4000 cal. yr BP, depending on the region, in the Northern Hemisphere (Bond et al., 2001; Blaauw et al., 2004; Diefendorf et al., 2006; Daley et al., 2011; Renssen et al., 2012; Blaschek and Renssen, 2013; Marcott et al., 2013; Brooks and Langdon, 2014; Marsicek et al., 2018). These warmer phases were interrupted by numerous multi-decadal- to centennial-scale cold reversals (Wanner et al., 2011). Cooling in the late Holocene is well-documented from proxy reconstructions in the North Atlantic region; however, model reconstructions continuously simulate long-term warming associated with retreating ice-sheets and increasing carbon dioxide concentrations (Baker et al., 2017; Marsicek et al., 2018). From the discrepancies between these proxy reconstructions and the transient climate simulations, pertinent questions regarding climate evolution during the Holocene arise.

In recent years, there has been a proliferation of Holocene palaeoclimate research in Ireland (Caseldine et al., 2005; Caseldine and Fyfe, 2006; Langdon et al., 2012; Swindles et al., 2013). Only a small number of records continuously span the early to late Holocene (McDermott et al., 1999; Ahlberg et al., 2001; McDermott et al., 2001; Holmes et al., 2007). The majority of work tends to focus on the mid- to late Holocene (Caseldine et al., 2005;

Swindles et al., 2007; Holmes et al., 2010; Langdon et al., 2012; Swindles et al., 2013; Roland et al., 2014; Roland et al., 2015; Taylor et al., 2018), with few targeted reconstructions exploring short-term phases over the early Holocene, (Daley et al., 2011; Ghilardi and O'Connell, 2013; Holmes et al., 2016), and the transition from the Last Glacial Maximum (LGM) to the early/mid-Holocene (Diefendorf et al., 2006; Watson et al., 2010; van Asch et al., 2012). Most of these data are derived from peatlands (Caseldine et al., 2005; Plunkett, 2006; Swindles et al., 2010), speleothems (McDermott et al., 1999; McDermott et al., 2001), and lacustrine sediments (Diefendorf et al., 2006; Schettler et al., 2006; Holmes et al., 2007; Holmes et al., 2010; Ghilardi and O'Connell, 2013; Taylor et al., 2018). Despite this progress, a consensus on the prevailing pattern of Holocene climate variability in Ireland has not been reached.

The potential of chironomids (non-biting midge, Insecta; Diptera) as a Holocene palaeoclimatic proxy in Ireland has been demonstrated by Potito et al. (2014), McKeown and Potito (2016), and Taylor et al. (2018). As chironomids can track major and minor changes in temperature through time, independently of precipitation (Eggermont and Heiri, 2012), they have the potential to capture summer air temperature fluctuations inherent to the Irish climate system. Chironomid-based climate research in Ireland has largely concentrated on quantitative temperature reconstructions over the Pleistocene-Holocene transition (Watson et al., 2010; van Asch et al., 2012), using chironomid-temperature transfer functions generated from Scandinavian-based training sets (Heiri et al., 2011). When no transfer function is available for a region, calibration models from other regions can be used (Watson et al., 2010; van Asch et al., 2012). However, these models do not consider several factors that may undermine the reconstruction when applied to the Holocene, such as regional differences in chironomid biogeography and ecology, and possible lack of modern analogues (Heiri and Millet, 2005). With the development of the regional Ireland-based chironomid transfer function (Potito et al., 2014; Taylor et al., 2018), localised quantitative estimates of July air temperature can be reconstructed for the island. While the Irish-based training set has many benefits for reconstructing chironomid-inferred air temperatures for local sites through the Holocene, the Scandinavian-based training set allows a longer temperature gradient to be captured. Chironomid-inferences using the Irish model may not have good modern analogues in the earliest portion of the Holocene. Thus, the development of a European, and even hemisphere-wide, chironomid-air temperature transfer function would allow the biogeographical patterns of species and their temperature optima to be more comprehensively understood, along with maximising modern analogues. This has been successfully achieved using peatland testate amoebae for palaeohydrological reconstructions (Amesbury et al., 2016; Amesbury et al., 2018)

The complexity and sensitivity of the transfer function approach has been discussed in recent studies (Juggins, 2013; Luoto et al., 2014). The choice of parameters, calibration set, and regression method can alter reconstructed temperature models and caution should be exercised in the interpretation of transfer-functions in climate reconstructions (Velle et al., 2010; Brooks et al., 2012). Ecological systems are rarely as simple as transfer functions would imply. Criticisms suggest that variables other than the one being reconstructed have a negligible effect on abiotic assemblages (Juggins, 2013). To complicate matters further, the chironomid-temperature relationship can be decoupled by non-climate variables such as human activities in the lake catchment (McKeown, 2013; McKeown and Potito, 2016; Taylor et al., 2017; Chique et al., 2018). Pollen can be used as an indicator of human activity through the identification of cereal-type pollen, *Plantago* sp. - which is primarily used as an indicator of pastoral farming in Europe - and other pastoral indicators (Behre, 1981). This multi-proxy approach to reconstructing palaeo-environments can allow vegetation/landscape changes to be tracked alongside chironomid community change, while also allowing a critical assessment of the transfer function during periods of notable human impacts.

Comparing pollen and chironomid records can be difficult in many cases, as the response of terrestrial (and aquatic) plants to fluctuations in climate will likely lag behind chironomid community shifts. While climate fluctuations directly influence the adult chironomids through changes in air temperature, the larval stage is driven by indirect climate effects, such as changes in water temperature, fluctuations in lake level, and alterations in the catchment (e.g., hydrology, vegetation, erosion). As chironomid larvae provide a vital role in biogeochemical cycling in lakes via the food web structure (Palmer et al., 1997), the feeding habits for chironomids have been identified as the most useful functional trait for ecological studies (Pinder, 1995; Schmera et al., 2017). Recent studies have demonstrated that chironomid functional traits are excellent indicators of nutrient enrichment and climate variability (Luoto et al., 2014; Luoto et al., 2016; Árva et al., 2017; Gomes et al., 2018; Luoto and Ojala, 2018). The potential to explore functional traits to characterise long-term environmental change has long been known (Jeppesen et al., 2001), but has recently gained momentum in chironomid research (Fournier et al., 2015; Gałka et al., 2017; Nevalainen and Luoto, 2017; Van Bellen et al., 2017; Luoto and Ojala, 2018), along with other palaeoecological indicators such as testate amoebae (Fournier et al., 2015; Marcisz et al., 2016; Lamentowicz et al., 2017; Van Bellen et al., 2017; Koenig et al., 2018) and diatoms (O'Donnell et al., 2017; McGowan et al., 2018; Stenger-Kovács et al., 2018). Thus, shifts in chironomid functional traits, explored through their feeding guilds, may provide a useful link between the faster response of the chironomid community and the slower plant response to climate fluctuations, as changes in various feeding guilds will, at times, be dependent on plant abundance.

To examine key periods of Holocene climate change, we statistically compare the chironomid records with other palaeoclimate reconstructions from fossil archives and climate model simulations for Ireland. This is an important and necessary exercise for bridging gaps in our knowledge of how to interpret climate proxies robustly (Marcott and Shakun, 2015). However, this process is challenging in and of itself. Palaeoclimate reconstructions present several technical challenges including chronological uncertainties (resulting from radiometric dating techniques), and variable temporal resolution of proxy records (variable sedimentation rates in lakes, differing growth rates in speleothem records). Additionally, different proxies respond to different climate variables and local-scale variations can occur (Hu et al., 2017; Sweeney et al., 2018). Thus, combining and comparing several climate proxies for a long-term climate synthesis can be challenging. Recent palaeoenvironmental reconstructions are associated with better chronologies, and many records have been compiled through 'tuning' and 'stacking' (Swindles et al., 2013). Running correlation analysis between forcing parameters and climate proxy data can also be applied to interrogate the temporal variation of correlations (Turner et al., 2016).

Well-documented disparities also exist between observed and simulated Holocene climate, particularly from the mid- to late Holocene period. Here, climate proxies have been interpreted to show long-term cooling (Marcott and Shakun, 2015), whereas computer-generated climate simulations show warming as a physically robust response to retreating ice sheets and rising atmospheric CO_2 (Liu et al., 2014). Marsicek et al. (2018) and Baker et al. (2017) suggest that late Holocene cooling, evident in proxy reconstructions, is limited to the North Atlantic records. As large areas of continental regions are under-represented in Holocene global climate studies, it is plausible that the North Atlantic is responsible for the contradiction. Furthermore, this discrepancy could be an over-representation of indicators towards summer temperatures (Baker et al., 2017). However, pollen-based Holocene temperatures from continental regions in the Northern Hemisphere follow the warming trend simulated by climate models (Marsicek et al., 2018). In order to fully understand the climate evolution over the Holocene, and reasons behind the Holocene 'conundrum', more research is needed comparing new palaeoclimate records and climate simulations (Marsicek et al., 2018).

This study endeavours to improve our understanding of Holocene climate variability in Ireland. The aims of this study are fourfold: 1) to investigate the potential of chironomid-July air temperature transfer functions to accurately reconstruct temperature change through the early to late Holocene, supplemented with pollen data to track landscape change; 2) to explore the use of chironomid functional traits as a tool for reconstructing ecosystem functioning and stability, along with testing the sensitivity of chironomid feeding guilds to modelled climate; 3) to assess the coherence with other well-established palaeoclimate records in Ireland spanning the Holocene and various climate model hindcasts, which have been downscaled and bias corrected to the west coast of Ireland; 4) to evaluate if there is a link between the Irish palaeoclimate records and climate forcing parameters, such as total solar irradiance and ice rafted debris from the North Atlantic.

2. Regional setting

Ireland's geographic position on the eastern seaboard of the Atlantic Ocean makes it an important location to investigate climate variability over the Holocene due to its sensitivity to oceanic conditions and air masses affecting thermal characteristics of the adjacent land. The climate of the island is characterised by low annual temperatures (between 9 °C and 10 °C mean annual temperature), low summer temperatures (14 °C mean July temperature), and high precipitation (between 1000 and 1400 mm of rainfall per annum along with west coast, and ~ 750 to 1000 mm of rainfall per annum on the eastern half of the island) (McKeown et al., 2012; Met Éireann, 2018).

Lough Nakeeroge (53 ° 59.53 ’N, 10 ° 08.25 ’W) is located on the northern coast of Achill Island, Co. Mayo, in the west of Ireland. Achill Island’s geology is composed of acidic Dalradian and Moinian schists, which have been folded into the dominating peaks of the island, with summit heights of up to 671 m a.s.l. (Chew et al., 2003). The region was extensively glaciated during the last ice age by inland and local ice sheets (Knight, 2015). Sea-levels have been modelled close to Achill Island, which was at the boundary of the Celtic Ice sheet (Patton et al., 2017). They were estimated to be around minus 80 m by 20,000 cal. yr BP, and rose rapidly to minus 30 m by 10,000 cal. yr BP, reaching around minus 5 m by 8000 cal. yr BP (Shennan et al., 2018).

Achill Island has been subject to several palaeoenvironmental studies (Caseldine et al., 2005; Caseldine et al., 2007; Head et al., 2007). The present landscape is covered with extensive ombrotrophic blanket peat, and it is suggested that peat initiation began in the early Holocene and became a dominant form on the landscape by the late-Holocene (Caseldine et al., 2007). The treeless landscape of the island bears little resemblance to that of the early to mid-Holocene, when Achill Island was covered with extensive forest of *Pinus*, *Quercus*, *Betula*, *Corylus*, *Alnu*s, and *Ulmus* (Caseldine et al., 2007). Lough Nakeeroge is adjacent to the coast at 20 m a.s.l. (Annagh Beach, located only meters to the north) with steep hill slopes to the south, east and west (Fig 1). No bathymetric maps were generated, but spot measurements were taken on the day of coring. The maximum depth of the water column is 9 m towards the centre of the larger basin and 4 m towards the centre of the smaller one, which is located at the western edge of the lake. The lake is 0.65 km long and 0.2 km wide with two basins. The catchment slopes consist of shallow peat soils on granite schist bedrock. *Molinia caerulea*, *Schoenus nigricans* and *Sphagnum* spp. are dominant along the slopes and the lower plateaus. There are limited areas of *Phragmites* around the periphery of the lake. Despite the lake's remote location, prehistoric features such as unclassified megalithic tombs and a stone circle have been identified on the nearby headlands (archaeology.ie, 2018).

Figure 1 here

3. Materials and methods

3.1 Lake coring strategy and core realignment

Two overlapping cores, core A and core B, were extracted in June 2009 in 1 m segments to a maximum depth of 4 m, from the smaller basin of the Lough Nakeeroge. This was carried out using a Livingstone corer (Wright Jr, 1980) from an anchored boat. The smaller basin was selected to avoid slumping from steeper slopes. The cores were labelled and wrapped in plastic film and aluminium foil before being transported to the Geography Department's laboratory at the University of Exeter, where they were stored at c. 4°C to minimise biological activity.

During the analysis of the Lough Nakeeroge sediment core, uncertainties in core recovery were identified from an evaluation of the ^{14}C dating model, percentage weight of loss-on-ignition after being dried at 550 ºC and 950 ºC (LOI_{550} and LOI_{950}), and chironomid assemblages from core A and core B (see Sup Fig. 1-2, supplementary material).

3.2 Age-depth model

Age-depth models for the Lough Nakeeroge core were based on AMS ^{14}C ages of bulk sediment, due to the absence of suitable macrofossils. Humic acid and bulk humin were the fractions chosen for dating and samples were pre-treated according to Lowe et al. (2004). Five AMS radiocarbon dates were obtained along the sediment master core (Table 1). The five dates for this lake were calibrated using IntCal 13 (Reimer et al. 2013) on *Bacon* version 2.2 (Blaauw and Christen, 2013) and R version 3.5.2. (R Core Team, 2018). Dates for this lake are reported throughout the paper in calibrated years before present and rounded to the nearest 10 years (cal. yr BP).

Table 1 Here

3.3 Laboratory analyses

Sediment organic (LOI_{550}) and inorganic content (LOI_{950}) was calculated using loss-on-ignition, following using standard methods (Heiri et al. 2001). This was carried out at continuous 1 cm intervals. Chironomid analysis was carried out at 2 cm intervals at the top of core A from 50 cm to 66 cm, and at 4 cm intervals hereafter. Chironomid analysis followed standard procedures outlined by Walker (2001). Chironomids were handpicked with forceps using 10-40 x magnification and permanently mounted on slides for identification. A minimum of 150 chironomid head capsules was picked for each sample. Chironomid identifications were made using a compound microscope at 100-400 x magnification. Taxa were identified to genus, sub-genus and species-type based on

Wiederholm (1983), Rieradevall and Brooks (2001), and Brooks et al. (2007). Samples for pollen analysis were taken volumetrically (0.4 cm^3) at 4 cm intervals and prepared using standard methods including KOH digestion, HF treatment and acetylation (Moore et al., 1991).

3.4 Numerical and statistical analysis

A chironomid stratigraphy was created using C2 version 1.4, and stratigraphic changes in the composition of chironomid and pollen assemblages were assessed by sum-of-squares partitioning and statistically significant zones were identified using Psimpoll 4.27 (Bennett, 2009). All ordinations were produced using square-root transformed chironomid percentage data for all common taxa. Common taxa were identified as those present in at least two samples with a relative abundance of > 2 % in at least one sample (Heiri and Lotter, 2001).

Chironomid-inferred temperatures were reconstructed from the chironomid assemblages using an inference model generated using the 50-lake training set from Western Ireland (Potito et al., 2014; Taylor et al., 2018). Based on a weighted-average (WA) classic model of lake characteristics, chironomid assemblages were deemed a good predictor of summer air temperature in west of Ireland region (r^2_{jack} = 0.63, RMSEP = 0.56 °C) (Potito et al., 2014, Taylor et al., 2018). The reliability of the chironomid-inferred temperature model was assessed with a chi-squared ‘goodness-of-fit’ to temperature test whereby fossil samples were passively positioned on a Canonical Correspondence Analysis (CCA) of the modern training set constrained solely against July air temperature (Heiri and Lotter, 2001). Any fossil samples that had a squared residual distance value within the 10th percentile of values in the modern training set were considered to have a poor fit-to-temperature (Birks, 1998). Chi chord-squared distances were calculated, and CCA were performed using CANOCO version 4.54 (Ter Braak and Smilauer, 2002). Non-metric multidimensional scaling (NMDS) was performed on the chironomid community data to further explore changes through time using vegan version 2.5-4 (Oksanen et al., 2015) in R version 3.5.2. Chironomids were divided into five guilds based on their primary feeding preferences: collector-gatherers, collector-filterers, scrapers, shredders, and predators (Merritt and Cummins, 1996; Luoto and Nevalainen, 2015b).

3.6 Data compilation

The Lough Nakeeroge chironomid-inferred temperature model (C-IT) and functional trait (using collector-filterer guild) records were compared with Holocene palaeoclimate data from Ireland to test the strength of coherence, if any, between the reconstructions. The Irish palaeoclimate data is composed of peatland water table reconstructions combined and detrended from eight sites across Ireland (Swindles et al., 2013), and the $\delta^{18}O$ record sourced from the Crag Cave speleothem (McDermott et al., 1999; McDermott et al., 2001). Although palaeoclimate evidence differs in the degree to which it records specific climate parameters, statistical comparisons between the proxy reconstructions and palaeoclimate simulations from a coupled atmosphere-ocean-vegetation general circulation model, the Hadley Centre Coupled Model, version 3 (HadCM3; Valdes et al., 2017), was carried out to explore connections between the different climate parameters and the proxy datasets. Whilst this climate model is not in the latest generation of general circulation or earth system models, its relatively fast integration speed on few cores (e.g. achieving ~100 model years per wall-clock day on 24 processors of a Tier 3, i.e. University, supercomputing facility) makes it feasible to carry out the number of simulations required for comparison to the climate proxy data presented here. Furthermore, HadCM3 performs well, simulating mean present-day climate and Last Glacial Maximum climate (21 ka) with comparable skill to other and more recent models (DiNezio and Tierney, 2013; Valdes et al., 2017). The climate model also performs well when compared to a range of palaeoenvironmental records over the last glacial cycle (120 ka to present) (Singarayer et al., 2011; Hoogakker et al., 2016; Davies-Barnard et al., 2017).

The equilibrium-type simulations used in this study were run at intervals of 500 years from 12,500 to 0 yr BP and are the same simulations as those used by Gandy et al. (2018), Swindles et al. (2018) and Morris et al. (2018). The simulations are based on the previous 1750-year long runs performed by Singarayer et al. (2011) with model developments and the dynamic vegetation module described by Davies-Barnard et al. (2017) as HadCM3BM2.1aD. For each time interval, the model setup was updated to be broadly consistent with the Paleoclimate Model Intercomparison Project Phase Four (PMIP4) protocol for the last deglaciation (Ivanovic et al., 2016) and run for a further 500 years with the new boundary conditions (such as orbital parameters, atmospheric trace gases, bathymetry, land sea mask, ice mask, orography) held constant through time. The climate means used in this study were calculated from the last 50 years of the simulations, by which time the model had reached near steady-state. The model outputs were then regionally downscaled and bias corrected to 0.5° x 0.5° resolution using bi-cubic spline (see Morris et al., 2018; SI Materials and Methods for more details), which is c. 50 x 50 km in the mid-latitudes. This provided estimates of climate to be localised to northern Achill Island. For this study, five climate variables were extracted from the simulation output: 1) annual air temperature at 2 m above the ground surface (°C); 2) July air temperature at 2 m above the ground surface (°C); 3) total annual precipitation (mm); 4) total July precipitation (mm); 5) total annual potential evaporation (mm). Each variable was statistically assessed with each of the Irish proxy reconstructions by placing all records on the same 500-year window. The climate proxy data were tested for normality using the Sharpo-Wilk test and Pearson correlations were performed across all datasets. Running correlations were then performed to statistically interrogate the relationship among the proxy records, and then with the five computer simulated climate variables. This was carried out between 9500 to 2000 cal. yr BP for all records, apart from the standardised water table compilation (Swindles et al., 2013), which was assessed between 6000 and 2000 cal. yr BP.

All palaeoclimate records (proxy and simulated) were used to determine the correlation between each variable and two climate forcing datasets, Total Solar Irradiance (TSI) (Steinhilber et al., 2009), and Ice Rafted Debris (IRD) in the North Atlantic (Bond et al., 2001), and then with the $\delta^{18}O$ from the Greenland NGRIP record (North Greenland Ice Core Project members, 2004). TSI was selected as a forcing parameter to determine if solar signals are present in the proxy reconstructions. The IRD record has been recently linked to storm activity throughout the Holocene in Denmark, where shifts in North Atlantic westerlies and storm tracks were modulated by persistent North Atlantic Oscillation-like phases (Goslin et al., 2018). The IRD record was chosen to determine if we see similar links in the Irish palaeoclimate data, given that Lough Nakeeroge is a high-energy lake adjacent to the coast. The $\delta^{18}O$ of the Greenland NGRIP record was used to determine if we can see wider regional-scale teleconnections in Holocene climate.

4. Results

4.1 Age-Depth Model

The sedimentation rate throughout the dated levels of the master core maintains a relatively consistent pattern based on the weighted mean of the age model, with no significant irregularities. Between 10,050 cal. yr BP and 2050 cal. yr BP (389 cm to 76 cm), the sedimentation rate was modelled at an average rate of 0.045 cm yr^{-1} (26 yr cm^{-1}).

Figure 2 Here

4.2 Organic Carbon (LOI_{550})

Organic carbon (LOI_{550}) ranges from 3.2 % to 39.1 % over the length of the master core (Fig 3). The section of the core that is > 10,000 cal. yr BP is marked by the lowest values of organic carbon (~ 4-9 %). By 9960 cal. yr BP, LOI_{550} increases to ~ 17 % and continues to rise hereafter, reaching an average of 25 % between 9300 and 8100 cal. yr BP. LOI_{550} values decrease to ~ 10 to 17 % between 7860 and 7600. This is followed by a marked rise in organic carbon, where LOI_{550} reaches a maximum of 39 % by 6500 cal. yr BP. LOI_{550} values largely stabilise from the mid-Holocene, fluctuating between 25 and 30 %. However, two notable drops in LOI_{550} values occur at 3900 and 1700 cal. yr BP.

4.3 Chironomid community analysis and functional traits

The succession was divided into five statistically significant chironomid assemblage zones (CAZs). In total, 54 different taxa were identified in Lough Nakeeroge, with 36 common taxa (Fig. 3). There was an average of 17 different taxa per sample.

Figure 3 Here

4.3.1 CAZ1 ca. > 10,000 cal. yr BP (404 – 393 cm)

Micropsectra insignilobus-type (64 %), *Tanytarsus lugens*-type (8 %), *Tanytarsus chinyensis*-type (8 %) and *Protanypus* (4 %) comprise 84 % of the taxa in this zone.

Microtendipes pedellus-type (3 %), *Polypedilum nubifer*-type (3 %) and *Cladopelma* (2 %) are present, albeit in low numbers. These samples lie below the last radiocarbon date in the inorganic portion of the core, and denoted > 10,000 cal. yr BP. Collector-filterers are the largest guild in this zone (84 %), while predators (7 %), shredders (5 %), collector-gatherers (2 %) are present but at low abundance. Scrapers are not present in this zone.

4.3.2 CAZ2 ca. 10,050 – 8400 cal. yr BP (389 – 320 cm)

CAZ2 is characterised by a rise in *M. pedellus*-type (6%), *Psectrocladius sordidellus/psilopterus*-type (6 %) and *Procladius* (6 %). *Dicrotendipes nervosus*-type (20 %) and *Ablabesmyia* (10 %) appear for the first time in this zone and are the most dominant taxa. These taxa make up around half of the chironomid community in CAZ2. *M. insignilobus*-type (3 %), *T. lugens*-type (<1 %) and *Protanypus* (<1 %) notably decrease. *Heterotanytarsus* (3.5 %) appears for the first time in this zone. Collector-gatherers (49 %), predators (19 %) and shredders (6 %) show a sharp increase at the start of the zone, while collector-filterers show a notable decline by 10,050 cal. yr BP and a progressive decline through the rest of the zone (33 – 22 %). Scrapers appear for the first time in the record (1 %).

4.3.3 CAZ3 ca. 8310 – 7760 cal. yr BP (317 – 300 cm)

In CAZ3 there is an increase in *P. septentrionalis*-type (19 %), *H. marcidus*-type (6 %), *Pseudochironomus* (5 %) and *M. insignilobus*-type (4 %). *P. septentrionalis*-type reaches its highest abundance between 8100 cal. yr BP and 7800 cal. yr BP. *D. nervosus*-type decrease through this zone, while *Chironomus anthracinus*-type and *Tanytarsus mendax*-type, disappear entirely. *Lauterborniella* is only present in the lake between 8200 cal. yr BP and 8000 cal. yr BP. Collector-gatherers (67 %) reach their greatest abundance throughout this zone, while collector-filterers present a trough (12 %). Predators (15 %), scrapers (< 1 %), and shredders (3 %) all show minor decreases in percentage abundance.

4.3.4 CAZ4 ca. 7690 – 6000 cal. yr BP (297 – 238 cm)

H. marcidus-type, *Thienemannimyia*, *Pseudochironomus* and *M. insignilobus*-type are abundant at the beginning of CAZ4 between 7700 to 7550 cal. yr BP, and decrease quickly after 7550 cal. yr BP. *T. chinyensis*-type (18 %) is quite dominant. *D. nervosus*-type (17 %), *M. pedellus*-type (~8 %), *T. glabrescens*-type (6 %), *T. mendax*-type (3 %) and *C. edwardsi*-type (2 %) remain abundant. Collector-filters recover in this zone (35 %), while collector-gatherers decrease (46 %). Between 6150 and 6000 cal. yr BP, at the end of this zone, there is a sharp shift in the abundance of both guilds, with collector-filterers increasing (32 - 45 %) and collector-gatherers decreasing (53 – 33 %). Predators are variable throughout the zone (max = 17 %, min = 0 %, average = 12 %). Scrapers (2 %) and shredders (3 %) show a relatively stable low abundance apart from a notable shift at the end of the zone, where the former falls by 6 % and the latter increases by 6 %.

4.3.5 CAZ5 ca. 5900 – 1500 cal. yr BP (236 – 50 cm)

Overall, CAZ5 is dominated by *T. chinyensis*-type (19%), *T. mendax*-type (10%) and *T. glabrescens*-type (8 %), together comprising around one third of the chironomid community. *Heterotanytarsus* (14 %) is also quite prominent. The zone comprises the sub-section of core A, with the notable decrease in *D. nervosus*-type taking place towards the bottom of the core. *H. marcidus*-type (2-14 %), *T. chinyensis*-type (23-34 %) and *Thienemannimyia* (4-11 %) increase in numbers between 6050 cal. yr BP and 5700 cal. yr BP. While, *D. nervosus*-type (15-0 %), *P. nubifer*-type (7-0 %), *M. pedellus*-type (7-4 %), *T. mendax*-type (2-0 %) and *T. glabrescens*-type (11-6.5 %) all decrease. Two shifts in chironomid community structure are evident in the Late Holocene; the first is between 4150 and 3700 cal. yr BP, and the second more abrupt shift occurs between 1750 and 1700 cal. yr BP. The former phase shows a decline in *M. pedellus*-type, *Procladius* and *T. glabrescens*-type after 4150 cal. yr BP. The latter abrupt decline shows a brief but rapid increase in *Thienemannimyia*, *M. insignilobus*-type and *H. marcidus*-type.

Collector-gatherers and collector-filterers show an opposing and variable trend in this zone. This is particularly evident between 1750 and 1700 cal. yr BP, when collector-filterers decrease from 49 % to 33 %, and collector-gatherers replace them with a notable rise from 28 % to 45 %. Predators notably increase by 1790 cal. yr BP to 24%, remaining relatively high (~ 17-18 %) until 1660 cal. yr BP. Shredders and scrapers stay relatively stable at this time but show minor variability throughout the zone.

4.3.6 Non-metric multidimensional scaling

The non-metric multidimensional scaling (NMDS) applied to the chironomid stratigraphy shows an overview of community change through time. CAZ1 is spaced further from all other zones in the ordination space and is driven by cool adapted taxa such as *T. lugens*, *M. insignilobus*-type, and *Protanypus*. CAZ2-CAZ3 overlap, with CAZ3 located further to the right of the bottom quantrant, which is driven by *Lauterborniella*, *Psectrocladius septentrionalis*-type, and *Pseudochironomus*. The ordination space occupied by CAZ2, CAZ4 and CAZ5 is much larger than the other two zones, provides a general overview of lake development over the Holocene along NMDS Axis 1 (Fig. 4(i) and 4(ii)). The shift towards the left of the graph is driven by T. *palidicornis*-type, Polypedilum *sordens*-type, *Stempellina*, *Tanytarus* undefined, and *Eukiefferiella*.

Figure 4 Here

4.3.7 Chironomid-inferred temperature model

The chironomid-inferred July air temperature model (C-IT) for Lough Nakeeroge ranged from 11.4 °C to 14.5 °C (Fig. 3). Potito et al (2014) states that the root-mean square error of prediction (RMSEP) of 0.56 °C is considerably smaller than errors reported from other regional training sets. Thus, the model has greater applicability for reconstructing Ireland's relatively subdued Holocene temperature fluctuations. The lowest C-IT estimates occur at > 10,000 cal. yr BP and the highest at 1990 cal. yr BP. The period < 10,000 cal. yr BP, is composed of three samples, which fall slightly outside the ordination space of the Western Ireland training set, but were still statistically calculated to be a good 'fit-to-temperature' (Fig 5). C-IT estimates increase from > 10,000 cal. yr BP, with sustained high values between 10,000 and 6000 cal. yr BP. Within this inferred warmer period, C-ITs show a decline 7800 and 7500 cal. yr BP (12.5 °C). Between 6030 and 5800 cal. yr BP the model shows a notable decline in C-IT over a 230-year period. By 5200 cal. yr BP inferred temperatures increase gradually, with a decline in values inferred between 4050 and 3400 cal. yr BP, and a marked abrupt decline between 1730 and 1690 cal. yr BP. A subsequent increase in C-IT is evident for the rest of the core with inferred values reaching an average of 13.8 °C, with the highest inferred temperature recorded at 1990 cal. yr BP (14.5 °C). The chironomid taxa identified in the Irish training set (Potito et al. 2014) are well represented throughout the Lough Nakeeroge core. The CCA shows that the downcore chironomid assemblage are located within the ordination space captured by the Western Ireland training set (Fig. 5) (Potito et al. 2014).

Figure 5 Here

4.4 Pollen Stratigraphy

The pollen profile was divided into four significant pollen assemblage zones (PAZs), with zone boundaries occurring at 9750 cal. yr BP, 7850 cal. yr BP, and 3125 cal. yr BP (Fig. 6). In total 48 different taxa were identified. Pollen concentrations ranged from 735,811 to 19,349 grains per ml^{-1} of wet sediment, with grains more densely concentrated in the bottom section of the core and decreasing towards the top.

4.4.1 PAZ1 ca. > 10,000 – 9750 cal. yr BP (404 – 377 cm)

In PAZ1, > 10,000 cal. yr BP, *Poaceae*, *Salix*, *Juniperus* and a range of ericaceous taxa dominated the landscape, comprising around 70 % of the pollen record. This open herbaceous landscape with dwarf shrubs declined by 9850 cal. yr BP and a *Betula*-dominant woodland began to establish. Unfortunately, due to the lack of pollen in the sediment, notable gaps in the pollen record exists between 9650 cal. yr BP and 8800 cal. yr BP, and again between 8725 cal. yr BP and 8100 cal. yr BP.

4.4.2 PAZ2 ca. 9650 – 7890 cal. yr BP (373 – 305 cm)

In PAZ2, *Betula* becomes more dominant and by 8700 cal. yr BP *Pinus* and *Corylus* increase in abundance. *Ulmus* and *Quercus* also appear at the end of PAZ2 and all Ericales decrease to 2 %. By 7800 cal. yr BP mixed woodland is well established with *Corylus* (9 %), *Pinus* (23 %), *Betula* (21 %). *Isoetes* also increases towards the end of the Zone from 2 % to 17 %. Ferns decrease throughout PAZ 2 (24 % to 2 %).

Figure 6 Here

4.4.3 PAZ3 ca. 7790 – 3220 cal. yr BP (301 – 130 cm)

Throughout PAZ3 mixed woodland continues to dominate and *Isoetes* becomes more common. Total Ericales, most notably *Calluna*, was recorded relatively continuously throughout the zone with evident increases at times of notably lower woodland cover, which punctuate the record between 5550 cal. yr BP and 5450 cal. yr BP, and again at 4850 cal. yr BP. Between 5900 cal. yr BP and 5450 cal. yr BP, *Betula*, *Pinus*, *Ulmus*, *Quercus*, *Alnus* and *Corylus* decrease from 64 % to 20 % of the total landscape cover. *Calluna* increases from 15 % to 30 %, while *Isoetes* increases from 21 % to 57 %. By 5350 cal. yr BP, woodland recovers to 76 %, while *Calluna* and *Isoetes* decrease. A more abrupt decline in woodland (74 – 39 %) and increase in *Calluna* (13 – 34 %) is evident between 5000 cal. yr BP and 4850 cal. yr BP. PCA axis 1 for pollen shows two notable shifts at 5450 cal. yr BP and 4850 cal. yr BP, in a rather featureless record. Towards the end of the zone, between 4000 cal. yr BP and 3700 cal. yr BP, there is a fall in the abundance of most tree species once more (81 – 44 %) and *Calluna* becomes more dominant (4 – 19 %).

4.4.4 PAZ 4 ca. 3130 – 1500 cal. yr BP (126 – 50 cm)

Throughout PAZ 4 (3125 cal. yr BP to 1500 cal. yr BP) all trees decrease, most notably *Pinus* (15 – 2 %), *Betula* (11 – 2 %), *Quercus* (14 – 1 %) and *Ulmus* (1.5 – 0 %). There is also an increase in *Isoetes* between 3000 and 2600 cal. yr BP (6 – 56 %). By 1500 cal. yr BP, the landscape shifts from one dominated by woodland to one reflecting dwarf shrub colonisation.

5. Interpretation and discussion

5.1 Early Holocene

The early Holocene marks the period with the greatest taxa turnover and change in C-IT (Fig. 3). It must be noted that the dates for these samples are beyond the basal ^{14}C date (9830 cal. yr BP), and estimates have been attained through extrapolation of the Bayesian age-depth model (Blaauw and Christen, 2011). It is suspected that these sediments are older than the age-depth model implies. Taking this into consideration, a low C-IT of 11.4 ^{o}C is observed in this portion of the record (Fig 3). Taxa associated with cool, oligotrophic lake conditions dominate the earliest portion of the record before 10,000 cal. yr BP; taxa include

M. insignilobus-type, *T. lugens*-type, *T. chinyensis*-type and *Protanypus*. Species diversity is low in this portion of the stratigraphy. Here, the chironomid collector-filterer feeding guild dominates. This group filters small-sized organic particles from the water column, and are commonly found in tubes extending above the surface of the substrate (Cummins, 1973). Collector-filterers tend to thrive in cooler, less productive lakes, which are typically structured by benthic-food webs, and intermediate water depth (Cummins, 1973). A similar pattern is observed in Finland, where Luoto and Nevalainen (2015b) show that the collector-filterer guild is most abundant in the cold early Holocene (< 10,000 cal. yr BP). There is also a high concentration of chironomid head capsules and pollen grains, corresponding with a minimum in sediment organic carbon, likely indicating a slow rate of sedimentation, a typical feature of early lake ontology in an adjusting climate (Fig. 3 and Fig. 8). *Salix*, *Juniperus*, and a range of ericaceous taxa, are dominant reflecting dwarf shrub colonisation of the landscape during this phase.

At c. 10,000 cal. yr BP, the chironomid community appears to shift to an alternative ‘stable state’. There is an evident rise in taxa associated with warmer, more productive lake conditions, such as *M. pedellus*-type and *P. sordidellus/psilopterus*-type. Collector-filterers decline over the time, while collector-gatherers, predators, and shredders, notably increase. Collector-gatherers tends to be the most dominant feeding guild in contemporary, temperature, mid-latitude lakes; they are deposit feeders and consume organic detritus that accumulate on lake sediments (Cummins, 1973). Chironomid larvae with predatory feeding patterns tend to feed on small rotifers and cladocerans, which are more abundant in productive lakes (Vodopich and Cowell, 1984). Luoto and Nevalainen (2015a) suggest that predators and collector-gatherers may be indicators of climate-trophic coupling, as these feeding guilds tend to thrive in warmer, nutrient-rich lakes. Shredders are known to feed on course particles of organic matter, such as submerged wood, leaf litter, and algae; they are also associated with living vascular plants. These feeding guilds suggest an increase in lake productivity in a potentially warmer climate. At this time, frequencies of *Betula* rise (c. 9950 cal. yr BP), followed by *Juniperus* and *Poaceae*. Ericales notably decrease, indicating the growth of early forest. C-IT shows a marked increase from c. 10,000 - 8950 cal. yr BP. Thus, the chironomid community is responding indirectly to changes in trophic conditions, which is likely driven by a shift towards a warmer climate.

Between 8950 and 8000 cal. yr BP, the C-IT shows an overall decline, while taxa associated with warmer and more productive conditions continue to increase. Collector-filterers remain low, while collector-gatherers and predators continue to rise. By 8100 cal. yr BP, the Lough Nakeeroge pollen reconstruction shows an increase in *Pinus*, *Quercus* and *Corylus*, along with the colonisation of *Ulmus*, indicating a mature mixed tree canopy. *Lauterborniella* appears for the first time in the stratigraphy at c. 8200 cal. yr BP, and aligns with a notable increase in *Isoetes*. This chironomid taxon is well-known to be indicative of well-developed macrophytes stands (Merritt and Cummins, 1996; Heino, 2008; Kowalewski et al., 2016). Shredders and scrapers also show a minor, but notable, increase. As mentioned above, these guilds tend to be associated with diverse macrophyte communities (Alahuhta et al., 2011), and it is suggested that an increase in their abundance is linked to the availability of plant material (Luoto and Nevalainen, 2015a). At 8200 cal. yr BP, the chironomid assemblage, and functional traits of the community, are probably responding to altered macrophyte abundance, indirectly driving the community into an alternative ‘stable state’.

By 7000 cal. yr BP, trees show an overall decline, and *Calluna* increases, indicating peat expansion across the landscape. *Isoetes* follow a similar pattern to *Calluna*. Shredders and scrapers also increase. This may indicate a rise in lake level, driven by a shift in hydrogeological conditions associated with decreased tree cover and expansion of bog, allowing water-tables to rise, and lake shelves to flood, where *Isoetes* can further expand and thrive (Fig. 7). The shift in chironomid functional traits likely indicates a transition towards higher organic production through littoral aquatic vegetation expansion (*Isoetes*) and pelagic productivity. As mentioned above, shredders and scrapers are associated with diverse macrophyte communities (Alahuhta et al., 2011), and collector-gatherers consume organic detritus that accumulate on lake sediments (Cummins, 1973). Between 7800 and 6030 cal. yr BP, the collector-filterers increase once again, while the collector-gatherers decrease slightly but remain dominant. Shredders, scrapers, and predators, stay relatively stable. This likely indicates active pelagic, benthic, and littoral production in Lough Nakeeroge. However, the C-IT increases over this time, which seems counter-intuitive to the functional trait argument.

Figure 7 Here

5.2 Mid-Holocene

While the presence of megalithic tombs in northern Achill Island does suggest human habitation in the region (archaeology.ie, 2018), the Lough Nakeeroge pollen record only shows evidence of some small-scale human activity; traditional indicators, such as *Plantago* and *Rumex* are present albeit in only very low abundances. Charcoal evidence from the region shows levels too high to reflect solely domestic fires (Caseldine et al., 2005). As human activity is present, albeit only likely to be minor, caution is exerted with C-IT interpretation and there is the potential for human activity to influence the lake system and thus the chironomid community. It is difficult to determine a decline in Elm for the region as *Ulmus* abundance is relatively low and variable between 5500 and 4500 cal. yr BP; however, two notable periods where *Ulmus* declines occur at c. 5450 and 4850 cal. yr BP.

Lough Nakeeroge C-IT shows a notable decline between 6050 cal. yr BP and 5800 cal. yr BP, with continued low values until 5350 cal. yr BP. This is being driven by an increase in *H. marcidus*-type and *Thienemannimyia*, along with an increase in *Heterotanytarsus*. There is also a notable decrease in *D. nervosus*-type over this period; the taxon is well represented (15% of the chironomid assemblage) at 240 cm (6030 cal. yr BP), which is located at the bottom of the sub-section of core A (Sup. Fig. 2) and then decreases throughout the rest of the core. This species has been identified as a keystone indicator for identifying critical transitions to alternative stable states in lakes (Doncaster et al., 2016), and it clearly defines a shift in the chironomid community in Lough Nakeeroge. There is also a decrease in LOI_{550} around this time. Collector-gatherers decline and are briefly replaced by collector-filterers; this indicates a decrease in lake productivity, potentially forcing the lake, once again, into an alternative 'stable state'.

Heterotanytarus is inferred as a cooler-adapted species in the chironomid inference model. However, in the 50-lake training set from Western Ireland the higher elevation lakes were in catchments covered with blanket peat and contained a higher abundance of *Heterotanytarus*. As elevation decreases and temperatures rise, along with bogs becoming less dominant across the landscape due to drainage and conversion of peatland to pastoral land from human activities, *Heterotanytarus* may not be indicative of cooler temperatures but may be more related to acidic, peaty conditions, which occur in cool, higher elevation sites in western Ireland. In a catchment where peat is expanding, *Heterotanytarsus* will become more dominant but will also drive the model to infer cooler conditions. It is possible that the C-IT model may be 1) decoupled from temperature and responding to a changing landscape in the mid-Holocene or, 2) overestimating potential cooling. It is not clear that temperature is the main driver of chironomid community turnover and the C-IT should be interpreted with caution here.

The C-IT shows an increase between 5800 and 4150 cal. yr BP, with a notable lull between 5600 and 5200 cal. yr BP. Peatland was now well established in the catchment, as identified by the dominance of *Calluna*, *Cyperaceae*, and the chironomid taxon *Heterotanytarsus*. There is a notable abrupt decline in all trees and increase in *Calluna* and *Poaceae* between c. 5600 and 5400 cal. yr BP, with a parallel marked decrease in pollen concentration. The chironomid feeding guilds also show variability over this period, which is particularly evident in the collector-filterers and scrapers, with an overall increase in both guilds. As scrappers shave material from submerged objects, such as rocks and wood (Cummins, 1973), an expansion of this feeding guild may indicate an increase in the input of terrestrial material to the lake. Caseldine et al. (2005) suggest an extreme in-wash event from two peatlands on Achill island through humification and palynological data, which was associated with increased storminess between c. 5300 and 5050 cal. yr BP. Roland et al. (2015) suggests that the increase in storminess at 5200 cal. yr BP is an island-wide phenomenon, and wetter conditions have been largely reported across the Northern Europe at this time (Starkel, 1991; Haas et al., 1998; Magny, 1999; Hughes et al., 2000; Langdon et al., 2003; Blaauw et al., 2004; Magny et al., 2006). As Lough Nakeeroge is a coastal lake in a high-energy environment, in-wash events from stormier conditions c. 5600 and 5400 cal. yr BP may be responsible for the suggested decrease in lake productivity (increase in collector-filterers) in parallel with the increase in scrappers, which favour larger submerged material. Evidence for a stormy phase at the time could be further supported by the brief decrease in trees and the decline in LOI_{550}, where a marine in-wash event may have increased the percentage of terrigenous fractionation, thus, leading to a decrease in the percentage of organic carbon. However, as the resolution of our data is coarse and our dating model is composed of only 5 radiocarbon dates, we can only speculate about a 5.2 ka event. However, the timing of the suggested period of short-term environmental variability aligns well with lake level variability across Europe (Magny et al., 2006), but appears to be earlier then that recorded in Ireland (Caseldine et al., 2005; Roland et al., 2015).

5.3 Late Holocene

By the late Holocene, the chironomid community appears more stable. The C-IT shows a broad decline between 4150 and 3800 cal. yr BP. This change is mainly due to the replacement of *T. mendax*-type by the more cold-adapted *M. insignilobus*-type. Collector-filterers increase at the expense of collector-gatherers over this time, while shredders show a minor but stable increase. The is accompanied by a marked change in the pollen record with a rise in *Salix* and a fall in the abundance of most tree species. This may suggest a phase of cooler and wetter conditions in the region. Across Ireland and Britain evidence for wetter conditions is suggested in peat-based palaeoecological records c. 4250 – 3750 cal. yr BP (Hughes et al., 2000; Barber et al., 2003; Mauquoy et al., 2008; Daley and Barber, 2012; Roland et al., 2014). It has been suggested by Roland et al. (2014) that the manifestation of this ‘4.2 kyr event’ is unclear in Ireland. Caution is, once again, exercised with this interpretation of the Lough Nakeeroge reconstruction, as the resolution of the record is too coarse to confidently interpret short-term events/rapid climate shifts. More research is needed at a higher resolution to fully determine if the 4.2 and 5.2 ka events occur in Ireland.

Between 3000 and 2600 cal. yr BP, the Lough Nakeeroge C-IT increases. Here, the model is being driven by an increase in *T. mendax*-type and *T. glabrescens*-type. We also see a decrease in *Pinus*. Over this time there is a decline in predators, and an increase in collector-filterers, while collector-gatherers stay relatively stable. Luoto and Nevalainen (2015b) demonstrate that predators are associated with warmer lakes, while collector-filterers were largely found in cooler, less productive waters. The C-IT and chironomid guilds show conflicting inferences, with the former indicating warmer conditions and the latter suggesting a cooler climate. However, numerous palaeoecological studies from Ireland and Britain provide clear evidence for cooler and wetter conditions c. 2800 cal. yrs BP (Charman et al., 2006; Swindles et al., 2013; Roland et al., 2014). Thus, it is likely the C-IT is decoupled from temperature at this time and chironomid functional traits are more aligned with the evidence from Ireland and Britain.

For the rest of the record, there is a general replacement of trees with shrubs and grasses, and a minor decrease in the abundance of *Isoetes*. A final brief and notable fall in the Lough Nakeeroge C-IT and shift in functional traits occurs between 1750 and 1700 cal. yr BP. The resolution of the record is ~ 50 years in this later portion. During this time, collector-filterers decrease by 15 % and collector-gatherers increase by 18 %, and LOI_{550} notably declines. Predators markedly increase to 24 % by 1780, with a continued decrease for the rest of the record. No pollen was extracted over this brief period. It is not clear what is driving this change in the Lough Nakeeroge records at this time.

5.4 Comparison of Holocene proxy records and down-scaled climate simulations

The chironomid-inferred temperature and functional trait records were compared with existing palaeoclimate reconstructions from Ireland to decipher climate signals from autogenic processes. Peat-based records represent the most abundant paleoclimate data in

Ireland. These records are based on testate amoebae, plant macrofossils and humification values from ombrotrophic raised bogs and blanket peatlands (Swindles et al., 2013). Climate inferences are based on proxies of effective moisture (precipitation minus evaporation), reflecting periods of summer water deficit (Charman et al., 2009; Booth et al., 2010). These peatland records have been compiled from multiple sites across Ireland to decipher a climate signal from ‘noisy’ localised autogenic processes (Swindles et al., 2013), and provide quantitative curves of effective moisture at a centennial to multi-decadal scale from the mid- to late Holocene. The speleothem record from Crag Cave is a high-resolution temperature-sensitive proxy record from the south west of Ireland (Co. Kerry) spanning the full Holocene (McDermott et al., 1999; McDermott et al., 2001). It is inferred to be reflecting changes in isotopic values of the source moisture (McDermott et al., 2001). As air mass history and atmospheric circulation appear to influence the $\delta^{18}O$ signature in precipitation, palaeo-$\delta^{18}O$ reconstructions sourced from Irish proxy records are best interpreted as reflecting a combination of parameters, and not solely palaeoprecipitation or palaeotemperature (Baldini et al., 2010). While this speleothem record is a valuable climate archive, the interpretation of the $\delta^{18}O$ signature can at times be ambiguous.

Climate model hindcasts were used to simulate various climate parameters (with the annual and summer season output focused on here) to further explore climate change in Ireland. Although chironomid assemblages can be inferred climatically, there are other factors that can decouple the chironomid-temperature relationship. The simulated conditions provide another method to assess broader (500-yr) changes in climate throughout the Holocene in Ireland, which was then compared with the chironomid records from Lough Nakeeroge. This was carried out to assess if there was seasonal bias in the chironomid data and to decipher if this method could be used to determine time periods where the chironomid community may not be driven by temperature. This comparison was also carried out with the other Irish palaeoenvironmental records to gain a better understanding of climate fluctuations for Ireland.

Our results show that there is variable correspondence between the proxy reconstructions and the simulated climate variables (Fig. 8). There are some visible similarities, which we tested statistically. The results of the Pearson correlations show that simulated annual temperature ($r^2 = 0.56$, $p < 0.05$), annual potential evaporation ($r^2 = 0.58$, $p < 0.05$), and annual precipitation ($r^2 = 0.54$, $p < 0.05$), are all significantly negatively related to the Lough Nakeeroge C-IT (Table 2). Interestingly, simulated July temperature shows a much weaker relationship. This may imply that the chironomid-July air temperature inference model is being driven by changes in lake level throughout the Holocene as potential evaporation shows a strong negative relationship with the data. This suggests that increases in C-IT occurs when there is a fall in annual air temperature, annual precipitation, and annual potential evaporation, and vice versa. Thus, the Lough Nakeeroge C-IT represents a complicated signal driven by these three climate variables, which draws into question the chironomid-climate relationship and the validity of temperature reconstructions using the transfer function at this site.

Table 2 Here

The Lough Nakeeroge C-IT show little correspondence with the chironomid collector-filterer guild, apart from early Holocene warming (Fig 3 and Table 2). As collector-filterers tend to thrive in cooler, more oligotrophic lakes (Luoto and Nevalainen, 2015), they were selected as the best guild to explore alongside the chironomid-temperature inference model. When we explore the relationship between the simulated climate models and chironomid collector-filterer guild, which are typically structured by benthic-food webs

(Luoto and Nevalainen, 2015), annual temperature shows the strongest positive relationship to this guild ($r^2 = 0.51$, $p < 0.05$), and the relationship is less significant for modelled July temperature ($r^2 = 0.32$, $p = 0.23$). However, the positive relationship indicates that the collector-filterer guild increases when annual and July temperatures rise. As this guild is associated with cooler, less productive lakes, the relationship appears to actually be negative. When we interrogate the statistical relationship between the collector-filterer guild and simulated annual temperature using running correlations through time, the percentage of collector-filterers is low (indicating possible warmer conditions) when modelled annual temperature is low but rising from c. 9500 to 7500 cal. yr BP (Sup Fig 5 (ii)). As modelled annual temperature rises throughout the rest of the Holocene (6000 cal. yr BP to 2000 cal. yr BP), the collector-filterers rise, indicating a cooler, late Holocene (Sup Fig 5 (ii)).

The isotope record from Crag Cave was significantly negatively correlated to annual precipitation and annual temperature (both have $r^2 = 0.52$, $p < 0.05$). The relationship between the $\delta^{18}O$ of meteoric precipitation and precipitation amount at both modern event and daily timescales has been identified as negative in numerous observational and modelling studies (Noone and Simmonds, 2002; Celle-Jeanton et al., 2004; Treble et al., 2005; Lee and Fung, 2008). The negative correlation between the Crag Cave $\delta^{18}O$ record and the precipitation amount simulated by the GCM could be due to the “amount effect” in the former record, whereby heavier rainfall is more ^{18}O depleted (Dansgaard, 1964). Baldini et al. (2010) attributes 20 % of the $\delta^{18}O$ variability in Irish meteoric precipitation to the “amount effect”. Thus, precipitation amount, inferred from the depletion of $\delta^{18}O$, may be a useful indicator of heavy rainfall phases, and shifts in these values may reflect shifts in air mass history and atmospheric circulation.

Both Lough Nakeeroge C-IT and Crag Cave records show a strong negative relationship with modelled annual precipitation and temperature, and show a strong positive relationship to each other (r^2 = 0.43, p = 0.1). It is possible, and we speculate, that the C-IT may be complicated by changes in lake level, possibly through periods of heavy rainfall, where littoral shelves become flooded. However, more research is needed on lakes with a well constrained lake-level record to determine if any link exists.

When we interrogate the statistical relationship between the proxy records and GCM hindcasts through running correlations the relationships are highly variable. However, the Monte Carlo significance test further suggests that the relationship between each proxy and/or climate variable is mostly non-significant through time (Sup Fig. 3-12). While the climate model hindcasts can provide another method of exploring Holocene climate change alongside palaeoclimate proxies, it is important to remember the data-model disparity for global surface temperature during the late Holocene, with proxies recording overall cooling (Marcott et al., 2013), and climate models consistently simulating warming (Liu et al., 2014). This disparity is evident in our dataset. Marcott and Shakun (2014) argue that this Holocene climate “conundrum” relates to incomplete forcings and/or insufficient sensitivity to feedbacks in the models. However, Marsicek et al. (2018) and Baker et al. (2017) suggest that the contradiction may be due to palaeoclimate reconstructions primarily being carried out in the Northern Hemisphere mid-latitudes, where pronounced late Holocene cooling is largely inferred from maritime proximal sites using multiple approaches, while continental regions are largely underrepresented. Carbon and oxygen isotopes from two stalagmites in the Ural mountains, suggest that continental Eurasian warming over the Holocene, not only contradicts the widely recognised inferred-warmth between ~ 10,000 to 5000 cal. yr BP, followed by late Holocene cooling (Marcott and Shakun, 2015), but instead match the late

Holocene warming trend captured by the transient model simulations (Baker et al., 2017). More recent evidence shows that temperatures reconstructed from sub-fossil pollen across 642 sites, extending from Europe to North America, closely match climate model simulations, indicating the long-term warming defined the late Holocene up to ~ 2000 cal. yr BP, and that reconstructions demonstrating long-term cooling are confined to the North Atlantic Region (Marsicek et al., 2018). Our analysis shows that there is a link between specific simulated climate models and Lough Nakeeroge C-IT, chironomid collector-filter guild, and Crag Cave $\delta^{18}O$ records. As both sites are located in western Ireland and at the fringe of the Atlantic Ocean, the disparity between the proxy reconstructions and climate models is not surprising, and even supports the assumptions of Marsicek et al. (2018) and Baker et al. (2017).

5.5 Climate drivers

The palaeoclimate proxy records and model simulations were compared with $\delta^{18}O$ record from the NGRIP ice core (North Greenland Ice Core Project members, 2004), along with the TSI (Steinhilber et al., 2009) IRD records (Bond et al., 2001). It is evident that there is a high degree of variability between all three records and the Irish proxy and simulated climate records (Table 2); however, some patterns of coherence are evident.

Figure 8 Here

In the early Holocene, the Lough Nakeeroge FT, C-IT and Crag Cave $\delta^{18}O$ records indicate warming conditions c. 10,000 to 8000 cal. yr BP. The NGRIP $\delta^{18}O$ record also suggests overall warming during this early Holocene period. As the C-IT appears to be statistically related to modelled annual air temperature, precipitation and potential evaporation, caution is exercised with the interpretation of this transfer function solely as a

July air temperature reconstruction. TSI is high at the start of the record to 8000 cal. yr BP, which suggests that the early Holocene warming may be related to orbital-induced insolation. However, short lived cooler phases punctuate this overall warmer early Holocene climate. A 150-yr short lived decline in $\delta^{18}O$ is evident from the Crag Cave record between 9350 and 9200 cal. yr BP, and a more subtle change is also evident in the Lough Nakeeroge C-IT, FT, and NGRIP $\delta^{18}O$ records. However, the coarser resolution of the chironomid reconstructions makes it difficult to confidently interpret such short-lived fluctuations. Numerous studies have attributed these fluctuations to the interaction between solar insolation, ice-sheets dynamics and heat transport of the North Atlantic (Kaufman et al., 2004; Kim et al., 2004; Hald et al., 2007; Renssen et al., 2012; Blaschek and Renssen, 2013; Marcott et al., 2013).

Between 8700 and 7800 cal. yr BP, the FT record suggest peak annual warmth. The C-IT signal is not clear; however, it may suggest increased fluctuations in lake levels, possibly through the close relationship between C-IT and annual temperature, precipitation and potential evaporation. The collector-gatherer, shredder, and scraper, feeding guilds increase at the expense of the collector-filterers. This likely indicates greater organic production in the littoral aquatic vegetation and pelagic zones. An increase in *Isoetes* in the pollen record supports the change in chironomid functionality. It suggests that the lake's water column deepened so that it flooded the littoral shelves, which may have been the result of increased precipitation. The $\delta^{18}O$ record from Crag Cave shows variability over this time period, where the record fluctuates between low and high $\delta^{18}O$ values. Although the precise nature of what is driving the variability in chironomids is unclear and more research is needed at a higher temporal resolution.

Apart from the NGRIP $\delta^{18}O$ record, there is no clear evidence of the short lived 8.2 kyr event. This event was not detected in the conventional stalagmite (CC3) from Crag Cave $\delta^{18}O$ record; the large (~8 %) decrease in $\delta^{18}O$ is now known to be an analytical artefact (McDermott et al., 2001; Fairchild et al., 2006). The lack of an 8.2 ka event signal may be due to the coarse temporal resolution of the palaeoclimate records, as this event has been observed in other Irish lakes (Holmes et al., 2016). A cooler phase with variable precipitation from c. 7700 to 6800 is suggested from the Crag Cave $\delta^{18}O$, Lough Nakeeroge FT and CIT records. TSI is low over this period and the NGRIP $\delta^{18}O$ record shows variability similar to Crag Cave.

The Lough Nakeeroge FT, Crag Cave $\delta^{18}O$ record, and standardised water table compilation, show similar trends between 6500 and 5200 cal. yr BP, which suggests warmer/drier conditions before 5800 cal. yr BP with a shift to cooler/wetter conditions. Figure 8 demonstrates that these cooler/wetter conditions between c. 5800 and 5200 cal. yr BP occurred during a peak in IRD (Bond et al., 2001), along with reduced TSI. There is also evidence for cooler conditions across Greenland in the NGRIP $\delta^{18}O$ record (Fig. 8), and from the GISP2 $\delta^{18}O$ record (Stuiver et al., 1995; Alley, 2000). Modelling techniques have shown that the expansion of sea-ice led to cooler conditions across the North Atlantic at this time (Renssen et al., 2006). These conditions are perceived to be modulated by a persistent North Atlantic Oscillation-like system, most likely induced by changes in the strength and position of the Azores High pressure system, equivalent to the North Atlantic Oscillation (Goslin et al., 2018). Although the resolution of the Lough Nakeeroge chironomid record is not at a high temporal resolution to capture short-time climate fluctuations, it is suggested that a period of intense storminess coined the ‘5.2 ka event’ occurred during this cool/wet phase, which was characterised by the increased intensity of westerly winds over Ireland, with prevailing cyclonic activity and an associated increase in precipitation (Roland et al., 2015).

By 4150 and 3800 cal. yr BP, the standardised water table compilation indicates wetter conditions (Swindles et al., 2013). The collector-filterers display a subtle increase between 4150 and 3700 cal. yr BP, while the C-IT declines. This is accompanied by a marked change in the pollen record, with a rise in *Salix* and a fall in the abundance of Pinus, and most tree species, between 3900 and 3700 cal. yr BP. This may indicate cooler and wetter conditions between 4150 and 3800 cal. yr BP. However, Crag Cave $\delta^{18}O$ record shows a much earlier short-lived decline from 4500 to 4200 cal. yr BP. Peat-based palaeoecological records from Ireland and Britain indicate wetter conditions c. 4250 – 3750 cal. yr BP (Hughes et al., 2000; Barber et al., 2003; Mauquoy et al., 2008; Daley and Barber, 2012; Roland et al., 2014). TSI and IRD are stable at this time, suggesting that they are not driving this shift to cooler/wetter conditions.

The wet/cool phase in the late Holocene (c. 2700 to 2400 cal. yr BP) is well-documented across Ireland and Britain (Charman et al., 2006; Swindles et al., 2013; Roland et al., 2014) and is registered in the Lough Nakeeroge FT record, with an increase in the collector-filterer guild (Fig. 8). This climate phase is suggested to be widespread in the North Atlantic region and occurs when TSI and IRD are low (Fig. 8). Hereafter, the standardised water table record, Crag Cave $\delta^{18}O$ record, and the Lough Nakeeroge FT reconstruction suggests a shift to cooler/drier conditions between 2000 and 1700 cal. yr BP. This brief event has no clear connection to the IRD; however, it coincides with a subtle decline in TSI.

6. Conclusions

Our study is a contribution to the advancement of our understanding of Holocene climate variability in Ireland. We present a new chironomid-inferred July air temperature model, chironomid functional trait reconstruction, and palynological record, from a lake in western Ireland that spans the early to late Holocene (c. < 10,000 to 1500 cal. yr BP). While this study demonstrates the complexities of chironomid transfer functions in Irish lakes, it makes a valuable contribution to 1) our understanding of chironomids as palaeoindicators of climate and, 2) improves our knowledge of long-term Holocene climate variability in Ireland.

We can draw several conclusions from this study:

1. Our results show a connection between the collector-filterer feeding guild and simulated annual air temperature. As chironomids play a pivotal role in the biogeochemical cycling behind food-web structure in lakes, their feeding functions reflect the state of trophic levels. Functional traits expressed through chironomid feeding guilds may be sufficient for reconstructing past trends in temperature. However, other factors such as fluctuating lake level should also be considered. More research is needed to determine the strength of the relationship between chironomid feeding guilds, climate, and lake level. We suggest the development of a transfer function based on functional traits, which can be used alongside and complementary to the chironomid-inferred temperature models. This may help decipher autogenic and allogenic factors. The link between chironomid functional traits and palaeoclimate is only emerging, and more research is needed at a higher temporal resolution to determine if this relationship is evident in other regions of Ireland.

2. The chironomid-record from Lough Nakeeroge reflects a complicated range of driving factors. The Pearson’s correlations between the C-IT reconstruction and the five variables simulated from the climate models, suggest that the record is being driven by a

combination of annual air temperature, annual precipitation, and annual potential evaporation. Although the running correlations and Monte Carlo test show that this relationship is weak and, often, non-significant through time. Improvements can be made to the transfer function method by increasing the geographic scope of training sets to capture larger gradients in geographic zones, lake types and climate boundaries.

3. Although the palaeoclimate data is highly variable, several important phases and events can be identified from the records, and tied to recent studies from the Ireland, Britain, and North Atlantic region. Although, more research is needed in the early Holocene from terrestrial archives to fully understand climate variability and drivers at this time.

4. There is a clear contradiction between the proxy records and climate model hindcasts over the mid- to late Holocene. The discrepancy between late Holocene cooling inferred from proxy records and warming evident in the simulated climate models reflects the well-known Holocene temperature conundrum. Our data supports recent evidence, which suggests that the North Atlantic may be responsible for the ‘conundrum’. More research is needed comparing simulated climate models to proxy reconstructions from continental regions.

5. There is no clear evidence to link the terrestrial palaeoclimate records with changes in IRD, apart from one phase 5800 and 5200 cal. ye BP. There are times when changes in solar activity appear to be related to fluctuations in the proxy records. However, running correlation analysis shows that this relationship is generally weak and variable through time.

Acknowledgements

The authors would like to thank Irish Quaternary Association (IQUA), the Royal Irish Academy, and the School of Geography and Archaeology NUI Galway for funding the radiocarbon dating for this project. The contribution from RFI was partly supported by NERC grant NE/K008536/1. This research did not receive any specific grant from funding agencies in the public, commercial, or not-for-profit sectors. The authors would also like to thank the two anonymous reviewers for their constructive and valuable comments.

Reference List

AHLBERG, K., ALMGREN, E., WRIGHT JR, H. & ITO, E. 2001. Holocene stable-isotope stratigraphy at Lough Gur, County Limerick, Western Ireland. *The Holocene*, 11, 367-372.

ALAHUHTA, J., VUORI, K.-M. & LUOTO, M. 2011. Land use, geomorphology and climate as environmental determinants of emergent aquatic macrophytes in boreal catchments.

ALLEY, R. B. 2000. Ice-core evidence of abrupt climate changes. *Proceedings of the National Academy of Sciences*, 97, 1331-1334.

AMESBURY, M. J., BOOTH, R. K., ROLAND, T. P., BUNBURY, J., CLIFFORD, M. J., CHARMAN, D. J., ELLIOT, S., FINKELSTEIN, S., GARNEAU, M. & HUGHES, P. D. 2018. Towards a Holarctic synthesis of peatland testate amoeba ecology: Development of a new continental-scale palaeohydrological transfer function for North America and comparison to European data. *Quaternary Science Reviews*, 201, 483-500.

AMESBURY, M. J., SWINDLES, G. T., BOBROV, A., CHARMAN, D. J., HOLDEN, J., LAMENTOWICZ, M., MALLON, G., MAZEI, Y., MITCHELL, E. A. & PAYNE, R. J. 2016. Development of a new pan-European testate amoeba transfer function for reconstructing peatland palaeohydrology. *Quaternary Science Reviews*, 152, 132-151.

ARCHAEOLOGY.IE. 2018. Archaeology Survey Database

www.archaeology.ie [Online], Assessed on the 5th April 2018.

ÁRVA, D., TÓTH, M., MOZSÁR, A. & SPECZIÁR, A. 2017. The roles of environment, site position, and seasonality in taxonomic and functional organization of chironomid assemblages in a heterogeneous wetland, Kis-Balaton (Hungary). *Hydrobiologia*, 787, 353-373.

BAKER, J. L., LACHNIET, M. S., CHERVYATSOVA, O., ASMEROM, Y. & POLYAK, V. J. 2017. Holocene warming in western continental Eurasia driven by glacial retreat and greenhouse forcing. *Nature Geoscience*, 10, 430.

BALDINI, L. M., MCDERMOTT, F., BALDINI, J. U., FISCHER, M. J. & MÖLLHOFF, M. 2010. An investigation of the controls on Irish precipitation δ 18 O values on monthly and event timescales. *Climate dynamics*, 35, 977-993.

BARBER, K. E., CHAMBERS, F. M. & MADDY, D. 2003. Holocene palaeoclimates from peat stratigraphy: macrofossil proxy climate records from three oceanic raised bogs in England and Ireland. *Quaternary Science Reviews*, 22, 521-539.

BEHRE, K.-E. 1981. The interpretation of anthropogenic indicators in pollen diagrams. *Pollen et spores*, 23, 225-245.

BENNETT, K. 2009. psimpoll'and 'pscomb': C programs for analysing pollen data and plotting pollen diagrams (version 4.27) Available online from Queen's University Quaternary Geology program at URL.

BIRKS, H. 1998. DG Frey and ES Deevey Review 1: Numerical tools in palaeolimnology–Progress, potentialities, and problems. *Journal of paleolimnology*, 20, 307-332.

BLAAUW, M. & CHRISTEN, J. A. 2011. Flexible paleoclimate age-depth models using an autoregressive gamma process. *Bayesian analysis*, 6, 457-474.

BLAAUW, M. & CHRISTEN, J. A. 2013. Bacon Manual e v2. 2. *Blaauw, M., Wohlfarth, B., Christen, JA, Ampel, L., Veres, D., Hughen, KA, Preusser, F., et al.(2010),—Were Last Glacial Climate Events Simultaneous between Greenland and France*, 387-394.

BLAAUW, M., VAN GEEL, B. & VAN DER PLICHT, J. 2004. Solar forcing of climatic change during the mid-Holocene: indications from raised bogs in The Netherlands. *The Holocene*, 14, 35-44.

BLASCHEK, M. & RENSSEN, H. 2013. The Holocene thermal maximum in the Nordic Seas: the impact of Greenland Ice Sheet melt and other forcings in a coupled atmosphere-sea ice-ocean model.

BOND, G., KROMER, B., BEER, J., MUSCHELER, R., EVANS, M. N., SHOWERS, W., HOFFMANN, S., LOTTI-BOND, R., HAJDAS, I. & BONANI, G. 2001. Persistent solar influence on North Atlantic climate during the Holocene. *Science*, 294**,** 2130-2136.

BOOTH, R., LAMENTOWICZ, M. & CHARMAN, D. 2010. Preparation and analysis of testate amoebae in peatland palaeoenvironmental studies. *Mires & Peat*, 7.

BROOKS, S. J., AXFORD, Y., HEIRI, O., LANGDON, P. G. & LAROCQUE-TOBLER, I. 2012. Chironomids can be reliable proxies for Holocene temperatures. A comment on Velle et al.(2010). *The Holocene*, 22**,** 1495-1500.

BROOKS, S. J. & LANGDON, P. G. 2014. Summer temperature gradients in northwest Europe during the Lateglacial to early Holocene transition (15–8 ka BP) inferred from chironomid assemblages. *Quaternary International*, 341**,** 80-90.

BROOKS, S. J., LANGDON, P. G. & HEIRI, O. 2007. *The identification and use of Palaearctic Chironomidae larvae in palaeoecology*, Quaternary Research Association.

CASELDINE, C. & FYFE, R. 2006. A modelling approach to locating and characterising elm decline/landnam landscapes. *Quaternary science reviews*, 25**,** 632-644.

CASELDINE, C., FYFE, R., LANGDON, C. & THOMPSON, G. 2007. Simulating the nature of vegetation communities at the opening of the Neolithic on Achill Island, Co. Mayo, Ireland—the potential role of models of pollen dispersal and deposition. *Review of Palaeobotany and Palynology*, 144**,** 135-144.

CASELDINE, C., THOMPSON, G., LANGDON, C. & HENDON, D. 2005. Evidence for an extreme climatic event on Achill Island, Co. Mayo, Ireland around 5200–5100 cal. yr BP. *Journal of Quaternary Science: Published for the Quaternary Research Association*, 20**,** 169-178.

CELLE-JEANTON, H., GONFIANTINI, R., TRAVI, Y. & SOL, B. 2004. Oxygen-18 variations of rainwater during precipitation: application of the Rayleigh model to selected rainfalls in Southern France. *Journal of Hydrology*, 289, 165-177.

CHARMAN, D. J., BARBER, K. E., BLAAUW, M., LANGDON, P. G., MAUQUOY, D., DALEY, T. J., HUGHES, P. D. & KAROFELD, E. 2009. Climate drivers for peatland palaeoclimate records. *Quaternary Science Reviews*, 28, 1811-1819.

CHARMAN, D. J., BLUNDELL, A., CHIVERRELL, R. C., HENDON, D. & LANGDON, P. G. 2006. Compilation of non-annually resolved Holocene proxy climate records: stacked Holocene peatland palaeo-water table reconstructions from northern Britain. *Quaternary Science Reviews*, 25, 336-350.

CHEW, D. M., DALY, J. S., PAGE, L. & KENNEDY, M. 2003. Grampian orogenesis and the development of blueschist-facies metamorphism in western Ireland. *Journal of the Geological Society*, 160, 911-924.

CHIQUE, C., POTITO, A. P., MOLLOY, K. & CORNETT, J. 2018. Tracking recent human impacts on a nutrient sensitive Irish lake: integrating landscape to water linkages. *Hydrobiologia*, 807, 207-231.

CUMMINS, K. W. 1973. Trophic relations of aquatic insects. *Annual review of entomology*, 18, 183-206.

DALEY, T. & BARBER, K. 2012. Multi-proxy Holocene palaeoclimate records from Walton Moss, northern England and Dosenmoor, northern Germany, assessed using three statistical approaches. *Quaternary International*, 268, 111-127.

DALEY, T. J., THOMAS, E. R., HOLMES, J. A., STREET-PERROTT, F. A., CHAPMAN, M. R., TINDALL, J. C., VALDES, P. J., LOADER, N. J., MARSHALL, J. D. & WOLFF, E. W. 2011. The 8200 yr BP cold event in stable isotope records from the North Atlantic region. *Global and Planetary Change*, 79, 288-302.

DANSGAARD, W. 1964. Stable isotopes in precipitation. *Tellus*, 16, 436-468.

DAVIES-BARNARD, T., RIDGWELL, A., SINGARAYER, J. & VALDES, P. 2017. Quantifying the influence of the terrestrial biosphere on glacial–interglacial climate dynamics. *Climate of the Past*, 13, 1381-1401.

DIEFENDORF, A. F., PATTERSON, W. P., MULLINS, H. T., TIBERT, N. & MARTINI, A. 2006. Evidence for high-frequency late Glacial to mid-Holocene (16,800 to 5500 cal yr BP) climate variability from oxygen isotope values of Lough Inchiquin, Ireland. *Quaternary Research*, 65, 78-86.

DINEZIO, P. N. & TIERNEY, J. E. 2013. The effect of sea level on glacial Indo-Pacific climate. *Nature Geoscience*, 6, 485.

DONCASTER, C. P., CHÁVEZ, V. A., VIGUIER, C., WANG, R., ZHANG, E., DONG, X., DEARING, J. A., LANGDON, P. G. & DYKE, J. G. 2016. Early warning of critical transitions in biodiversity from compositional disorder. *Ecology*, 97, 3079-3090.

EGGERMONT, H. & HEIRI, O. 2012. The chironomid-temperature relationship: expression in nature and palaeoenvironmental implications. *Biological Reviews*, 87, 430-456.

FAIRCHILD, I. J., SMITH, C. L., BAKER, A., FULLER, L., SPÖTL, C., MATTEY, D. & MCDERMOTT, F. 2006. Modification and preservation of environmental signals in speleothems. *Earth-Science Reviews*, 75, 105-153.

FOURNIER, B., LARA, E., JASSEY, V. E. & MITCHELL, E. A. 2015. Functional traits as a new approach for interpreting testate amoeba palaeo-records in peatlands and assessing the causes and consequences of past changes in species composition. *The Holocene*, 25, 1375-1383.

GAŁKA, M., TOBOLSKI, K., GÓRSKA, A. & LAMENTOWICZ, M. 2017. Resilience of plant and testate amoeba communities after climatic and anthropogenic disturbances in a Baltic bog in Northern Poland: implications for ecological restoration. *The Holocene*, 27, 130-141.

GANDY, N., GREGOIRE, L. J., ELY, J. C., CLARK, C. D., HODGSON, D. M., LEE, V., BRADWELL, T. & IVANOVIC, R. F. 2018. Marine ice sheet instability and ice shelf buttressing of the Minch Ice Stream, northwest Scotland. *The Cryosphere*, 12, 3635-3651.

GHILARDI, B. & O'CONNELL, M. 2013. Early Holocene vegetation and climate dynamics with particular reference to the 8.2 ka event: pollen and macrofossil evidence from a small lake in western Ireland. *Vegetation History and Archaeobotany*, 22, 99-114.

GOMES, W. I. A., DA SILVA JOVEM-AZEVÊDO, D., PAIVA, F. F., MILESI, S. V. & MOLOZZI, J. 2018. Functional attributes of Chironomidae for detecting anthropogenic impacts on reservoirs: A biomonitoring approach. *Ecological Indicators*, 93, 404-410.

GOSLIN, J., FRUERGAARD, M., SANDER, L., GAŁKA, M., MENVIEL, L., MONKENBUSCH, J., THIBAULT, N. & CLEMMENSEN, L. B. 2018. Holocene centennial to millennial shifts in North-Atlantic storminess and ocean dynamics. *Scientific reports*, 8, 12778.

HAAS, J. N., RICHOZ, I., TINNER, W. & WICK, L. 1998. Synchronous Holocene climatic oscillations recorded on the Swiss Plateau and at timberline in the Alps. *The holocene*, 8, 301-309.

HALD, M., ANDERSSON, C., EBBESEN, H., JANSEN, E., KLITGAARD-KRISTENSEN, D., RISEBROBAKKEN, B., SALOMONSEN, G. R., SARNTHEIN, M., SEJRUP, H. P. & TELFORD, R. J. 2007. Variations in temperature and extent of Atlantic Water in the northern North Atlantic during the Holocene. *Quaternary Science Reviews*, 26, 3423-3440.

HEAD, K., TURNEY, C. S., PILCHER, J. R., PALMER, J. & BAILLIE, M. 2007. Problems with identifying the '8200-year cold event'in terrestrial records of the Atlantic seaboard: a case study from Dooagh, Achill Island, Ireland. *Journal of Quaternary Science*, 22, 65-75.

HEINO, J. 2008. Patterns of functional biodiversity and function-environment relationships in lake littoral macroinvertebrates. *Limnology and Oceanography*, 53, 1446-1455.

HEIRI, O., BROOKS, S. J., BIRKS, H. J. B. & LOTTER, A. F. 2011. A 274-lake calibration data-set and inference model for chironomid-based summer air temperature reconstruction in Europe. *Quaternary Science Reviews*, 30, 3445-3456.

HEIRI, O. & LOTTER, A. F. 2001. Effect of low count sums on quantitative environmental reconstructions: an example using subfossil chironomids. *Journal of Paleolimnology*, 26, 343-350.

HEIRI, O. & MILLET, L. 2005. Reconstruction of Late Glacial summer temperatures from chironomid assemblages in Lac Lautrey (Jura, France). *Journal of Quaternary Science*, 20**,** 33-44.

HOLMES, J., ARROWSMITH, C., AUSTIN, W., BOYLE, J., FISHER, E., HOLME, R., MARSHALL, J., OLDFIELD, F. & VAN DER POST, K. 2010. Climate and atmospheric circulation changes over the past 1000 years reconstructed from oxygen isotopes in lake-sediment carbonate from Ireland. *The Holocene*, 20**,** 1105-1111.

HOLMES, J., JONES, R., HAAS, J. N., MCDERMOTT, F., MOLLOY, K. & O'CONNELL, M. 2007. Multi-proxy evidence for Holocene lake-level and salinity changes at An Loch Mór, a coastal lake on the Aran Islands, western Ireland. *Quaternary Science Reviews*, 26**,** 2438-2462.

HOLMES, J. A., TINDALL, J., ROBERTS, N., MARSHALL, W., MARSHALL, J. D., BINGHAM, A., FEESER, I., O'CONNELL, M., ATKINSON, T. & JOURDAN, A.-L. 2016. Lake isotope records of the 8200-year cooling event in western Ireland: comparison with model simulations. *Quaternary Science Reviews*, 131**,** 341-349.

HOOGAKKER, B., SMITH, R. S., SINGARAYER, J. S., MARCHANT, R., PRENTICE, I., ALLEN, J., ANDERSON, R., BHAGWAT, S., BEHLING, H. & BORISOVA, O. 2016. Terrestrial biosphere changes over the last 120 kyr. *Climate of the Past*, 12**,** 51-73.

HU, J., EMILE-GEAY, J. & PARTIN, J. 2017. Correlation-based interpretations of paleoclimate data–where statistics meet past climates. *Earth and Planetary Science Letters*, 459**,** 362-371.

HUGHES, P. D., MAUQUOY, D., BARBER, K. & LANGDON, P. G. 2000. Mire-development pathways and palaeoclimatic records from a full Holocene peat archive at Walton Moss, Cumbria, England. *The Holocene*, 10**,** 465-479.

IVANOVIC, R., GREGOIRE, L., KAGEYAMA, M., ROCHE, D., VALDES, P., BURKE, A., DRUMMOND, R., PELTIER, W. R. & TARASOV, L. 2016. Transient climate simulations of the deglaciation 21-9 thousand years before present (version 1)-PMIP4 Core experiment design and boundary conditions. *Geoscientific Model Development*.

JEPPESEN, E., JENSEN, J. P., AMSINCK, S. L. & JOHANSSON, L. S. 2001. Paleoecological methods as tools in assessing the near-pristine state of lakes. *TemaNord*, 563, 45-49.

JUGGINS, S. 2013. Quantitative reconstructions in palaeolimnology: new paradigm or sick science? *Quaternary Science Reviews*, 64, 20-32.

KAUFMAN, D. S., AGER, T. A., ANDERSON, N. J., ANDERSON, P. M., ANDREWS, J. T., BARTLEIN, P. J., BRUBAKER, L. B., COATS, L. L., CWYNAR, L. C. & DUVALL, M. L. 2004. Holocene thermal maximum in the western Arctic (0–180 W). *Quaternary Science Reviews*, 23, 529-560.

KIM, J.-H., RIMBU, N., LORENZ, S. J., LOHMANN, G., NAM, S.-I., SCHOUTEN, S., RÜHLEMANN, C. & SCHNEIDER, R. R. 2004. North Pacific and North Atlantic sea-surface temperature variability during the Holocene. *Quaternary Science Reviews*, 23, 2141-2154.

KNIGHT, J. 2015. Ductile and brittle styles of subglacial sediment deformation: an example from western Ireland. *Sedimentary Geology*, 318, 85-96.

KOENIG, I., MULOT, M. & MITCHELL, E. A. 2018. Taxonomic and functional traits responses of Sphagnum peatland testate amoebae to experimentally manipulated water table. *Ecological Indicators*, 85, 342-351.

KOWALEWSKI, G. A., KORNIJÓW, R., MCGOWAN, S., KACZOROWSKA, A., BAŁAGA, K., NAMIOTKO, T., GĄSIOROWSKI, M. & WASIŁOWSKA, A. 2016. Disentangling natural and anthropogenic drivers of changes in a shallow lake using palaeolimnology and historical archives. *Hydrobiologia*, 767, 301-320.

LAMENTOWICZ, M., GALKA, M., TOBOLSKI, K., LAMENTOWICZ, L., ERSEK, V., JASSEY, V. E. & VAN DER KNAAP, W. O. Functional traits of testate amoebae and multi-proxy data unveil exceptional Baltic bog ecohydrology, autogenic succession and climate change during the last 2000 years in CE Europe. EGU General Assembly Conference Abstracts, 2017. 6705.

LANGDON, P., BARBER, K. & HUGHES, P. 2003. A 7500-year peat-based palaeoclimatic reconstruction and evidence for an 1100-year cyclicity in bog surface wetness from Temple Hill Moss, Pentland Hills, southeast Scotland. *Quaternary science reviews*, 22, 259-274.

LANGDON, P., BROWN, A., CASELDINE, C., BLOCKLEY, S. & STUIJTS, I. 2012. Regional climate change from peat stratigraphy for the mid-to late Holocene in central Ireland. *Quaternary International*, 268, 145-155.

LEE, J. E. & FUNG, I. 2008. “Amount effect” of water isotopes and quantitative analysis of post-condensation processes. *Hydrological Processes: An International Journal*, 22, 1-8.

LIU, Z., ZHU, J., ROSENTHAL, Y., ZHANG, X., OTTO-BLIESNER, B. L., TIMMERMANN, A., SMITH, R. S., LOHMANN, G., ZHENG, W. & TIMM, O. E. 2014. The Holocene temperature conundrum. *Proceedings of the National Academy of Sciences*, 111, E3501-E3505.

LUOTO, T. P., KAUKOLEHTO, M., WECKSTRÖM, J., KORHOLA, A. & VÄLIRANTA, M. 2014. New evidence of warm early-Holocene summers in subarctic Finland based on an enhanced regional chironomid-based temperature calibration model. *Quaternary Research*, 81, 50-62.

LUOTO, T. P. & NEVALAINEN, L. 2015a. Climate-forced patterns in midge feeding guilds. *Hydrobiologia*, 742, 141-152.

LUOTO, T. P. & NEVALAINEN, L. 2015b. Late Holocene precipitation and temperature changes in Northern Europe linked with North Atlantic forcing. *Climate Research*, 66, 37-48.

LUOTO, T. P. & OJALA, A. E. 2018. Controls of climate, catchment erosion and biological production on long-term community and functional changes of chironomids in High Arctic lakes (Svalbard). *Palaeogeography, Palaeoclimatology, Palaeoecology*, 505, 63-72.

LUOTO, T. P., RANTALA, M. V., GALKIN, A., RAUTIO, M. & NEVALAINEN, L. 2016. Environmental determinants of chironomid communities in remote northern lakes across the treeline–Implications for climate change assessments. *Ecological indicators*, 61, 991-999.

MAGNY, M. 1999. Lake-level fluctuations in the Jura and french subalpine ranges associated with ice-rafting events in the north atlantic and variations in the polar atmospheric circulation [Corrélations entre les fluctuations du niveau des lacs du Jura et des Alpes françaises du Nord, les débâcles d'icebergs dam l'Atlantique Nord et la circulation atmosphérique polaire]. *Quaternaire*, 10, 61-64.

MAGNY, M., LEUZINGER, U., BORTENSCHLAGER, S. & HAAS, J. N. 2006. Tripartite climate reversal in Central Europe 5600–5300 years ago. *Quaternary research*, 65, 3-19.

MARCISZ, K., COLOMBAROLI, D., JASSEY, V. E., TINNER, W., KOŁACZEK, P., GAŁKA, M., KARPIŃSKA-KOŁACZEK, M., SŁOWIŃSKI, M. & LAMENTOWICZ, M. 2016. A novel testate amoebae trait-based approach to infer environmental disturbance in Sphagnum peatlands. *Scientific reports*, 6, 33907.

MARCOTT, S. A. & SHAKUN, J. D. 2015. Holocene climate change and its context for the future. *PAGES*, 23, 28.

MARCOTT, S. A., SHAKUN, J. D., CLARK, P. U. & MIX, A. C. 2013. A Reconstruction of Regional and Global Temperature for the Past 11,300 Years. *Science*, 339, 1198-1201.

MARSICEK, J., SHUMAN, B. N., BARTLEIN, P. J., SHAFER, S. L. & BREWER, S. 2018. Reconciling divergent trends and millennial variations in Holocene temperatures. *Nature*, 554, 92.

MAUQUOY, D., YELOFF, D., VAN GEEL, B., CHARMAN, D. J. & BLUNDELL, A. 2008. Two decadally resolved records from north-west European peat bogs show rapid climate changes associated with solar variability during the mid–late Holocene. *Journal of Quaternary Science: Published for the Quaternary Research Association*, 23, 745-763.

MCDERMOTT, F., FRISIA, S., HUANG, Y., LONGINELLI, A., SPIRO, B., HEATON, T. H., HAWKESWORTH, C. J., BORSATO, A., KEPPENS, E. & FAIRCHILD, I. J. 1999. Holocene climate variability in Europe: evidence from δ18O, textural and extension-rate variations in three speleothems. *Quaternary Science Reviews*, 18, 1021-1038.

MCDERMOTT, F., MATTEY, D. P. & HAWKESWORTH, C. 2001. Centennial-scale Holocene climate variability revealed by a high-resolution speleothem δ18O record from SW Ireland. *Science*, 294, 1328-1331.

MCGOWAN, S., GUNN, H. V., WHITEFORD, E. J., ANDERSON, N. J., JONES, V. J. & LAW, A. C. 2018. Functional attributes of epilithic diatoms for palaeoenvironmental interpretations in South-West Greenland lakes. *Journal of paleolimnology*, 60, 273-298.

MCKEOWN, M. 2013. *A Palaeolimnological Assessment of Human and Climate Influences on Chironomid Communities in Western Ireland*.

MCKEOWN, M. & POTITO, A. P. 2016. Assessing recent climatic and human influences on chironomid communities from two moderately impacted lakes in western Ireland. *Hydrobiologia*, 765, 245-263.

MCKEOWN, M., POTITO, A. P. & HICKEY, K. R. 2012. The long-term temperature record from Markree Observatory, County Sligo, from 1842 to 2011. *Irish Geography*, 45, 257-282.

MERRITT, R. W. & CUMMINS, K. W. 1996. *An introduction to the aquatic insects of North America*, Kendall Hunt.

MET ÉIREANN. 2018. *Temperature* [Online]. [Accessed Accessed 3rd March 2018].

MOORE, P. D., WEBB, J. A. & COLLISON, M. E. 1991. *Pollen analysis*, Blackwell scientific publications.

MORRIS, P. J., SWINDLES, G. T., VALDES, P. J., IVANOVIC, R. F., GREGOIRE, L. J., SMITH, M. W., TARASOV, L., HAYWOOD, A. M. & BACON, K. L. 2018. Global peatland initiation driven by regionally asynchronous warming. *Proceedings of the National Academy of Sciences*, 115, 4851-4856.

NEVALAINEN, L. & LUOTO, T. P. 2017. Relationship between cladoceran (Crustacea) functional diversity and lake trophic gradients. *Functional ecology*, 31, 488-498.

NOONE, D. & SIMMONDS, I. 2002. Associations between δ 18O of water and climate parameters in a simulation of atmospheric circulation for 1979–95. *Journal of Climate*, 15, 3150-3169.

NORTH GREENLAND ICE CORE PROJECT MEMBERS 2004. High resolution record of Northern Hemisphere climate extending into the last interglacial period. *Nature*, 431, 147-151.

O'DONNELL, D. R., HAMMAN, C. R., JOHNSON, E. C., KLAUSMEIER, C. A. & LITCHMAN, E. 2017. Temperature selection drives evolution of function-valued traits in a marine diatom. *bioRxiv*, 167817.

OKSANEN, J., BLANCHET, F. G., KINDT, R., LEGENDRE, P., MINCHIN, P. R., O'HARA, R., SIMPSON, G. L., SOLYMOS, P., STEVENS, M. H. H. & WAGNER, H. 2015. Package 'vegan'. *Community ecology package, version*, 2.

PALMER, M. A., HAKENKAMP, C. C. & NELSON-BAKER, K. 1997. Ecological heterogeneity in streams: why variance matters. *Journal of the North American Benthological Society*, 16, 189-202.

PATTON, H., HUBBARD, A., ANDREASSEN, K., AURIAC, A., WHITEHOUSE, P. L., STROEVEN, A. P., SHACKLETON, C., WINSBORROW, M., HEYMAN, J. & HALL, A. M. 2017. Deglaciation of the Eurasian ice sheet complex. *Quaternary Science Reviews*, 169, 148-172.

PINDER, L. C. V. 1995. The habitats of chironomid larvae. *In:* ARMITAGE, P. D., CRANSTON, P. S. & PINDER, L. C. V. (eds.) *The Chironomidae: Biology and ecology of non-biting midges*. Dordrecht: Springer Netherlands.

PLUNKETT, G. 2006. Tephra-linked peat humification records from Irish ombrotrophic bogs question nature of solar forcing at 850 cal. yr BC. *Journal of Quaternary Science: Published for the Quaternary Research Association*, 21, 9-16.

POTITO, A. P., WOODWARD, C. A., MCKEOWN, M. & BEILMAN, D. W. 2014. Modern influences on chironomid distribution in western Ireland: potential for palaeoenvironmental reconstruction. *Journal of paleolimnology*, 52, 385-404.

R CORE TEAM. 2018. R: A language and environment for statistical computing. R Foundation for Statistical Computing.

RENSSEN, H., GOOSSE, H. & MUSCHELER, R. 2006. Coupled climate model simulation of Holocene cooling events: oceanic feedback amplifies solar forcing. *Climate of the Past*, 2, 79-90.

RENSSEN, H., SEPPÄ, H., CROSTA, X., GOOSSE, H. & ROCHE, D. 2012. Global characterization of the Holocene thermal maximum. *Quaternary Science Reviews*, 48, 7-19.

RIERADEVALL, M. & BROOKS, S. J. 2001. An identification guide to subfossil Tanypodinae larvae (Insecta: Diptera: Chrironomidae) based on cephalic setation. *Journal of paleolimnology*, 25, 81-99.

ROLAND, T., DALEY, T., CASELDINE, C., CHARMAN, D., TURNEY, C., AMESBURY, M., THOMPSON, G. & WOODLEY, E. 2015. The 5.2 ka climate event: Evidence from stable isotope and multi-proxy palaeoecological peatland records in Ireland. *Quaternary Science Reviews*, 124, 209-223.

ROLAND, T. P., CASELDINE, C., CHARMAN, D., TURNEY, C. & AMESBURY, M. 2014. Was there a '4.2 ka event'in Great Britain and Ireland? Evidence from the peatland record. *Quaternary Science Reviews*, 83, 11-27.

SCHETTLER, G., ROMER, R. L., O'CONNELL, M. & MOLLOY, K. 2006. Holocene climatic variations and postglacial sea-level rise geochemically recorded in the sediments of the brackish karst lake An Loch Mor, western Ireland. *Boreas*, 35, 674-693.

SCHMERA, D., HEINO, J., PODANI, J., ERŐS, T. & DOLÉDEC, S. 2017. Functional diversity: a review of methodology and current knowledge in freshwater macroinvertebrate research. *Hydrobiologia*, 787, 27-44.

SHENNAN, I., BRADLEY, S. L. & EDWARDS, R. 2018. Relative sea-level changes and crustal movements in Britain and Ireland since the Last Glacial Maximum. *Quaternary Science Reviews*, 188, 143-159.

SINGARAYER, J. S., VALDES, P. J., FRIEDLINGSTEIN, P., NELSON, S. & BEERLING, D. J. 2011. Late Holocene methane rise caused by orbitally controlled increase in tropical sources. *Nature*, 470, 82.

STARKEL, L. 1991. Long-distance correlation of fluvial events in the temperate zone. *Tem-perate Palaeohydrology*, 473-495.

STEINHILBER, F., BEER, J. & FRÖHLICH, C. 2009. Total solar irradiance during the Holocene. *Geophysical Research Letters*, 36.

STENGER-KOVÁCS, C., KÖRMENDI, K., LENGYEL, E., ABONYI, A., HAJNAL, É., SZABÓ, B., BUCZKÓ, K. & PADISÁK, J. 2018. Expanding the trait-based concept of benthic diatoms: Development of trait-and species-based indices for conductivity as the master variable of ecological status in continental saline lakes. *Ecological Indicators*, 95, 63-74.

STUIVER, M., GROOTES, P. M. & BRAZIUNAS, T. F. 1995. The GISP2 δ18O climate record of the past 16,500 years and the role of the sun, ocean, and volcanoes. *Quaternary research*, 44**,** 341-354.

SWEENEY, J., SALTER-TOWNSHEND, M., EDWARDS, T., BUCK, C. E. & PARNELL, A. C. 2018. Statistical challenges in estimating past climate changes. *Wiley Interdisciplinary Reviews: Computational Statistics*, 10**,** e1437.

SWINDLES, G., BLUNDELL, A., ROE, H. & HALL, V. 2010. A 4500-year proxy climate record from peatlands in the North of Ireland: the identification of widespread summer 'drought phases'? *Quaternary Science Reviews*, 29**,** 1577-1589.

SWINDLES, G. T., LAWSON, I. T., MATTHEWS, I. P., BLAAUW, M., DALEY, T. J., CHARMAN, D. J., ROLAND, T. P., PLUNKETT, G., SCHETTLER, G. & GEAREY, B. R. 2013. Centennial-scale climate change in Ireland during the Holocene. *Earth-Science Reviews*, 126**,** 300-320.

SWINDLES, G. T., MORRIS, P. J., WHITNEY, B., GALLOWAY, J. M., GAŁKA, M., GALLEGO-SALA, A., MACUMBER, A. L., MULLAN, D., SMITH, M. W. & AMESBURY, M. J. 2018. Ecosystem state shifts during long-term development of an Amazonian peatland. *Global change biology*, 24**,** 738-757.

SWINDLES, G. T., PLUNKETT, G. & ROE, H. M. 2007. A delayed climatic response to solar forcing at 2800 cal. BP: multiproxy evidence from three Irish peatlands. *The Holocene*, 17**,** 177-182.

TAYLOR, K. J., MCGINLEY, S., POTITO, A. P., MOLLOY, K. & BEILMAN, D. W. 2018. A mid to late Holocene chironomid-inferred temperature record from northwest Ireland. *Palaeogeography*, *Palaeoclimatology*, *Palaeoecology*, 505**,** 274-286.

TAYLOR, K. J., STOLZE, S., BEILMAN, D. W. & POTITO, A. P. 2017. Response of chironomids to Neolithic land-use change in north-west Ireland. *The Holocene*, 27**,** 879-889.

TER BRAAK, C. J. & SMILAUER, P. 2002. CANOCO reference manual and CanoDraw for Windows user's guide: software for canonical community ordination (version 4.5). www. canoco. com.

TREBLE, P., BUDD, W., HOPE, P. & RUSTOMJI, P. 2005. Synoptic-scale climate patterns associated with rainfall δ18O in southern Australia. *Journal of Hydrology*, 302, 270-282.

TURNER, T. E., SWINDLES, G. T., CHARMAN, D. J., LANGDON, P. G., MORRIS, P. J., BOOTH, R. K., PARRY, L. E. & NICHOLS, J. E. 2016. Solar cycles or random processes? Evaluating solar variability in Holocene climate records. *Scientific reports*, 6, 23961.

VALDES, P. J., ARMSTRONG, E., BADGER, M. P., BRADSHAW, C. D., BRAGG, F., DAVIES-BARNARD, T., DAY, J. J., FARNSWORTH, A., HOPCROFT, P. O. & KENNEDY, A. T. 2017. The BRIDGE HadCM3 family of climate models: HadCM3@ Bristol v1. 0. *Geoscientific Model Development*, 10, 3715-3743.

VAN ASCH, N., LUTZ, A. F., DUIJKERS, M. C., HEIRI, O., BROOKS, S. J. & HOEK, W. Z. 2012. Rapid climate change during the Weichselian Lateglacial in Ireland: Chironomid-inferred summer temperatures from Fiddaun, Co. Galway. *Palaeogeography, Palaeoclimatology, Palaeoecology*, 315, 1-11.

VAN BELLEN, S., MAUQUOY, D., PAYNE, R. J., ROLAND, T. P., HUGHES, P. D., DALEY, T. J., LOADER, N. J., STREET-PERROTT, F. A., RICE, E. M. & PANCOTTO, V. A. 2017. An alternative approach to transfer functions? Testing the performance of a functional trait-based model for testate amoebae. *Palaeogeography, palaeoclimatology, palaeoecology*, 468, 173-183.

VELLE, G., BRODERSEN, K., BIRKS, H. & WILLASSEN, E. 2010. Midges as quantitative temperature indicator species: Lessons for palaeoecology. *The Holocene*, 20, 989-1002.

VODOPICH, D. S. & COWELL, B. C. 1984. Interaction of factors governing the distribution of a predatory aquatic insect. *Ecology*, 65, 39-52.

WALKER, I. R. 2001. Midges: Chironomidae and related diptera. *Tracking environmental change using lake sediments*. Springer.

WANNER, H., SOLOMINA, O., GROSJEAN, M., RITZ, S. P. & JETEL, M. 2011. Structure and origin of Holocene cold events. *Quaternary Science Reviews*, 30, 3109-3123.

WATSON, J. E., BROOKS, S. J., WHITEHOUSE, N. J., REIMER, P. J., BIRKS, H. J. B. & TURNEY, C. 2010. Chironomid-inferred late-glacial summer air temperatures from Lough Nadourcan, Co. Donegal, Ireland. *Journal of Quaternary Science*, 25, 1200-1210.

WIEDERHOLM, T. 1983. Chironomidae of Holarctic region: keys and diagnoses. Part 1. *Larvae Entomol Scand Suppl*, 19, 1-457.

WRIGHT JR, H. E. 1980. Cores of soft lake sediments. *Boreas*, 9, 107-114.

Fig 1. Maps showing A. location of the study area in Ireland. B. location of Lough Nakeeroge in Achill island, Co. Mayo, including elevation (contour lines of 10 m intervals), and an arrow showing the direction and orientation photograph. C. A photograph of Lough Nakeeroge on the day of coring. The white star indicates the coring location.

Fig 2. Age-depth model obtained with use of Bacon software: (i) modeled age versus depth plot, gray shaded area represents 95.4 % probability range (ii) MCMC diagnostic plot, no observed trend indicates stable solution (iii) and (iv) prior (line) and posterior (gray shape) distributions of accumulation rate (iii) and memory R (iv), confirming the reasonable choice of the parameters.

Fig 3. Chironomid stratigraphy for Lough Nakeeroge including Shannon-Wiener Diversity for each sample, chironomid head-capsule concentrations, NMDS Axis 1 and Axis 2 scores from the chironomid data, and summer air temperatures inferred using Potito et al. (2014) transfer function with LOESS smoother (span = 0.2). Chironomid accumulation zones are named CAZ.

Fig 4. NMDS bi-plot (i) of samples (ii) of common taxa. Chironomid abbreviations in (ii) are as follows: ABLA *Ablabesmyi*a, CHIRO *Chironomus anthracinus*-type, CLADO *Cladopelma*, CORY *Corynoneura edwardsi*-type, CRICI *Cricotopus intersectus*-type, CRYP *Cryptochironomus*, DICR *Dircotendipes nervosus*-type, EUK *Eukiefferiella*, HETE *Heterotanytarsus*, HETM *Heterotrissocladius marcidus*-type, LAUT Lauterborniella, LIM *Limnophyes/Paralimnophyes*

MACR *Macropelopia*, MICJ *Micropsectra junci-type*, MICI *Micropsectra insign-type*, MICR *Microtendipes pedellus*-type, PAG *Pagastiella*, PARK *Parakiefferiella bathophila*-type, PARM *Paramerina*, PHAE *Phaenopsectra flavipes*-type, POLN *Polypedilum nubifer*-type, POLS *Polypedilum sordens*-type, PRO *Procladius*, PROT *Protanypus*, PSEC *Psectrocladius septentrionalis*-type, PSECS *Psectrocladius sordidellus/psiloperus*-type, PSEUC *Pseudochironomus*, STEM *Stempellina*, TCHI *Tanytarsus chinyensis*-type, TGLA *Tanytarsus glabrescens*-type, THIE *Thienemannimyia*-type, TLUG *Tanytarsus lugens*-type, TMEN *Tanytarsus mendax*-type, TPAL *Tanytarsus palidicornis*-type, TUND *Tanytarsus* undefined.

Fig 5. Conical Correspondence analysis (CCA) passively positioned the fossil samples from Lough Nakeeroge (black dots) with assemblages present in the modern Western Ireland training set (white dots) (Potito et al. 2014) solely constrained to July air temperature. All fossil samples had a squared residual distance value greater than the 10th percentile of values in the modern training set and are considered to have a good fit-to-temperature.

Fig 6. Pollen stratigraphy for Lough Nakeeroge including LOI_{550} and summer air temperatures inferred using Potito et al. (2014) transfer function with LOESS smoother (span =0.2), and total pollen concentration per sample. The black dots and lines indicate the depths where pollen was extracted for analysis.

Fig 7. Lake water column illustrating high and low lake levels. The chironomid community showing all four life stages, i) egg mass, ii) larvae, iii) pupae, iv) adult. Submerged and emerged vegetation and algae are included in the image as they are a food source for the larvae collector-gatherers, scrapers, and shredders, and collector-filterers. Allogenic inputs are also represented as they can alter the chironomid community in the lake. Finally, the midge assemblage is directly and indirectly influenced by temperature, radiation, precipitation, seasonality, and evaporation. This figure has been modified from Porinchu and MacDonald (2003).

Fig 8. Composite diagram including simulated climate from a coupled atmosphere-ocean-vegetation general circulation model, the Hadley Centre Coupled Model, version 3 (HadCM3) at intervals of 500 years from 12,500 to 0 yr BP. Including total annual potential evaporation (mm), total annual precipitation (mm), total July precipitation (mm), July air temperature at 2 m above the ground surface (ºC), annual air temperature at 2 m above the ground surface (ºC); total solar irradiance (Steinhibler et al. 2009), a North Atlantic IRD record (Bond et al. 2001), the $\delta^{18}O$ record from the Greenland NGRIP ice core (NGRIP members, 2004); peatland water table reconstructions combined and detrended from eight sites across Ireland (Swindles et al. 2013), and $\delta^{18}O$ records from a speleothem in Crag Cave; chironomid-inferred temperature model and collector-filterer guild (representing chironomid functional traits) for Lough Nakeeroge. Grey bands indicate potential phases of climate correspondence between the records.

Sup Fig 1 (i) to (ii). The master core was corrected by aligning the LOI_{550} and LOI_{950} information from both cores A and B, along with the duplication in chironomid community structure (Sup Fig 2). Organic carbon (LOI_{550}) and inorganic carbon (LOI_{950}) for core A and core B sediment sequences for Lough Nakeeroge (i) LOI_{550} and LOI_{950} for core A and core B before realignment, and (ii) LOI_{550} and LOI_{950} for core A and core B after realignment. To realign the cores, core B was shifted down 42 cm, transferred from a depth of (i) 359-100 cm to (ii) 401-142 cm, while the bottom segment of core A was shifted down 13 cm, from (i) 352-280 cm to (ii) 365-293.

Sup Fig 1 (iii) to (iv). The portions of core A (dark grey) and core B (light grey) that were used to construct the mastercore (iii) before realignment, and (iv) after realignment. Black dots indicate the levels, and the cores, where samples were sub-sectioned for ^{14}C analysis. The areas marked with a star symbol in the (iii) core A and B are the areas where chironomid duplication was observed and (iv) shows where the core realignment corrects the duplication (see Sup. Fig 2). The realigned master core from (iv) begins at 50 cm below the sediment surface, avoiding the uppermost unconsolidated material, and reaches a depth of 401 cm (Sup Fig. 1). The master core is composed of sediment from core A taken at depths of 365-293 cm, 240-150 cm and 143-50 cm. Gaps in core A exists at 292-241 cm and 149-144 cm. Sediment from core B was taken at depths of 401-369 cm and 320-244 cm in the master core.

Sup Fig 1 (v) to (vi). Age-depth models obtained with use of Bacon software for (v) before core realignment, and (vi) after core realignment. A sixth AMS radiocarbon date was obtained for the top section of core B (120 cm); however, this date was omitted from both age-depth models as it was decided to use the continuous section of core A from 240 – 50 cm rather than shirting back and forth between cores A and B. The ^{14}C dating model of the realigned mastercore presents an almost linear accumulation rate in the age-depth model, and the chironomid community becomes synchronous (Sup Fig 2).

Sup Fig 2. The chironomid stratigraphy showing the sections of the mastercore that are composed of core A (black filled) and core B (white with black outline). The chironomid taxa where the duplication was corrected by core re-alignment are shown between 7560 and 8300 cal. yr BP (292 – 321 cm). The taxa that show a good overlap between both cores are *Lauterborniella* (the only instances of this taxa in both cores), *Psectrocladius septentrionalis*-type, *Tanytarsus chinyensis*-type and *Heterotrissocladius marcidus*-type. Core A, core B, and the master core from Sup Fig 1 (iv) is reproduced alongside the stratigraphy so the taxa overlap and core alignment care be observed together.

Sup Fig 3 (i) to (iii). Running correlations between the proxy climate records from 2000 to 9500 cal. yr BP (time windows = 500 years). The statistical significance was calculated using a Monte Carlo simulation to determine the null hypothesis (bottom graph); coarsely dashed lines indicate significance at 95 %. Proxy records are Lough Nakeeroge chironomid-inferred temperature reconstruction (C-IT), Lough Nakeeroge chironomid collector-filterer guild (FT) (percentage compared to all other guilds), and Crag Cave $\delta^{18}0$ record.

Sup Fig 4 (i) to (iii). Running correlations between the standardized water table reconstruction for Ireland (STD WTD units) and the proxy climate records from 2000 to 6000 cal. yr BP (time windows = 500 years). The statistical significance was calculated using a Monte Carlo simulation to determine the null hypothesis (bottom graph); coarsely dashed lines indicate significance at 95 %.

Sup Fig 5 (i) to (iv). Running correlations between simulated annual surface air temperature and climate proxy records from 2000 to 9500 cal. yr BP and for STD WTD units from 2000 to 6000 cal. yr BP (time windows = 500 years). The statistical significance was calculated using a Monte Carlo simulation to determine the null hypothesis (bottom graph); coarsely dashed lines indicate significance at 95 %.

Sup Fig 6 (i) to (iv). Running correlations between simulated total annual precipitation and climate proxy records from 2000 to 9500 cal. yr BP and for STD WTD units from 2000 to 6000 cal. yr BP (time windows = 500 years). The statistical significance was calculated using a Monte Carlo simulation to determine the null hypothesis (bottom graph); coarsely dashed lines indicate significance at 95 %.

Sup Fig 7 (i) to (iv). Running correlations between simulated total annual potential evaporation and climate proxy records from 2000 to 9500 cal. yr BP and for STD WTD units from 2000 to 6000 cal. yr BP (time windows = 500 years). The statistical significance was calculated using a Monte Carlo simulation to determine the null hypothesis (bottom graph); coarsely dashed lines indicate significance at 95 %.

Sup Fig 8 (i) to (iv). Running correlations between simulated July surface air temperature and climate proxy records from 2000 to 9500 cal. yr BP and for STD WTD units from 2000 to 6000 cal. yr BP (time windows = 500 years). The statistical significance was calculated using a Monte Carlo simulation to determine the null hypothesis (bottom graph); coarsely dashed lines indicate significance at 95 %.

Sup Fig 9 (i) to (iv). Running correlations between simulated July total precipitation and climate proxy records from 2000 to 9500 cal. yr BP and for STD WTD units from 2000 to 6000 cal. yr BP (time windows = 500 years). The statistical significance was calculated using a Monte Carlo simulation to determine the null hypothesis (bottom graph); coarsely dashed lines indicate significance at 95 %.

Sup Fig 10 (i) to (iv). Running correlations between the NGRIP $\delta^{18}0$ record (members, 2004) and proxy climate records from 2000 to 9500 cal. yr BP and for STD WTD units from 2000 to 6000 cal. yr BP (time windows = 500 years). The statistical significance was calculated using a Monte Carlo simulation to determine the null hypothesis (bottom graph); coarsely dashed lines indicate significance at 95 %.

Sup Fig 11 (i) to (iv). Running correlations between the Total Solar Irradiance (W/m^2) (TSI) record (Steinhilber et al., 2009) and proxy climate records from 2000 to 9500 cal. yr BP and for STD WTD units from 2000 to 6000 cal. yr BP (time windows = 500 years). The statistical significance was calculated using a Monte Carlo simulation to determine the null hypothesis (bottom graph); coarsely dashed lines indicate significance at 95 %.

Sup Fig 12 (i) to (iv). Running correlations between the Ice Rafted Debris (IRD) record from the North Atlantic (Bond et al., 2001). and proxy climate records from 2000 to 9500 cal. yr BP and for STD WTD units from 2000 to 6000 cal. yr BP (time windows = 500 years). The statistical significance was calculated using a Monte Carlo simulation to determine the null hypothesis (bottom graph); coarsely dashed lines indicate significance at 95 %.

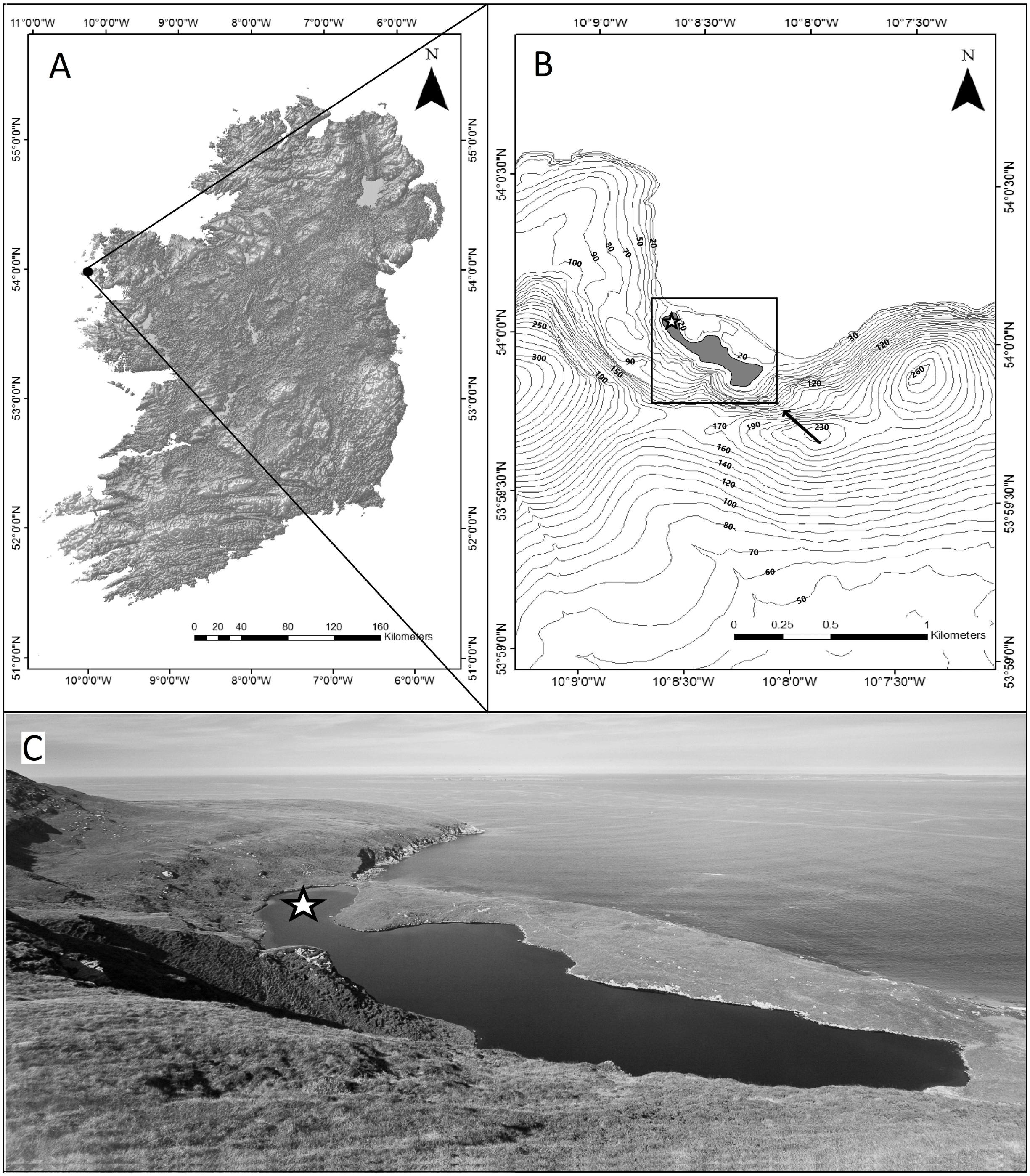
A
B
C
N
11°0'0"W
10°0'0"W
9°0'0"W
8°0'0"W
7°0'0"W
6°0'0"W
55°0'0"N
54°0'0"N
53°0'0"N
52°0'0"N
51°0'0"N
0 20 40 80 120 160
Kilometers
10°9'0"W
10°8'30"W
10°8'0"W
10°7'30"W
54°0'30"N
54°0'0"N
53°59'30"N
53°59'0"N
0 0.25 0.5 1
Kilometers

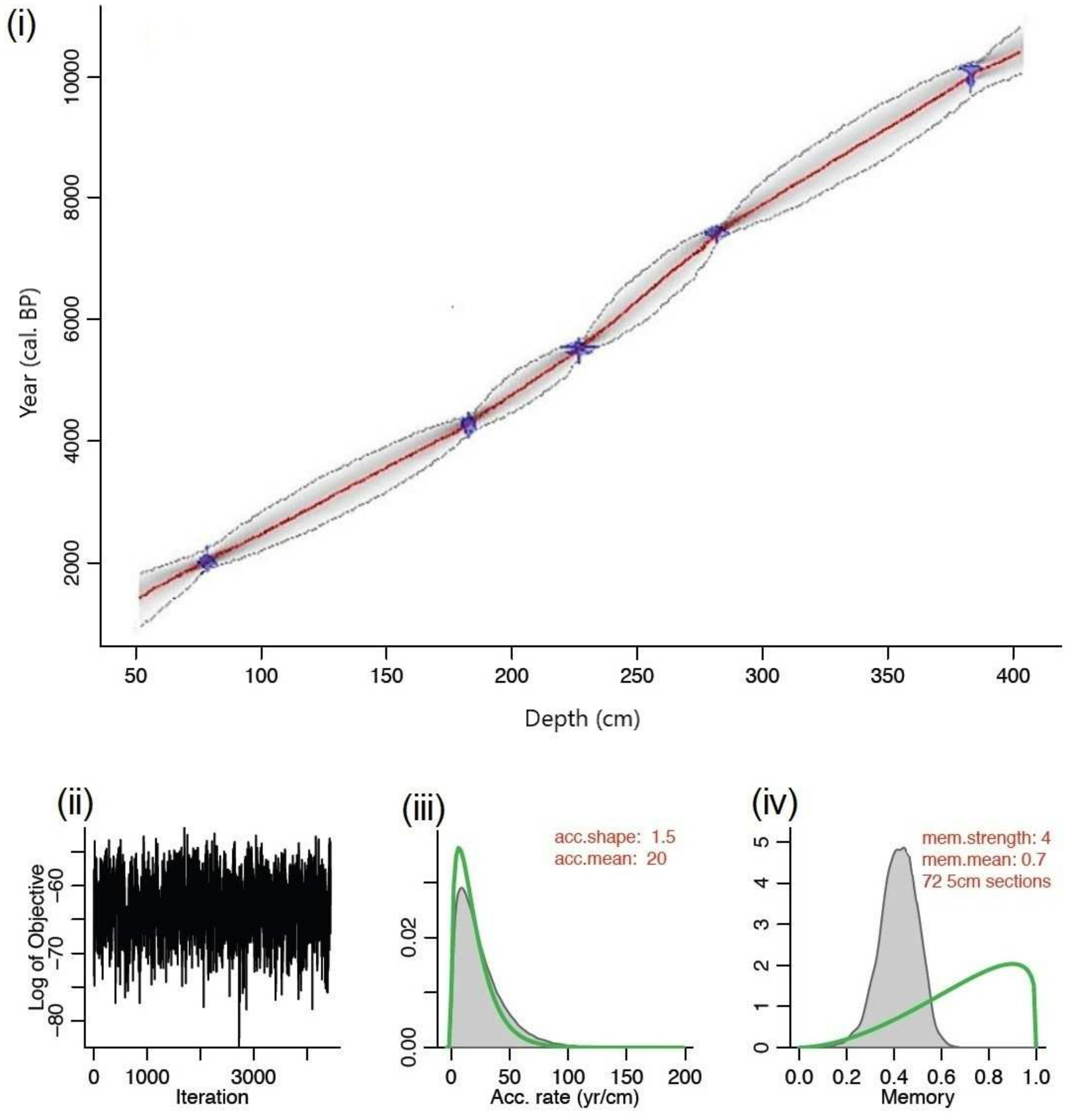
(i)
Year (cal. BP)
2000
4000
6000
8000
10000
50
100
150
200
250
300
350
400
Depth (cm)
(ii)
Log of Objective
−80
−70
−60
0
1000
3000
Iteration
(iii)
acc.shape: 1.5
acc.mean: 20
0.00
0.02
0
50
100
150
200
Acc. rate (yr/cm)
(iv)
mem.strength: 4
mem.mean: 0.7
72 5cm sections
0
1
2
3
4
5
0.0
0.2
0.4
0.6
0.8
1.0
Memory

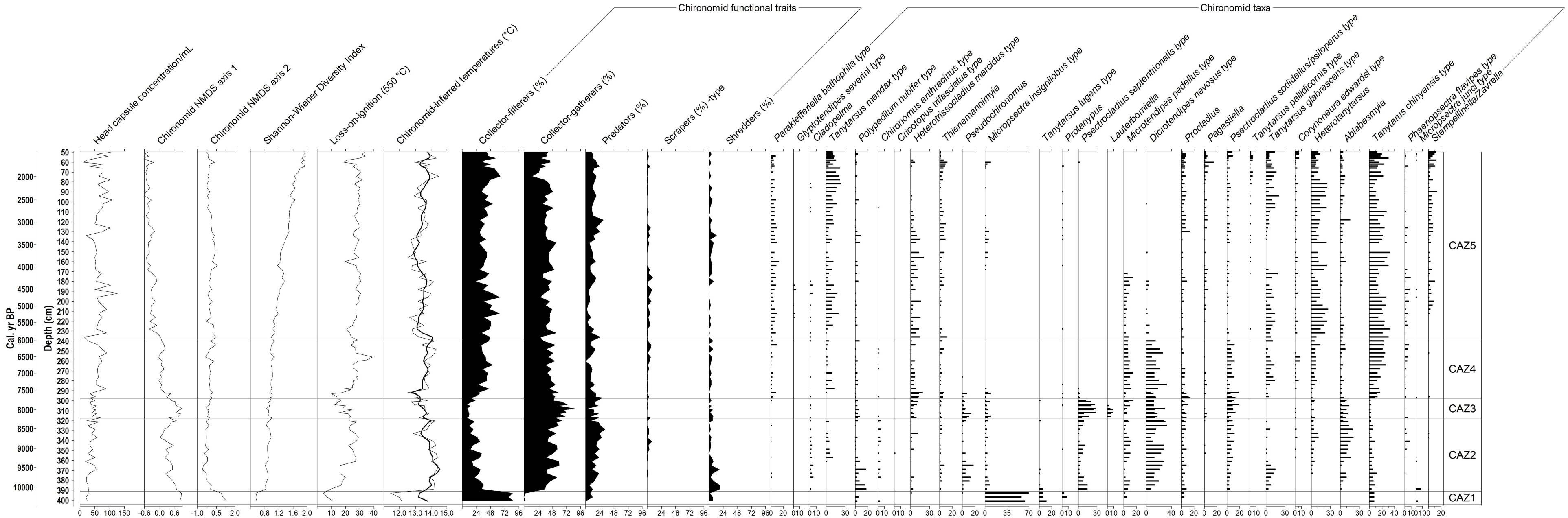
Chironomid functional traits
Chironomid taxa
Head capsule concentration/mL
Chironomid NMDS axis 1
Chironomid NMDS axis 2
Shannon-Wiener Diversity Index
Loss-on-ignition (550 °C)
Chironomid-inferred temperatures (°C)
Collector-filterers (%)
Collector-gatherers (%)
Predators (%)
Scrapers (%) -type
Shredders (%)
Parakiefferiella bathophila type
Glyptotendipes severini type
Cladopelma
Tanytarsus mendax type
Polypedilum nubifer type
Chironomus anthracinus type
Cricotopus trifasciatus type
Heterotrissocladius marcidus type
Thienemannimyia
Pseudochironomus
Micropsectra insignilobus type
Tanytarsus lugens type
Protanypus
Psectrocladius septentrionalis type
Lauterborniella
Microtendipes pedellus type
Dicrotendipes nervosus type
Procladius
Pagastiella
Psectrocladius sordidellus/psilopterus type
Tanytarsus pallidicornis type
Tanytarsus glabrescens type
Corynoneura edwardsi type
Heterotanytarsus
Ablabesmyia
Tanytarsus chinyensis type
Phaenopsectra flavipes type
Micropsectra junci type
Stempellinella/Zavrelia
Cal. yr BP
Depth (cm)
CAZ5
CAZ4
CAZ3
CAZ2
CAZ1

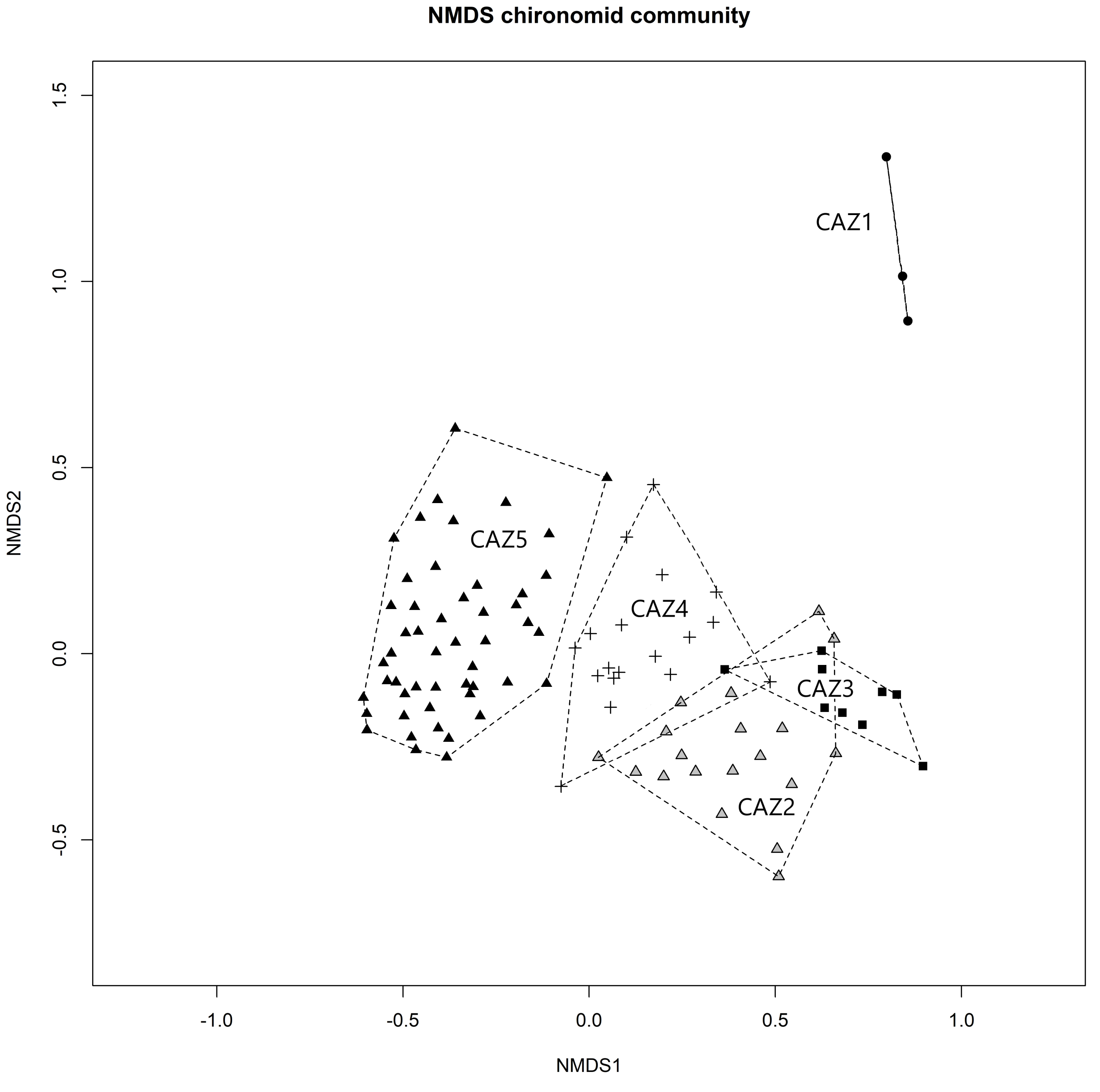

NMDS chironomid community
CAZ1
CAZ2
CAZ3
CAZ4
CAZ5
NMDS1
NMDS2
-1.0
-0.5
0.0
0.5
1.0
1.5

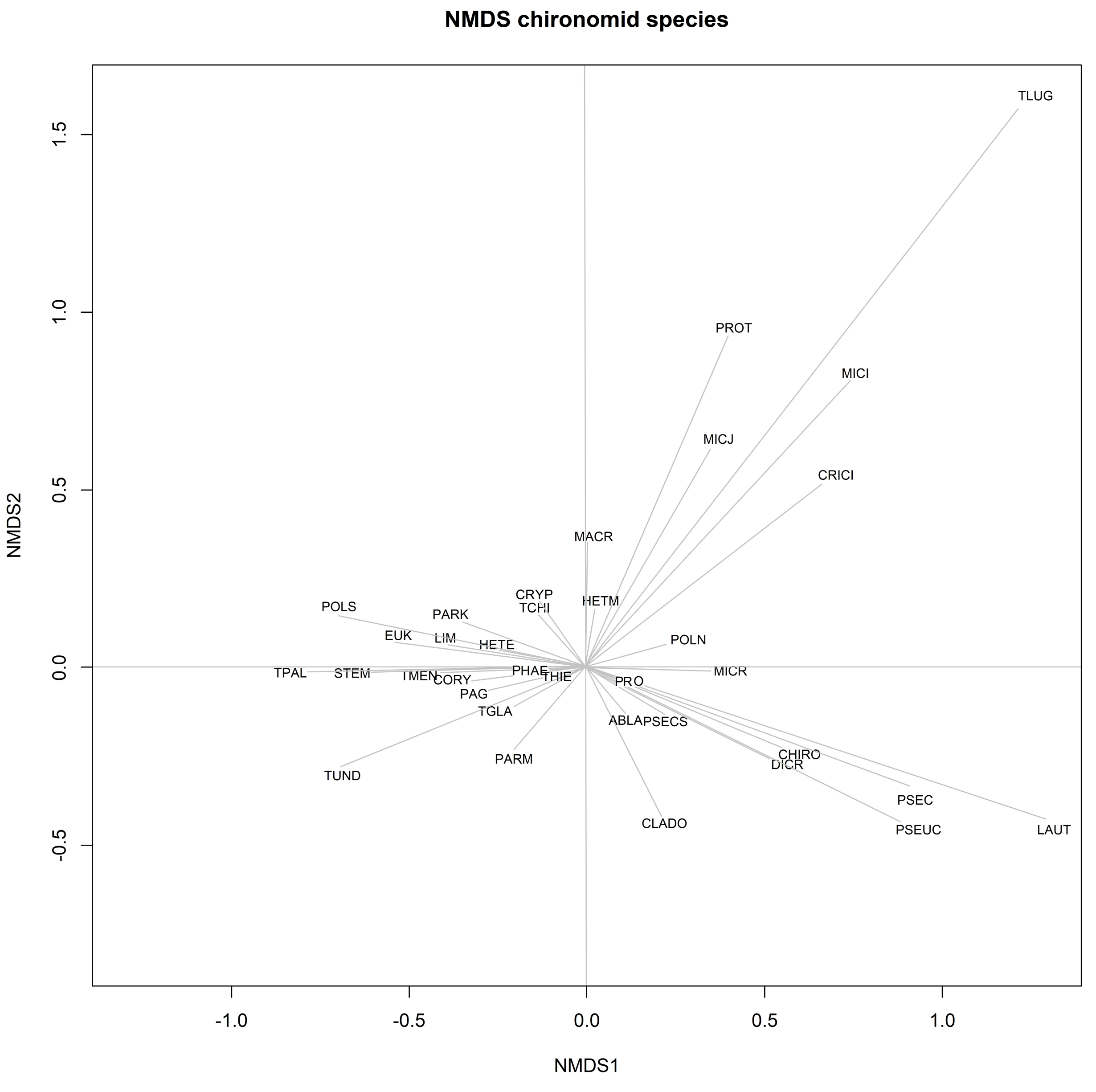
NMDS chironomid species
NMDS2
NMDS1
1.5
1.0
0.5
0.0
-0.5
-1.0
-0.5
0.0
0.5
1.0
TLUG
PROT
MICI
MICJ
CRICI
MACR
CRYP
TCHI
HETM
POLS
PARK
EUK
LIM
HETE
POLN
TPAL
STEM
TMEN
CORY
PHAE
THIE
MICR
PRO
PAG
TGLA
ABLA
PSECS
PARM
TUND
CHIRO
DICR
PSEC
CLADO
PSEUC
LAUT

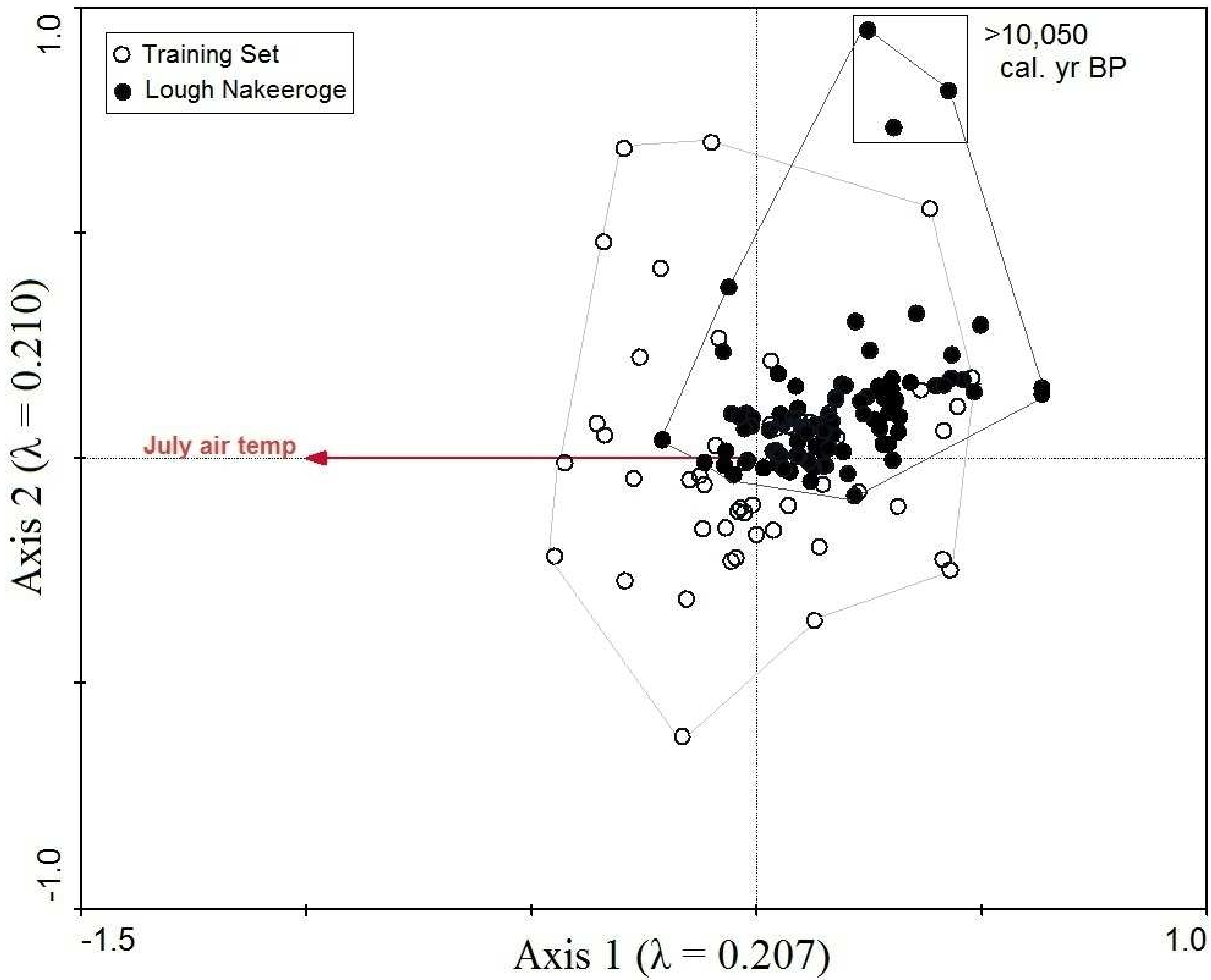

1.0
-1.0
-1.5
1.0
Axis 1 (λ = 0.207)
Axis 2 (λ = 0.210)
Training Set
Lough Nakeeroge
>10,050
cal. yr BP
July air temp

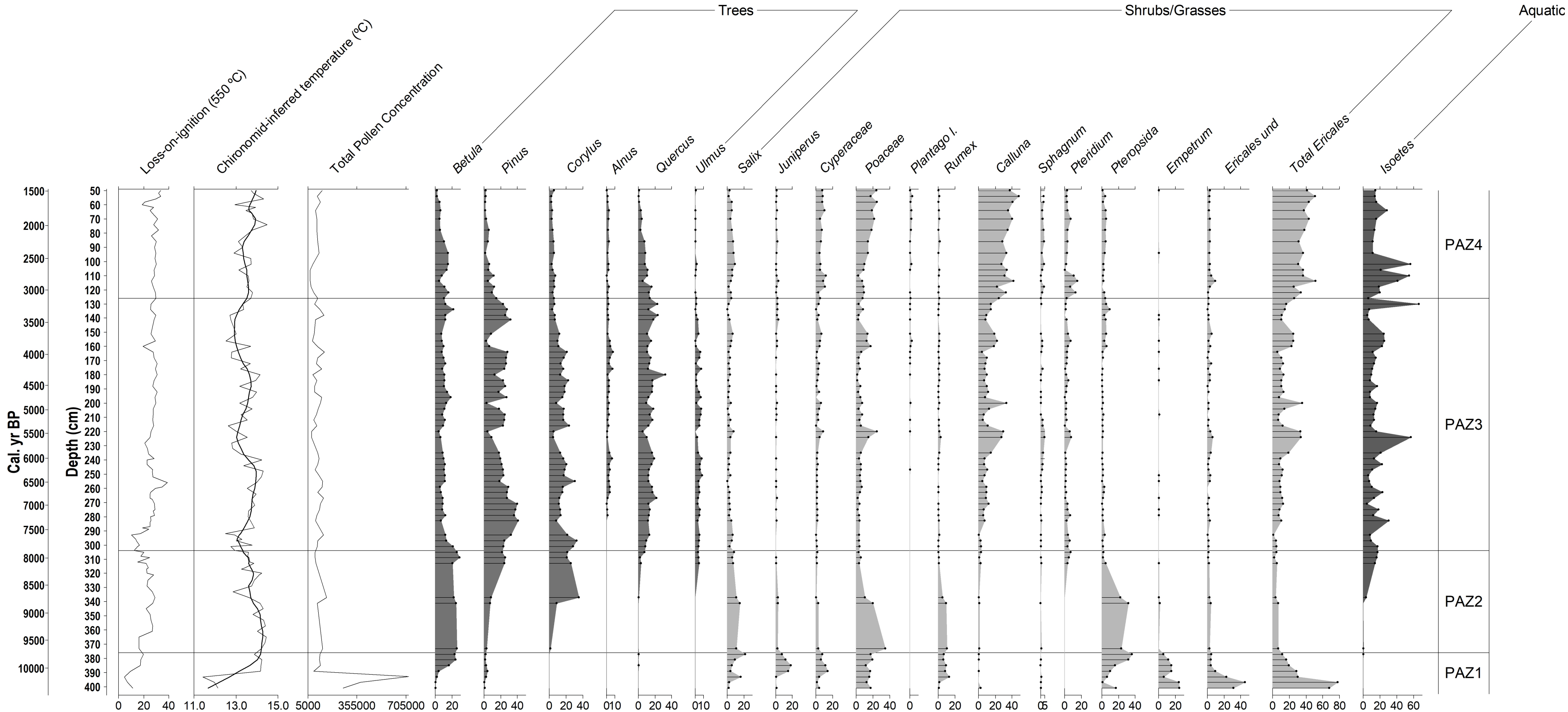

Trees
Shrubs/Grasses
Aquatic
Loss-on-ignition (550 ºC)
Chironomid-inferred temperature (ºC)
Total Pollen Concentration
Betula
Pinus
Corylus
Alnus
Quercus
Ulmus
Salix
Juniperus
Cyperaceae
Poaceae
Plantago l.
Rumex
Calluna
Sphagnum
Pteridium
Pteropsida
Empetrum
Ericales und
Total Ericales
Isoetes
Cal. yr BP
Depth (cm)
PAZ4
PAZ3
PAZ2
PAZ1

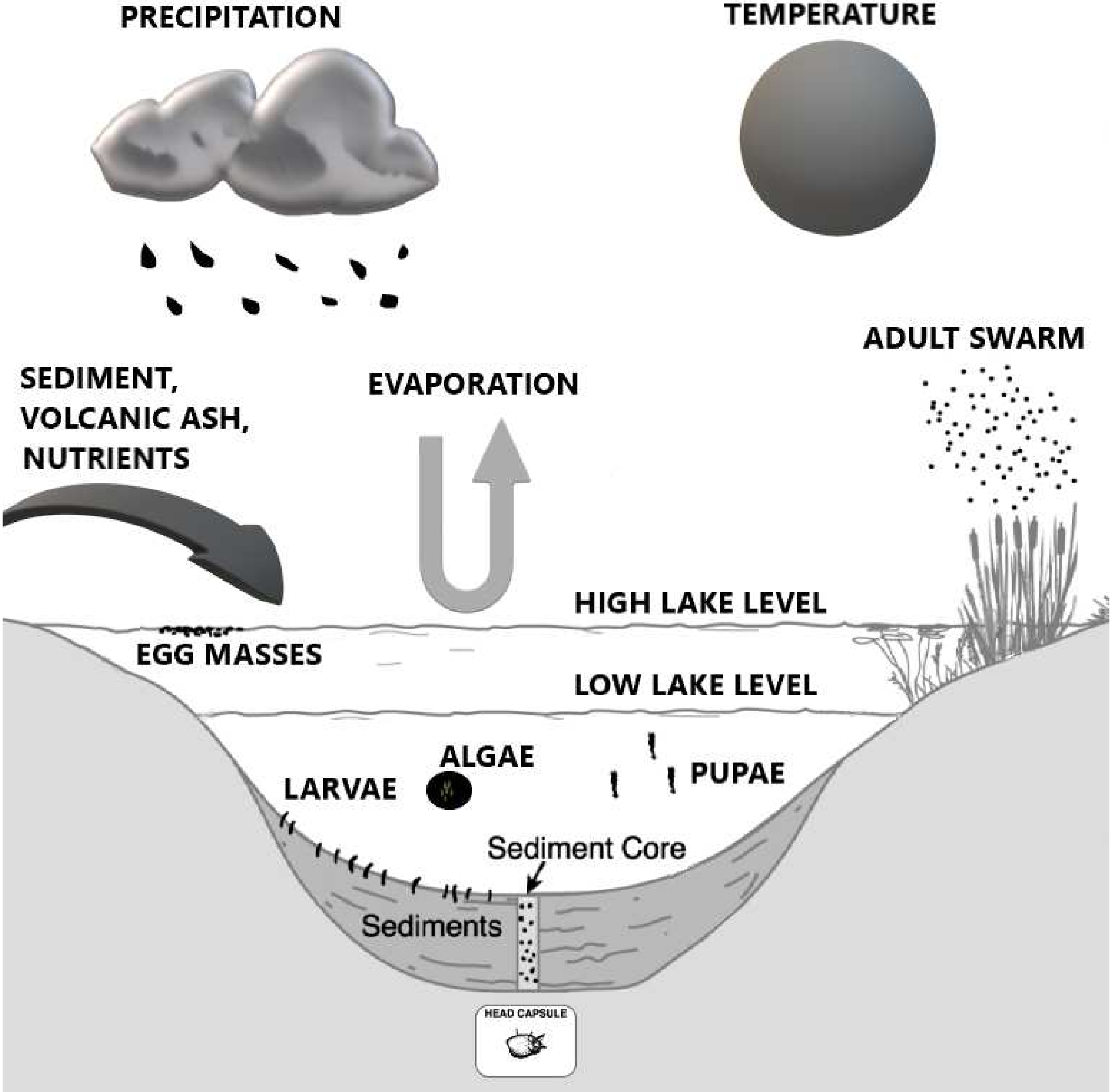
PRECIPITATION
TEMPERATURE
ADULT SWARM
SEDIMENT,
VOLCANIC ASH,
NUTRIENTS
EVAPORATION
HIGH LAKE LEVEL
EGG MASSES
LOW LAKE LEVEL
ALGAE
PUPAE
LARVAE
Sediment Core
Sediments
HEAD CAPSULE

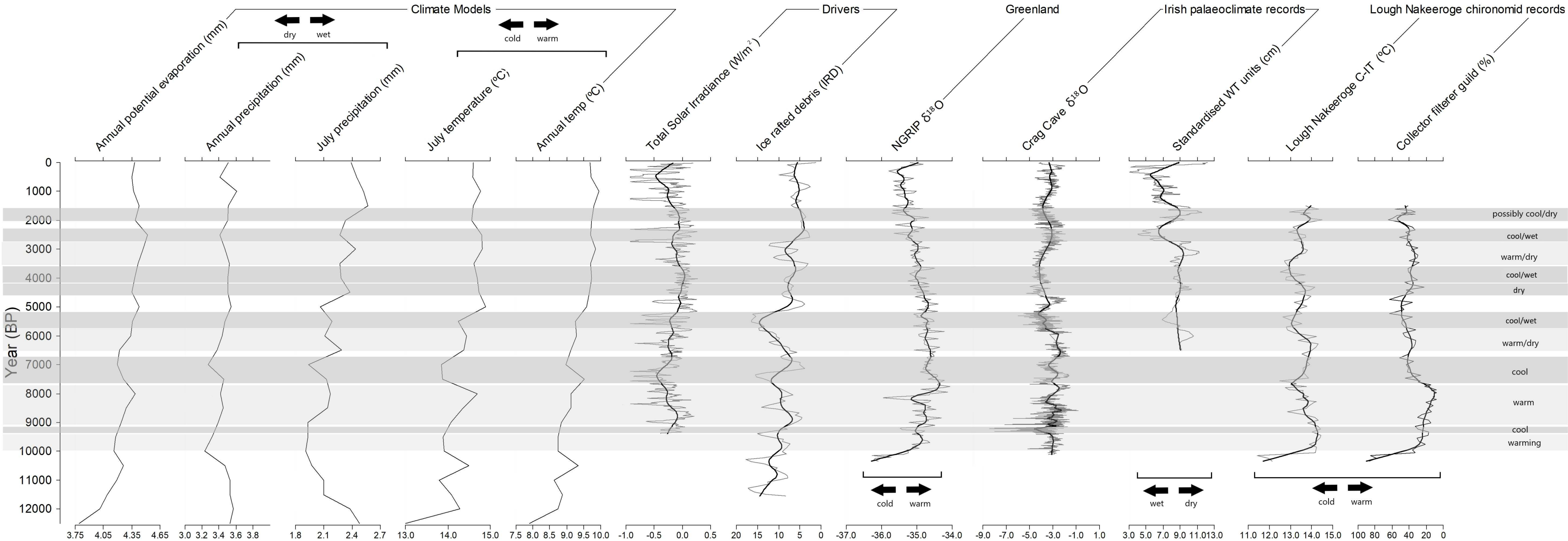

Climate Models
Drivers
Greenland
Irish palaeoclimate records
Lough Nakeeroge chironomid records
dry
wet
cold
warm
Annual potential evaporation (mm)
Annual precipitation (mm)
July precipitation (mm)
July temperature (ºC)
Annual temp (ºC)
Total Solar Irradiance (W/m²)
Ice rafted debris (IRD)
NGRIP δ¹⁸O
Crag Cave δ¹⁸O
Standardised WT units (cm)
Lough Nakeeroge C-IT (ºC)
Collector filterer guild (%)
Year (BP)
possibly cool/dry
cool/wet
warm/dry
cool/wet
dry
cool/wet
warm/dry
cool
warm
cool
warming
cold
warm
wet
dry
cold
warm

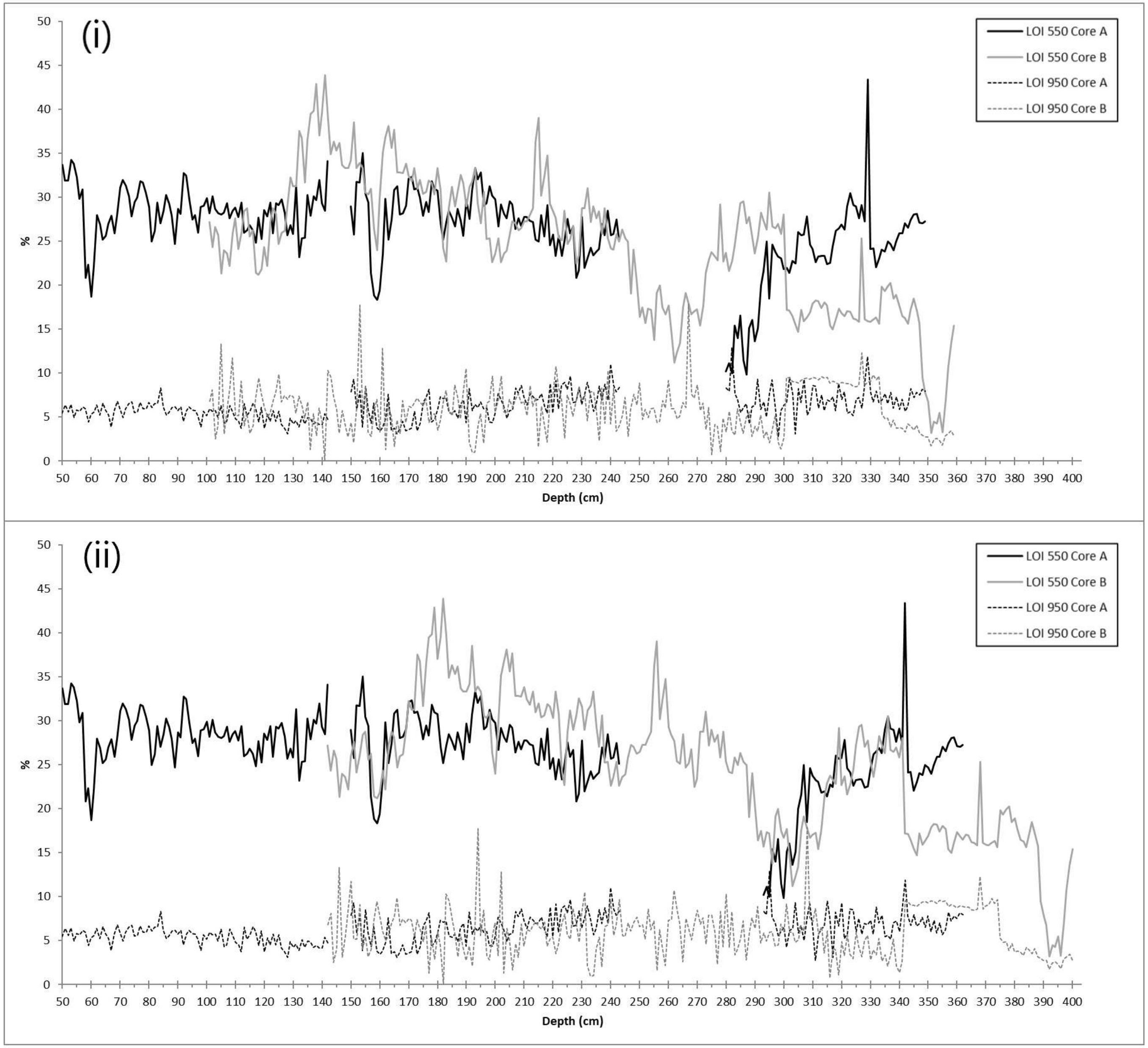
(i)
LOI 550 Core A
LOI 550 Core B
LOI 950 Core A
LOI 950 Core B
%
Depth (cm)
0 5 10 15 20 25 30 35 40 45 50
50 60 70 80 90 100 110 120 130 140 150 160 170 180 190 200 210 220 230 240 250 260 270 280 290 300 310 320 330 340 350 360 370 380 390 400
(ii)
LOI 550 Core A
LOI 550 Core B
LOI 950 Core A
LOI 950 Core B
%
Depth (cm)
0 5 10 15 20 25 30 35 40 45 50
50 60 70 80 90 100 110 120 130 140 150 160 170 180 190 200 210 220 230 240 250 260 270 280 290 300 310 320 330 340 350 360 370 380 390 400

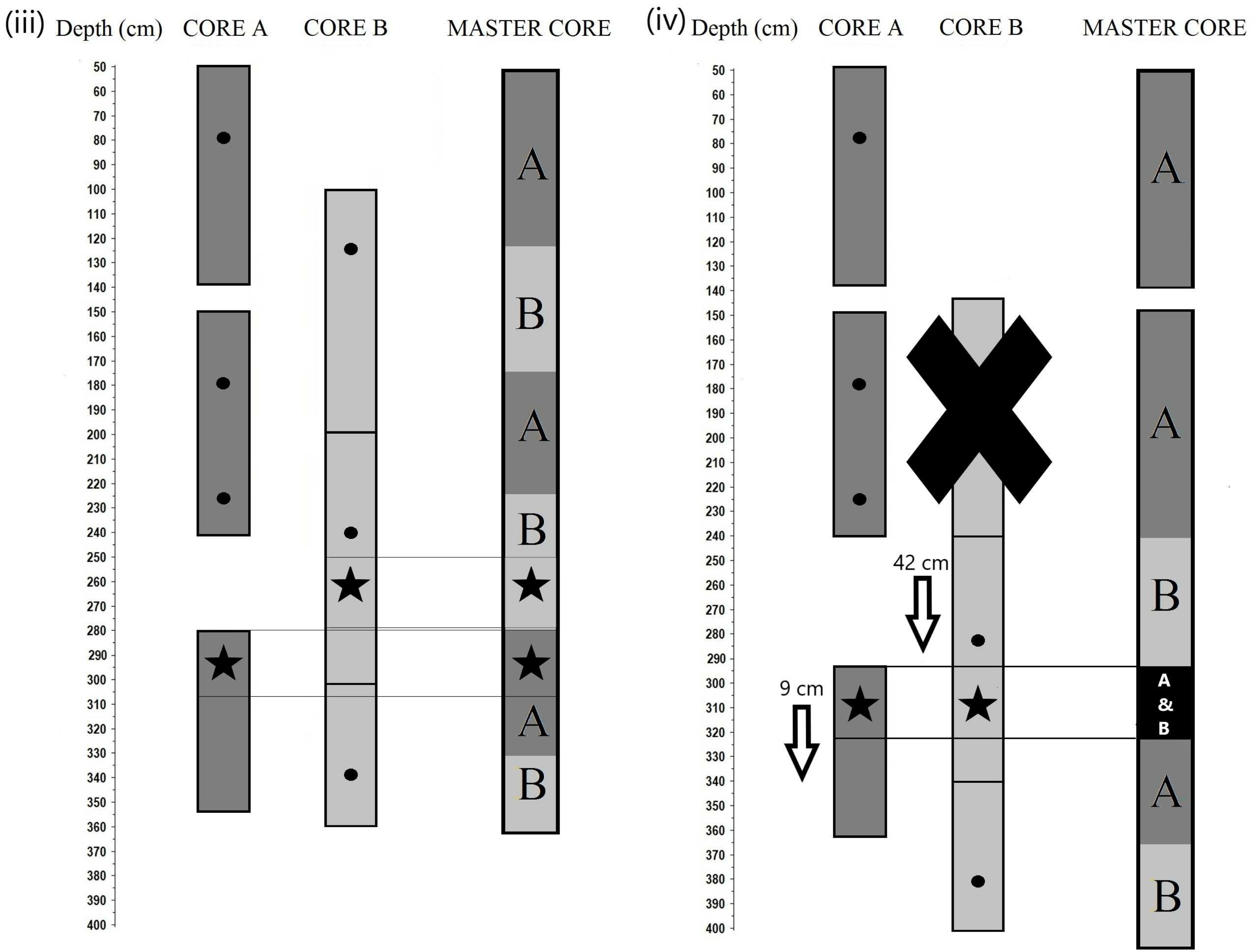

(iii)
Depth (cm)
CORE A
CORE B
MASTER CORE
50
60
70
80
90
100
110
120
130
140
150
160
170
180
190
200
210
220
230
240
250
260
270
280
290
300
310
320
330
340
350
360
370
380
390
400
A
B
A
B
A
B
(iv)
Depth (cm)
CORE A
CORE B
MASTER CORE
42 cm
9 cm
A
A
B
A & B
A
B

(v)

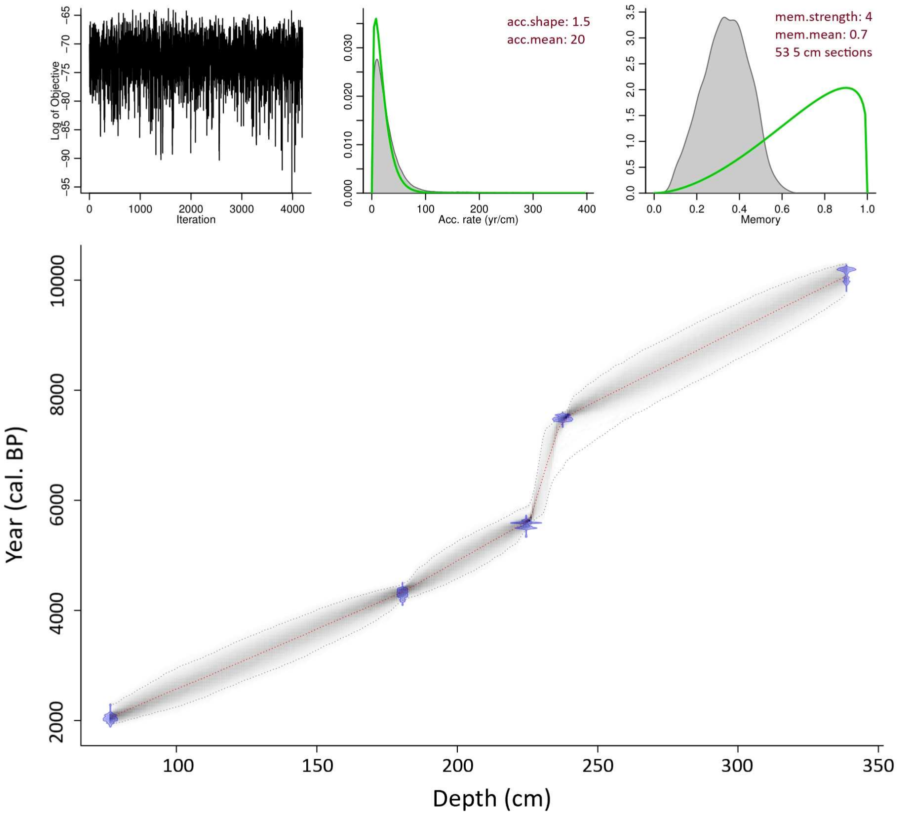

Log of Objective
Iteration
acc.shape: 1.5
acc.mean: 20
Acc. rate (yr/cm)
mem.strength: 4
mem.mean: 0.7
53 5 cm sections
Memory
Year (cal. BP)
Depth (cm)

(vi)

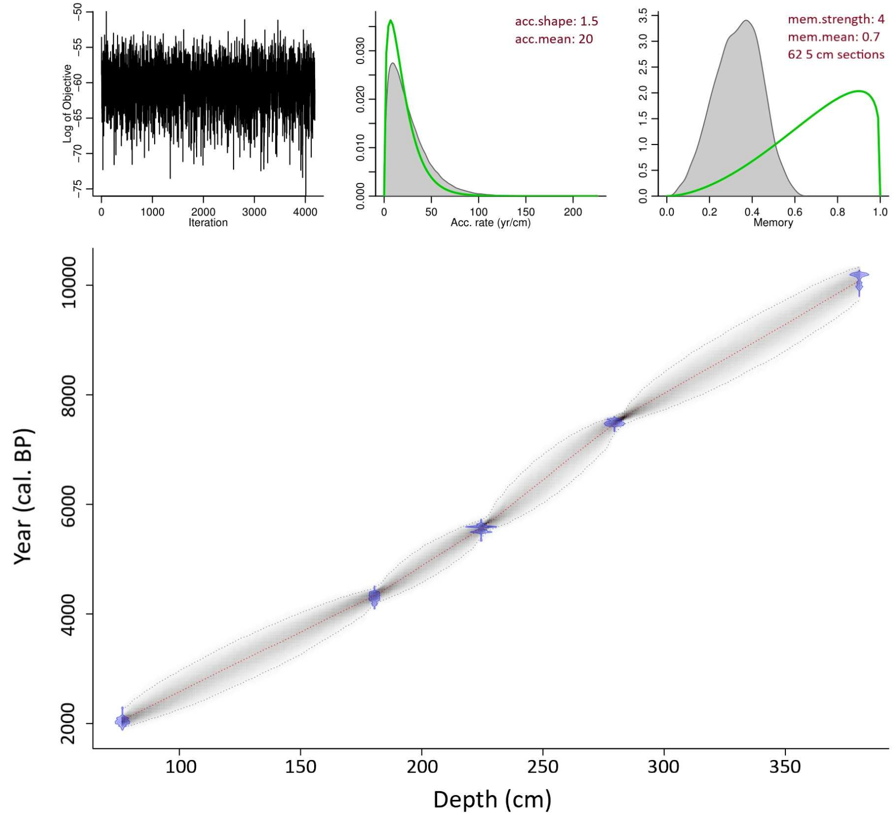

Log of Objective
Iteration
acc.shape: 1.5
acc.mean: 20
Acc. rate (yr/cm)
mem.strength: 4
mem.mean: 0.7
62 5 cm sections
Memory
Year (cal. BP)
Depth (cm)

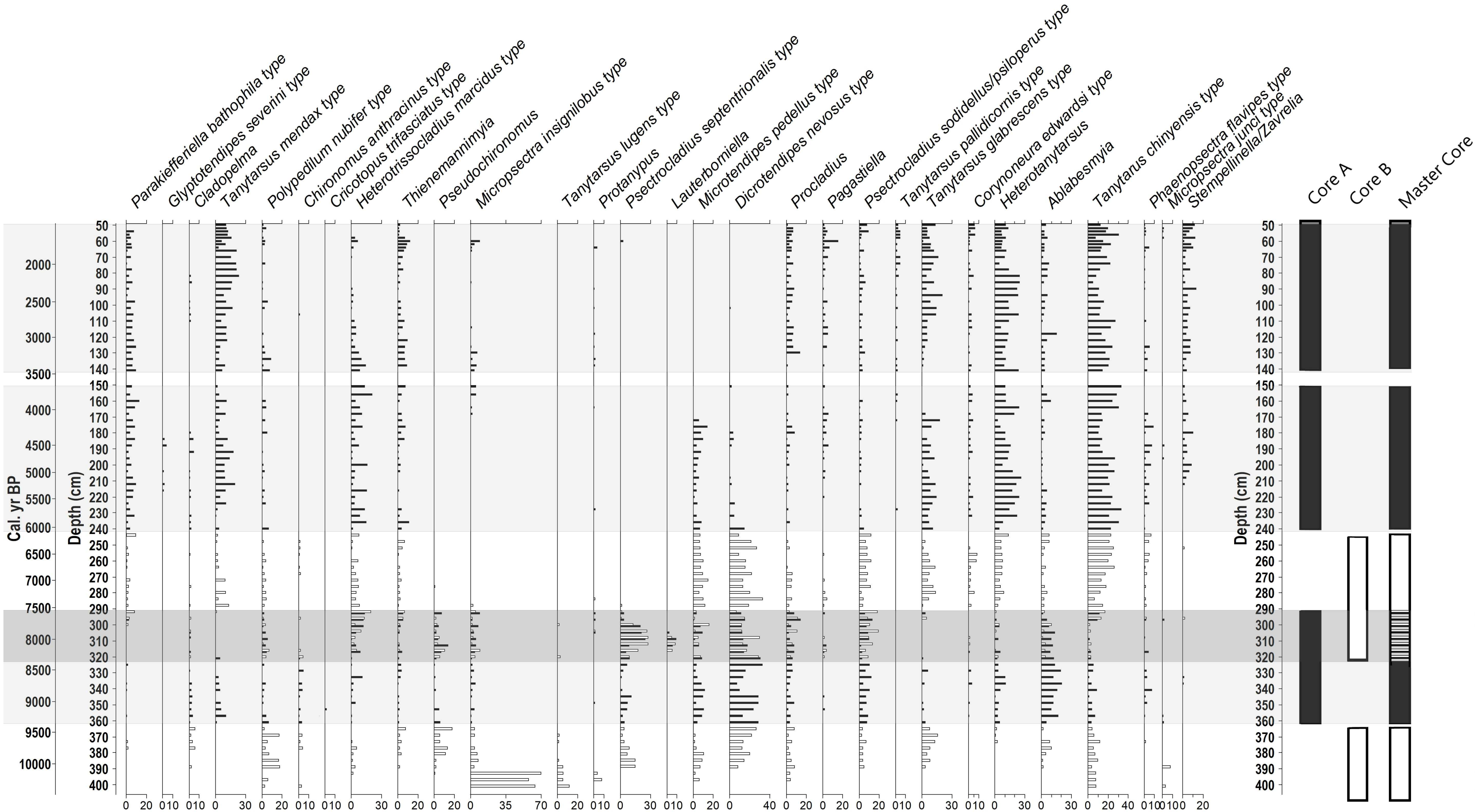

Parakiefferiella bathophila type
Glyptotendipes severini type
Cladopelma
Tanytarsus mendax type
Polypedilum nubifer type
Chironomus anthracinus type
Cricotopus trifasciatus type
Heterotrissocladius marcidus type
Thienemannimyia
Pseudochironomus
Micropsectra insignilobus type
Tanytarsus lugens type
Protanypus
Psectrocladius septentrionalis type
Lauterborniella
Microtendipes pedellus type
Dicrotendipes nevosus type
Procladius
Pagastiella
Psectrocladius sodidellus/psiloperus type
Tanytarsus pallidicornis type
Tanytarsus glabrescens type
Corynoneura edwardsi type
Heterotanytarsus
Ablabesmyia
Tanytarus chinyensis type
Phaenopsectra flavipes type
Micropsectra junci type
Stempellinella/Zavrelia
Core A
Core B
Master Core
Cal. yr BP
Depth (cm)

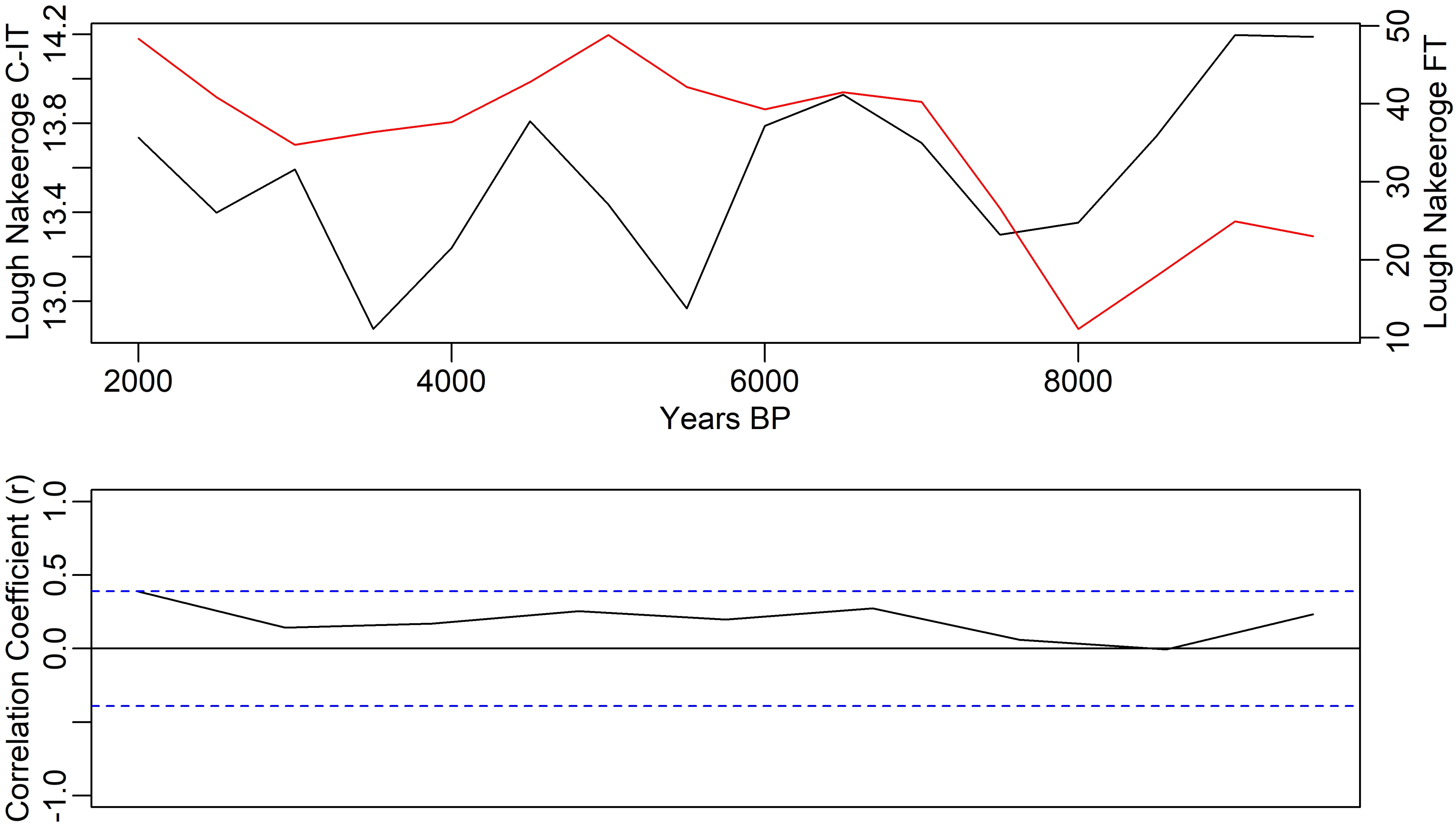

Lough Nakeeroge C-IT
Lough Nakeeroge FT
Years BP
Correlation Coefficient (r)

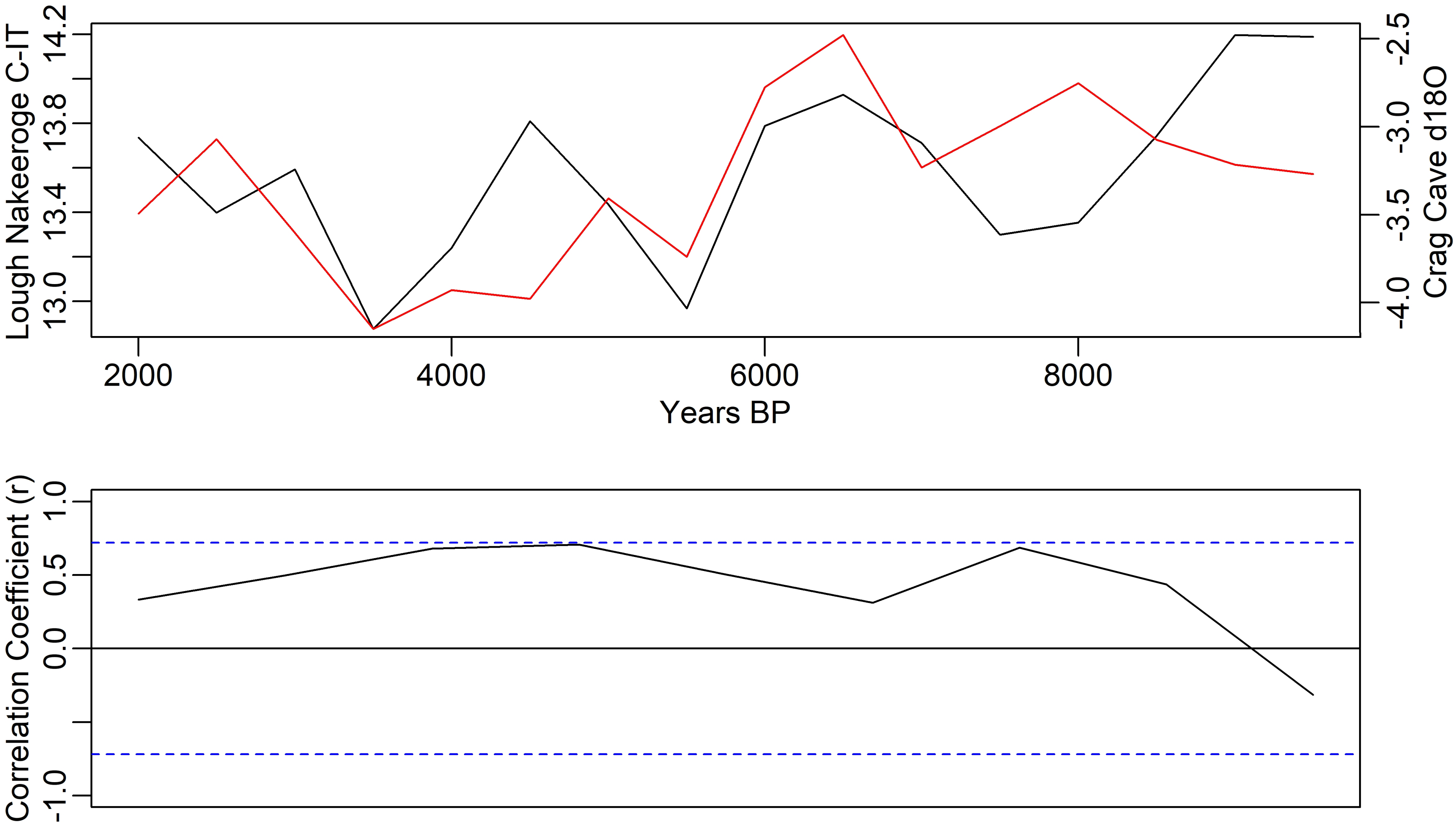

Lough Nakeeroge C-IT
13.0
13.4
13.8
14.2
Crag Cave d18O
-4.0
-3.5
-3.0
-2.5
2000
4000
6000
8000
Years BP
Correlation Coefficient (r)
-1.0
0.0
0.5
1.0

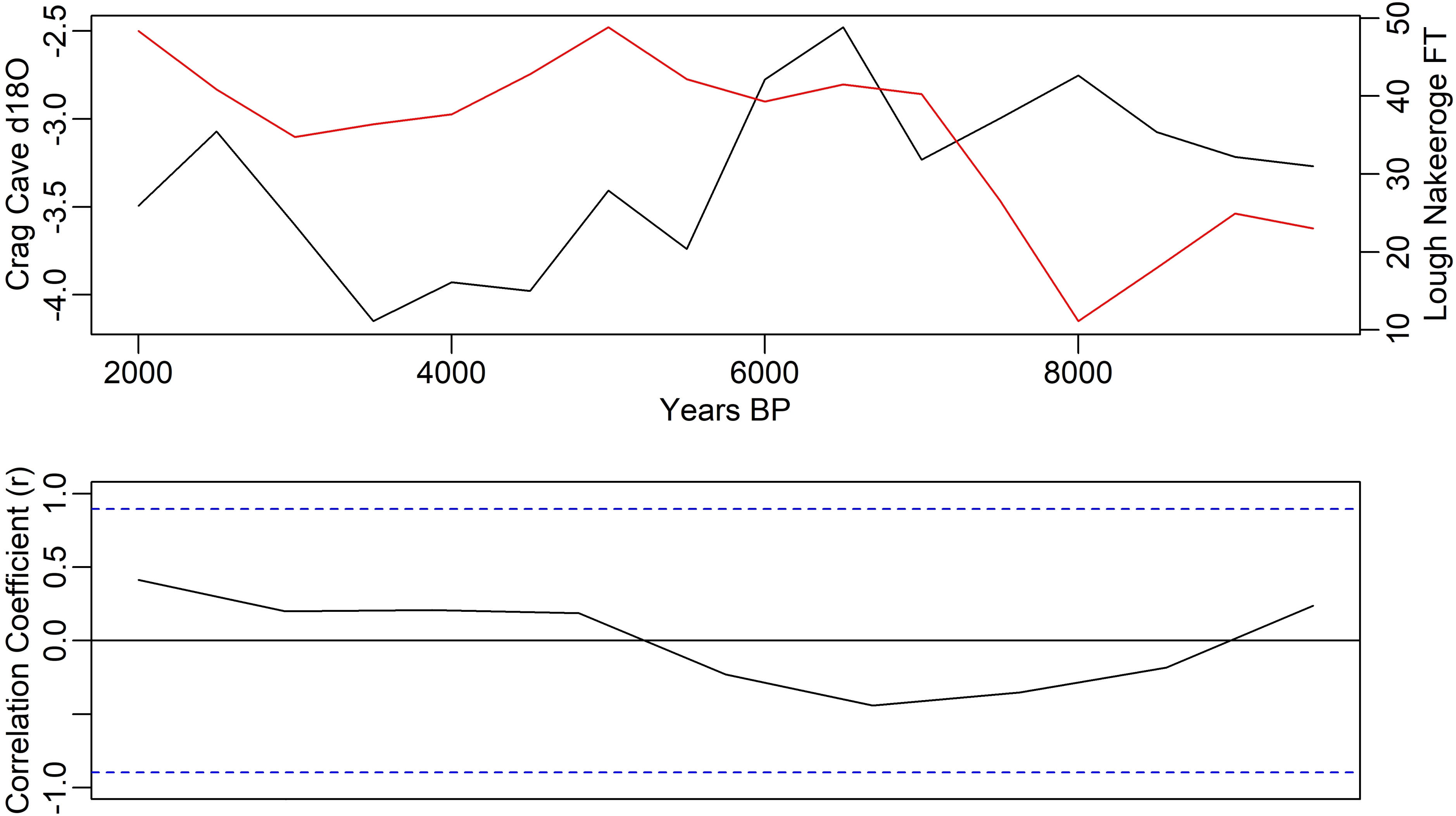
Crag Cave d18O
-2.5
-3.0
-3.5
-4.0
Lough Nakeeroge FT
50
40
30
20
10
2000
4000
6000
8000
Years BP
Correlation Coefficient (r)
1.0
0.5
0.0
-1.0

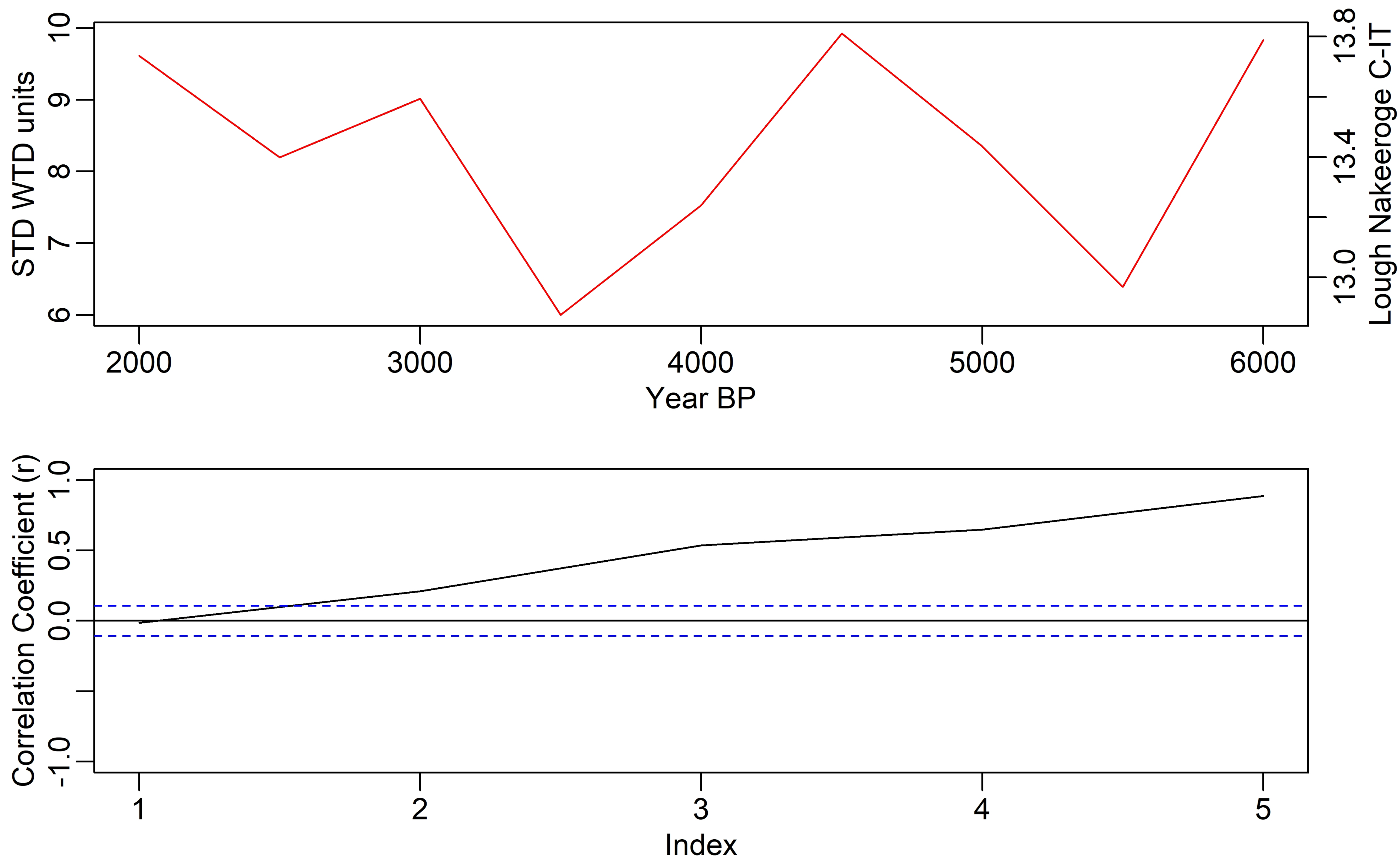
STD WTD units
10
9
8
7
6
Lough Nakeeroge C-IT
13.8
13.4
13.0
2000
3000
4000
5000
6000
Year BP
Correlation Coefficient (r)
1.0
0.5
0.0
-1.0
1
2
3
4
5
Index

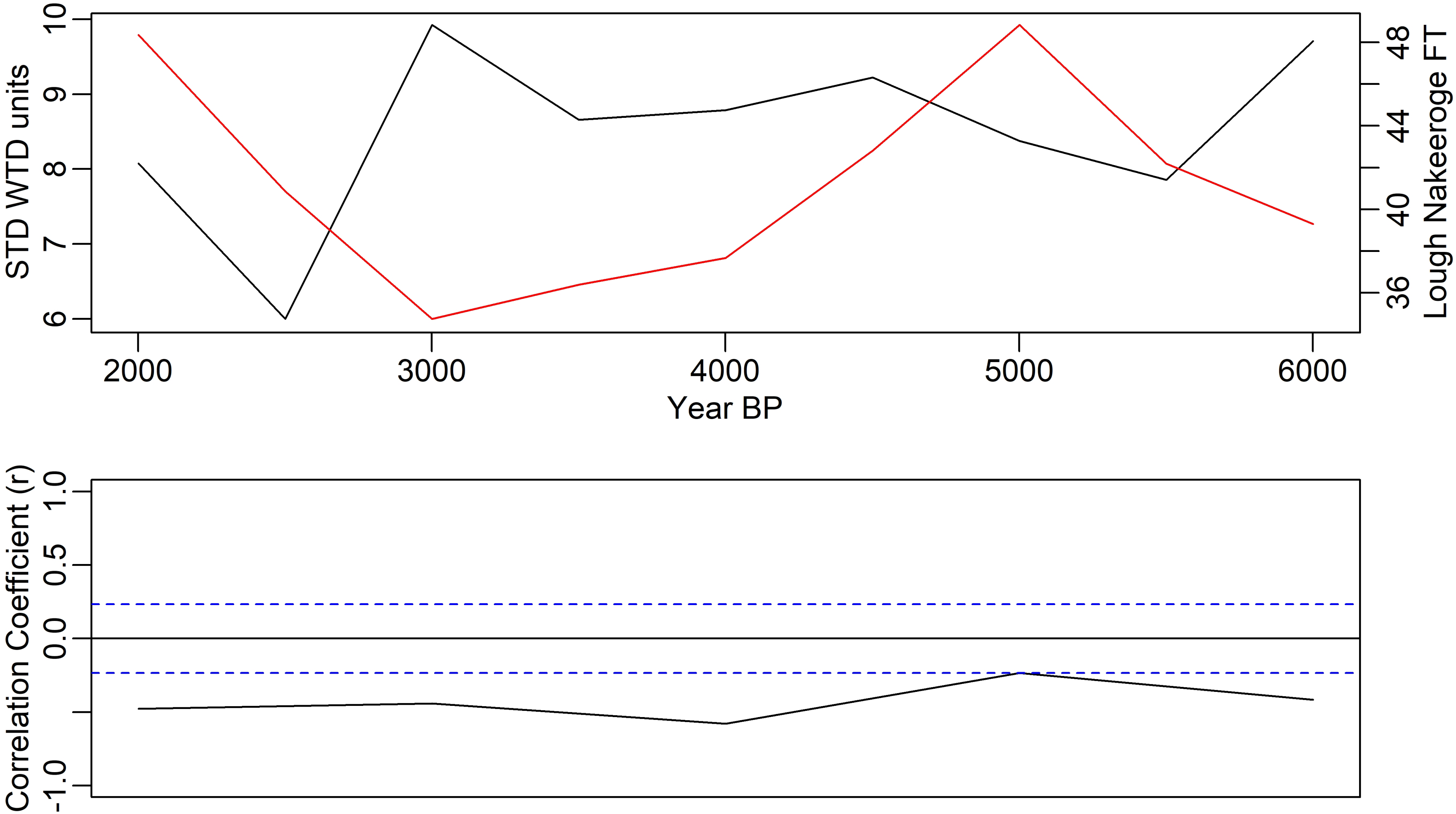

STD WTD units
10
9
8
7
6
Lough Nakeeroge FT
48
44
40
36
2000
3000
4000
5000
6000
Year BP
Correlation Coefficient (r)
1.0
0.5
0.0
-1.0

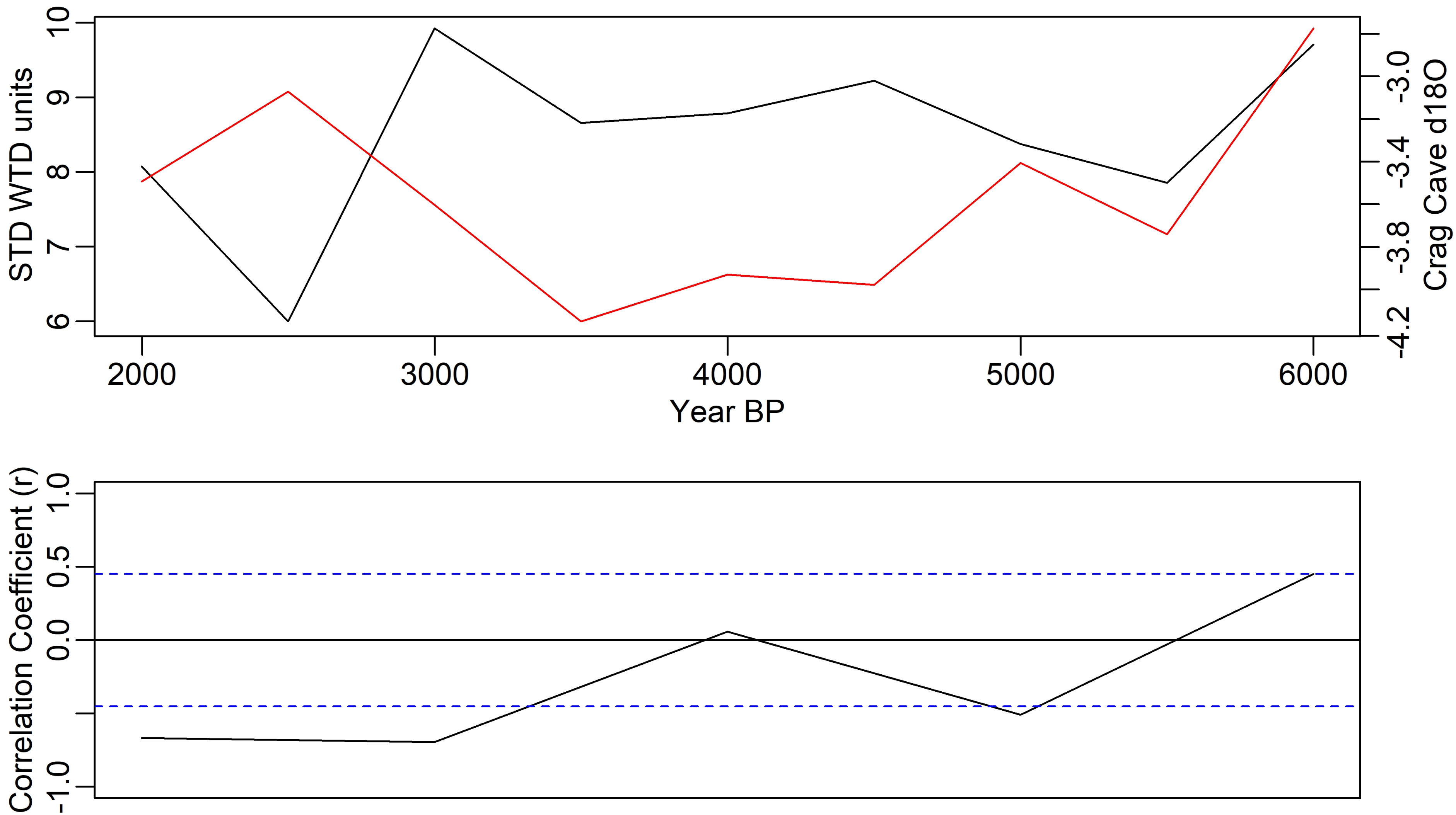

STD WTD units
10
9
8
7
6
-3.0
-3.4
-3.8
-4.2
Crag Cave d18O
2000
3000
4000
5000
6000
Year BP
Correlation Coefficient (r)
1.0
0.5
0.0
-1.0

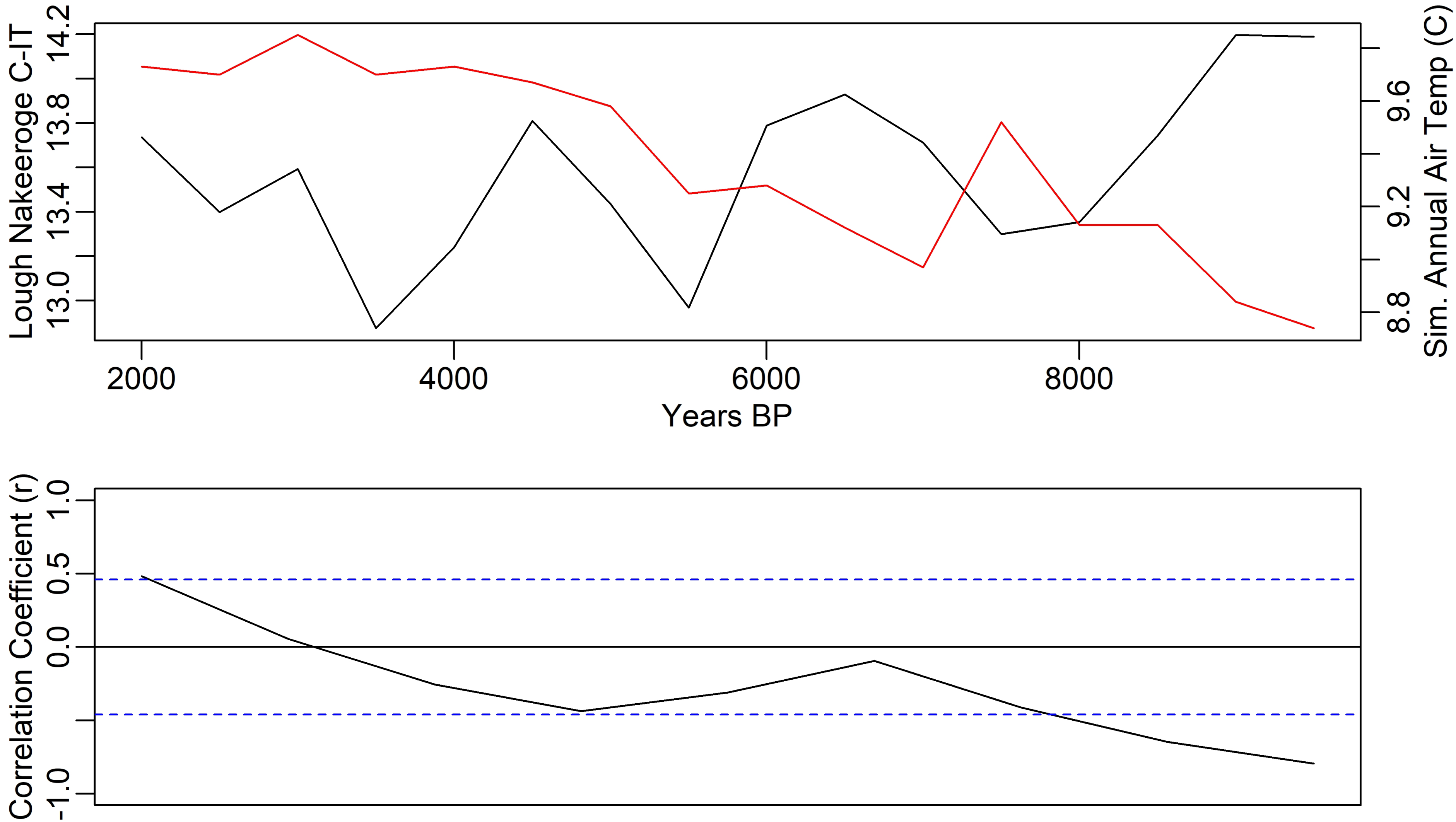

Lough Nakeeroge C-IT
14.2
13.8
13.4
13.0
Sim. Annual Air Temp (C)
9.6
9.2
8.8
2000
4000
6000
8000
Years BP
Correlation Coefficient (r)
1.0
0.5
0.0
-1.0

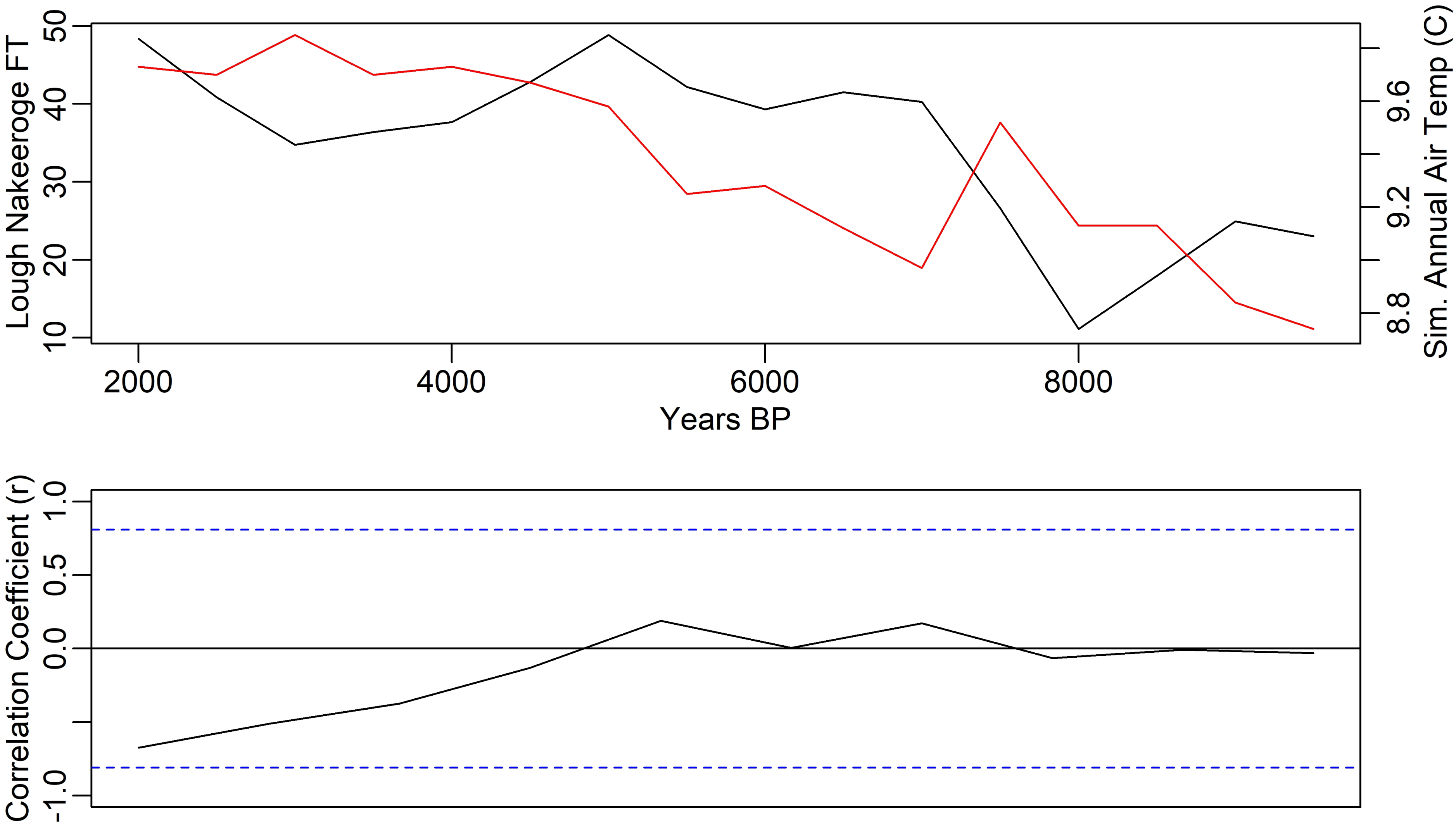

Lough Nakeeroge FT
50
40
30
20
10
Sim. Annual Air Temp (C)
9.6
9.2
8.8
2000
4000
6000
8000
Years BP
Correlation Coefficient (r)
1.0
0.5
0.0
-1.0

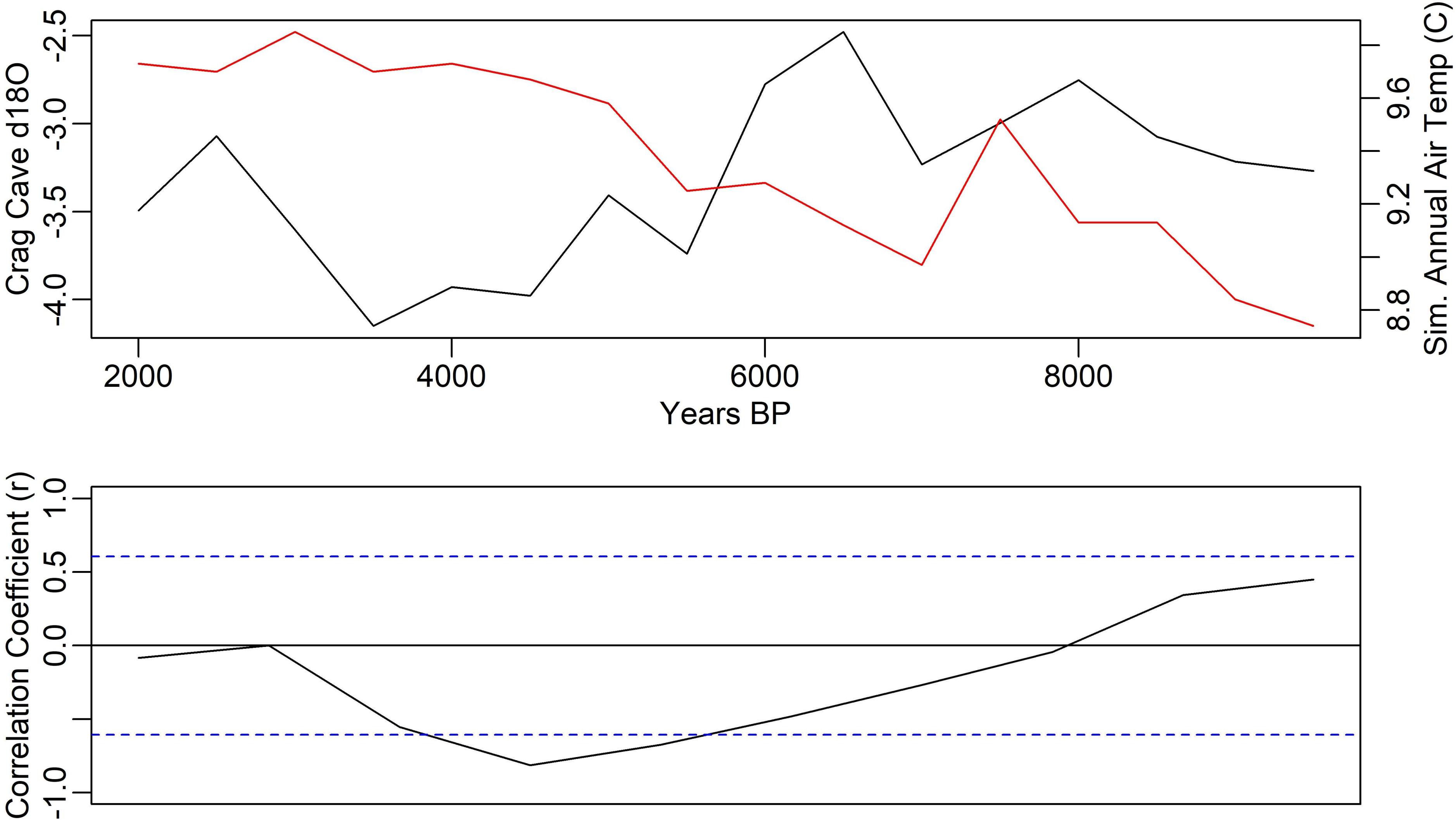

Crag Cave d18O
-2.5
-3.0
-3.5
-4.0
Sim. Annual Air Temp (C)
9.6
9.2
8.8
2000
4000
6000
8000
Years BP
Correlation Coefficient (r)
1.0
0.5
0.0
-1.0

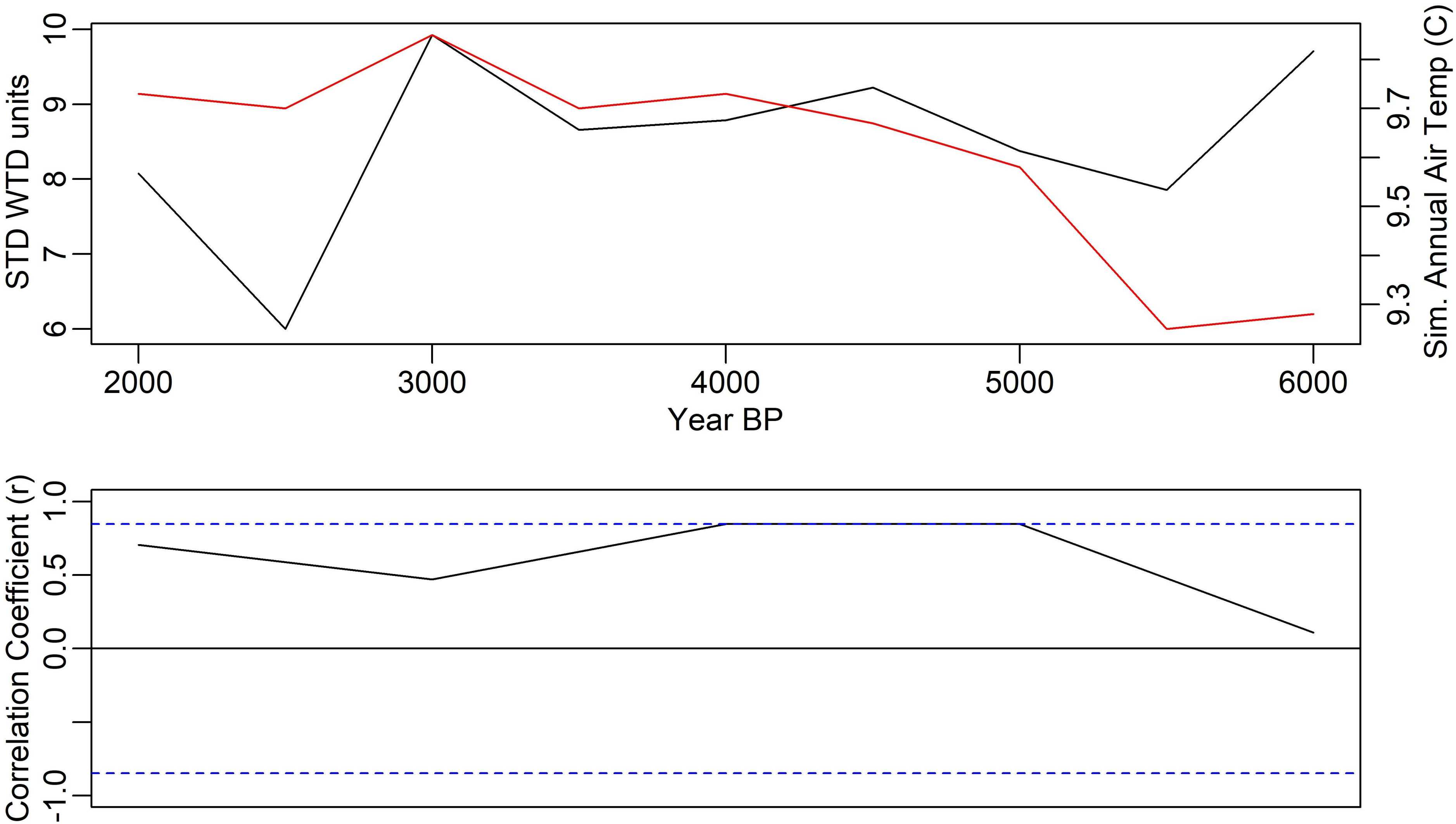

STD WTD units
Sim. Annual Air Temp (C)
Year BP
2000
3000
4000
5000
6000
6
7
8
9
10
9.3
9.5
9.7
Correlation Coefficient (r)
-1.0
0.0
0.5
1.0

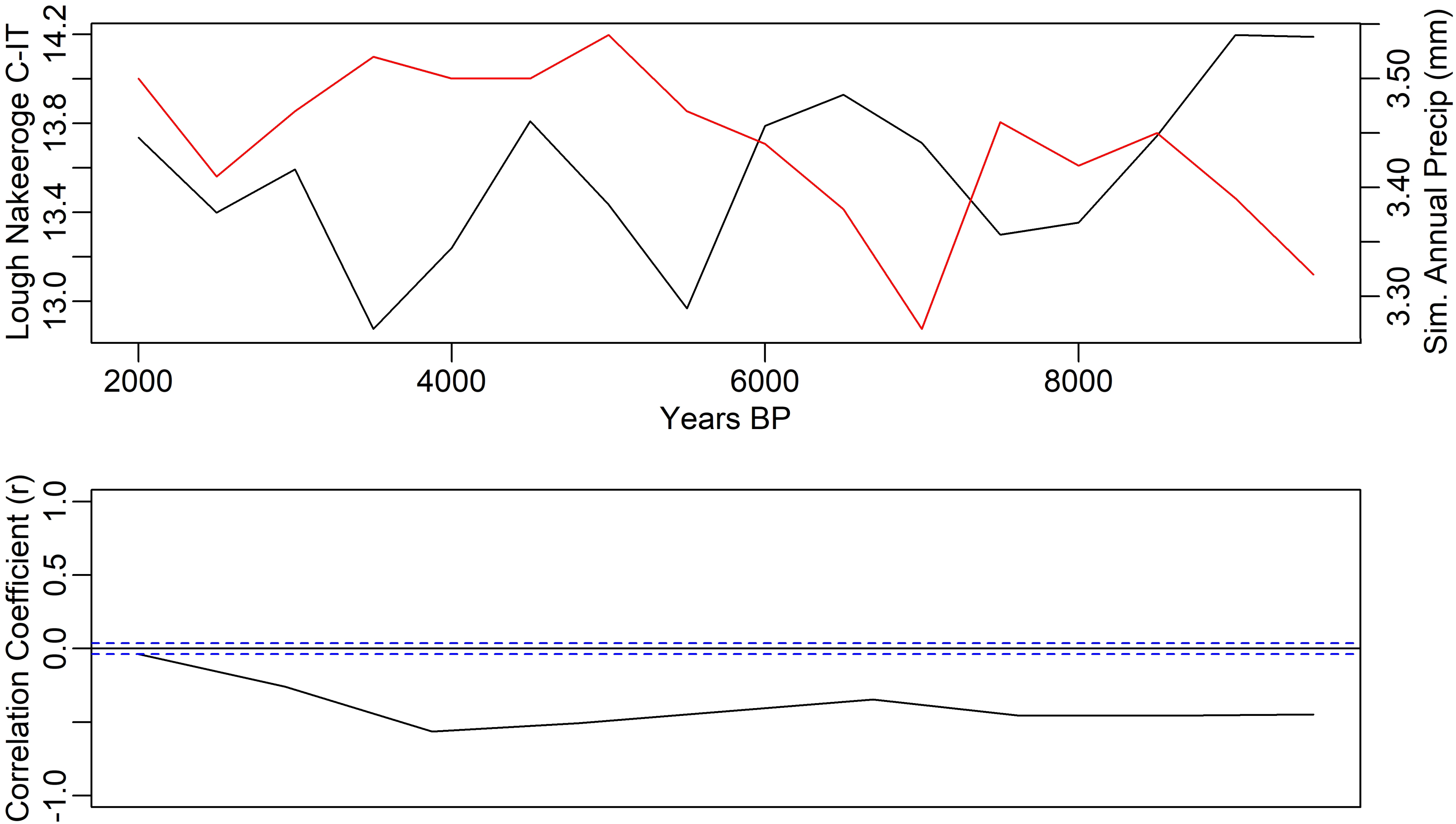

Lough Nakeeroge C-IT
13.0
13.4
13.8
14.2
Sim. Annual Precip (mm)
3.30
3.40
3.50
2000
4000
6000
8000
Years BP
Correlation Coefficient (r)
-1.0
0.0
0.5
1.0

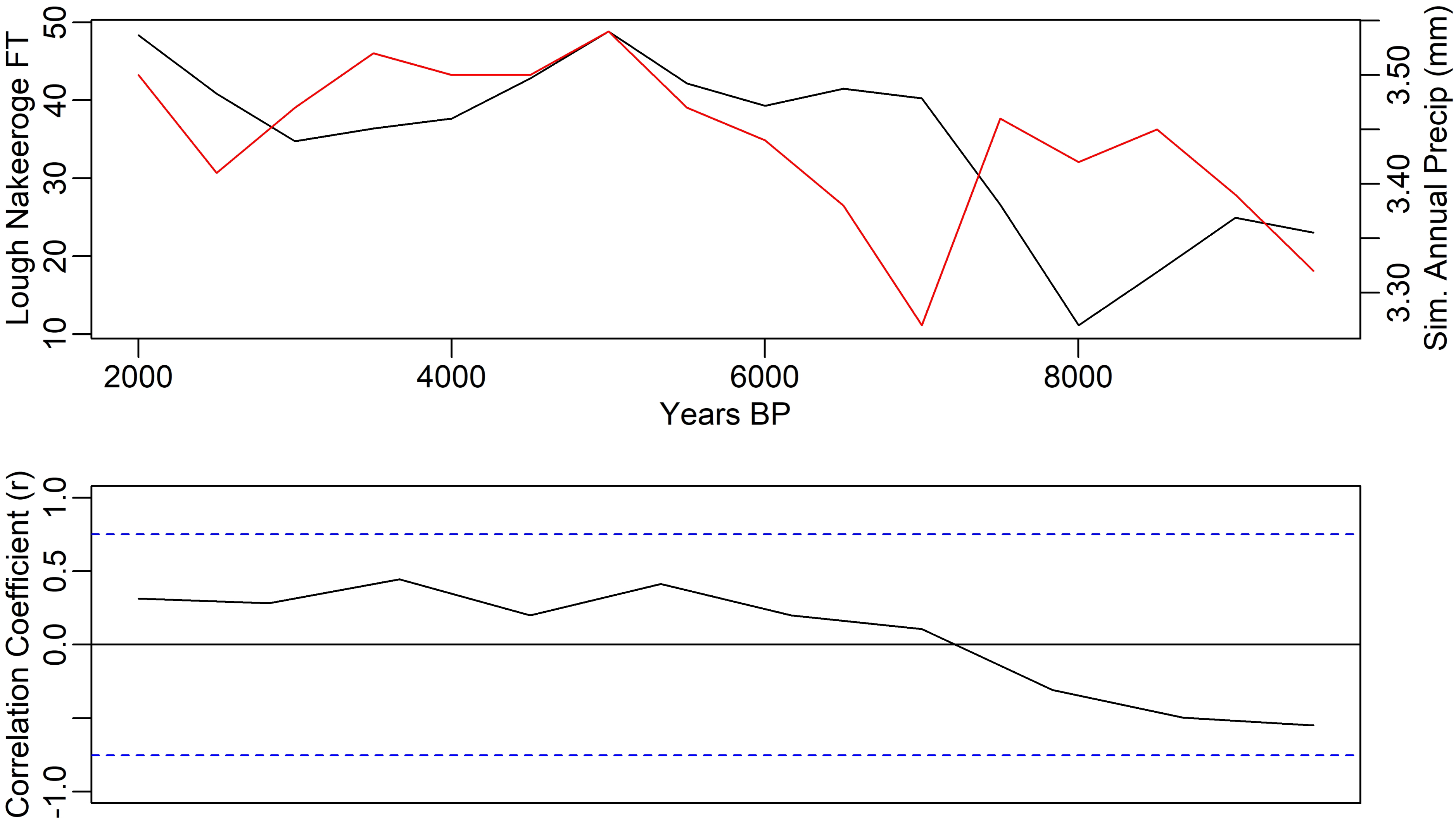

Lough Nakeeroge FT
50
40
30
20
10
Sim. Annual Precip (mm)
3.50
3.40
3.30
2000
4000
6000
8000
Years BP
Correlation Coefficient (r)
1.0
0.5
0.0
-1.0

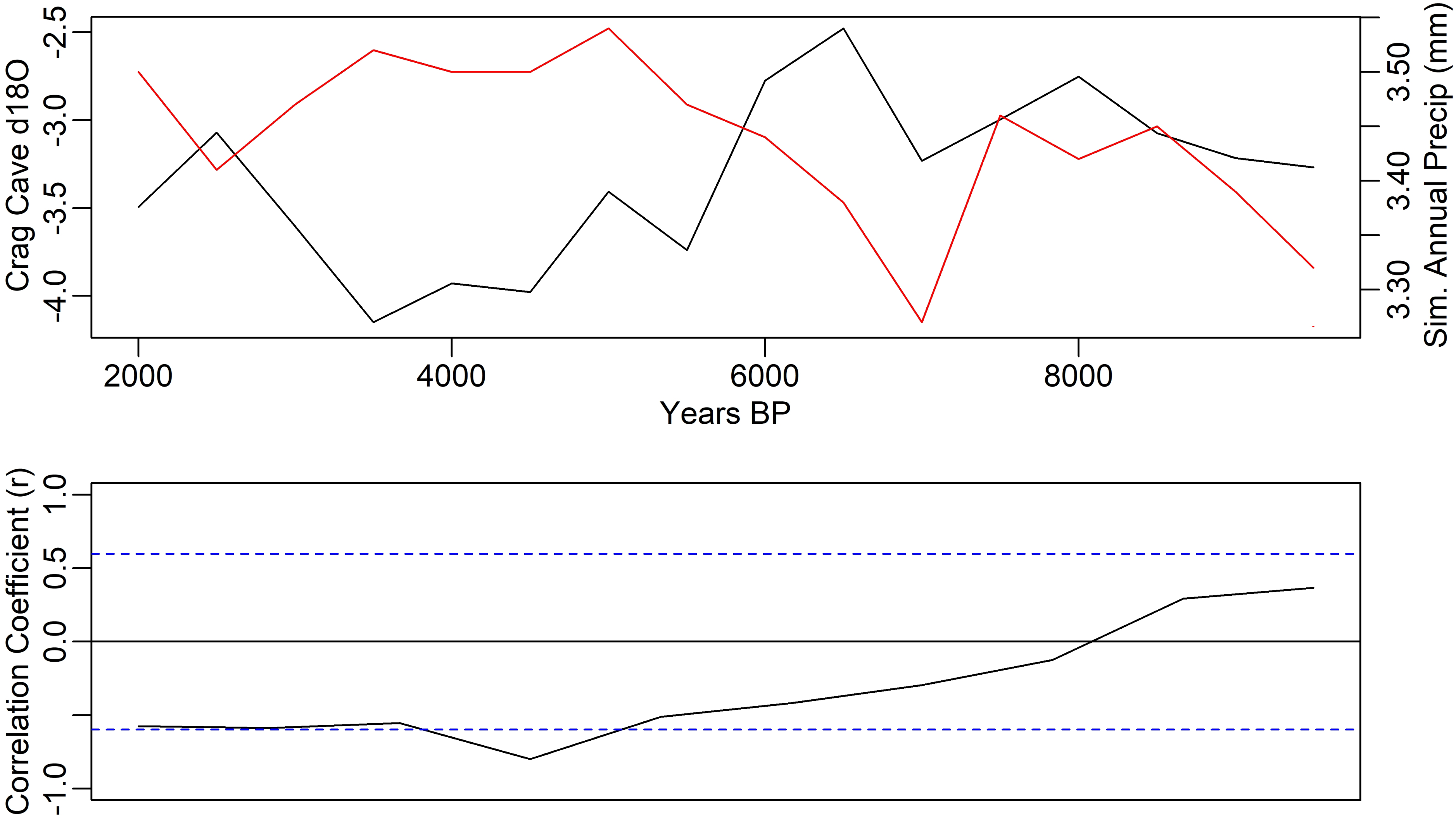

Crag Cave d18O
-2.5
-3.0
-3.5
-4.0
Sim. Annual Precip (mm)
3.50
3.40
3.30
2000
4000
6000
8000
Years BP
Correlation Coefficient (r)
1.0
0.5
0.0
-1.0

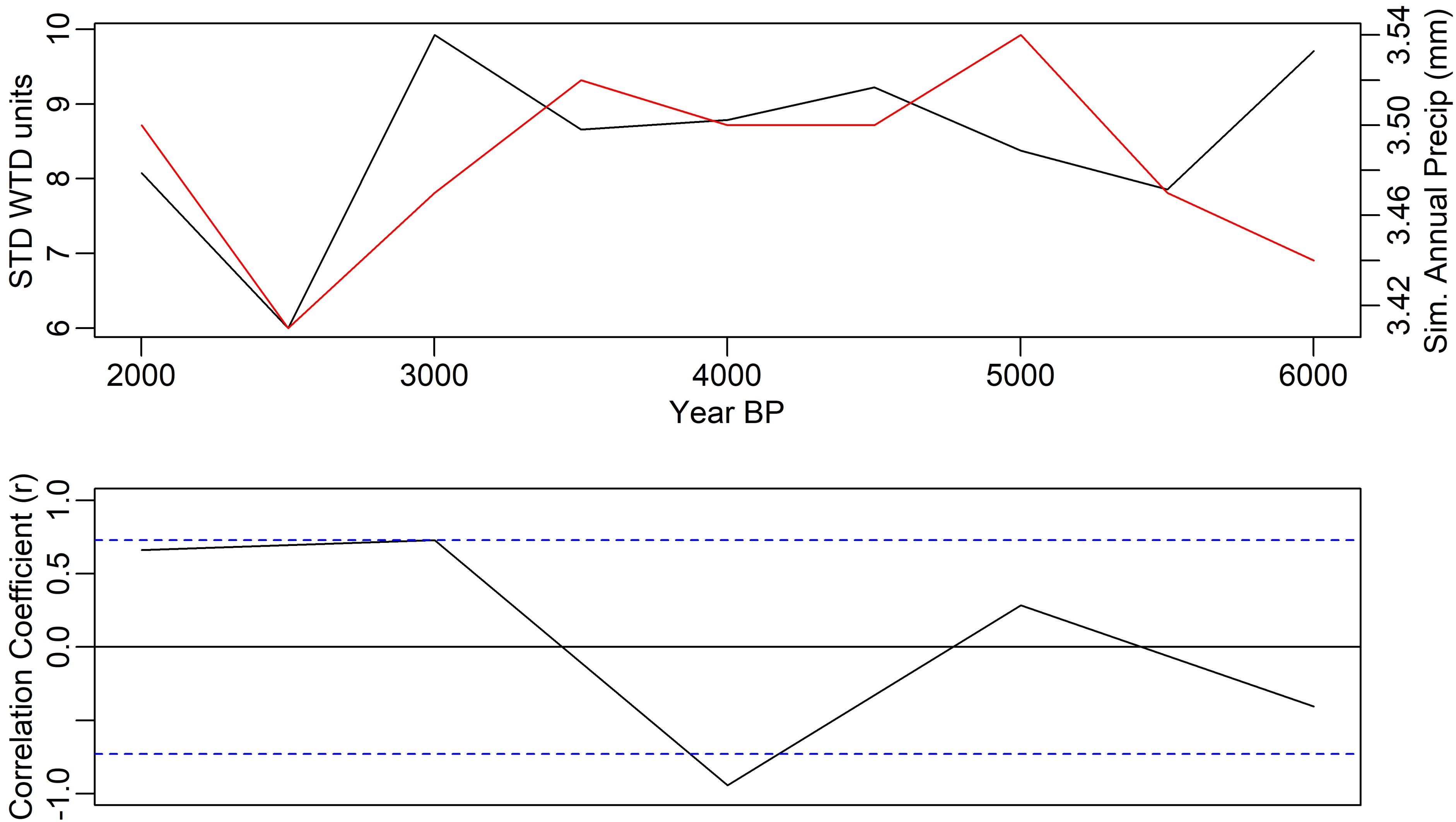

STD WTD units
10
9
8
7
6
Sim. Annual Precip (mm)
3.54
3.50
3.46
3.42
2000
3000
4000
5000
6000
Year BP
Correlation Coefficient (r)
1.0
0.5
0.0
-1.0

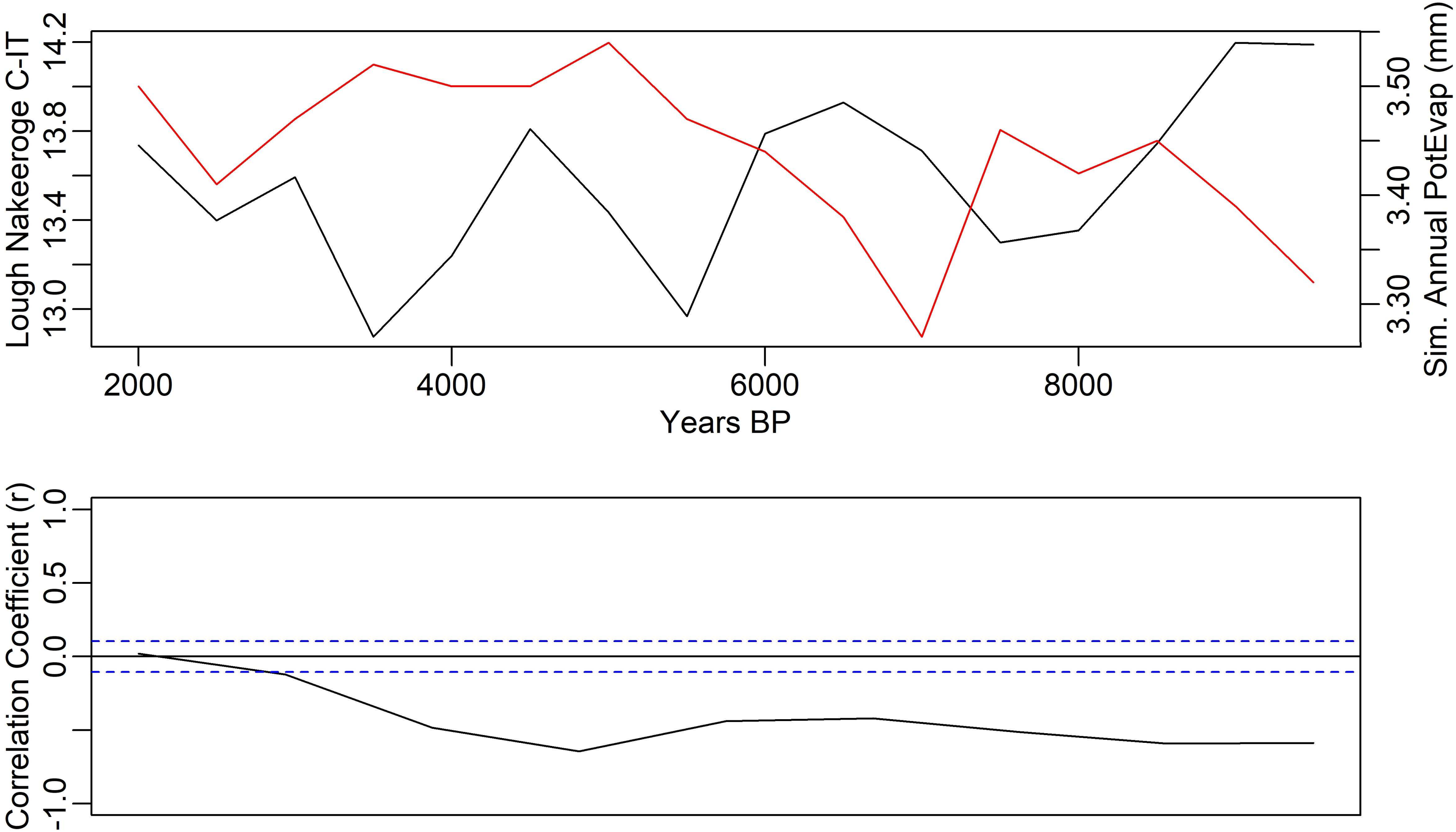

Lough Nakeeroge C-IT
13.0
13.4
13.8
14.2
Sim. Annual PotEvap (mm)
3.30
3.40
3.50
2000
4000
6000
8000
Years BP
Correlation Coefficient (r)
-1.0
0.0
0.5
1.0

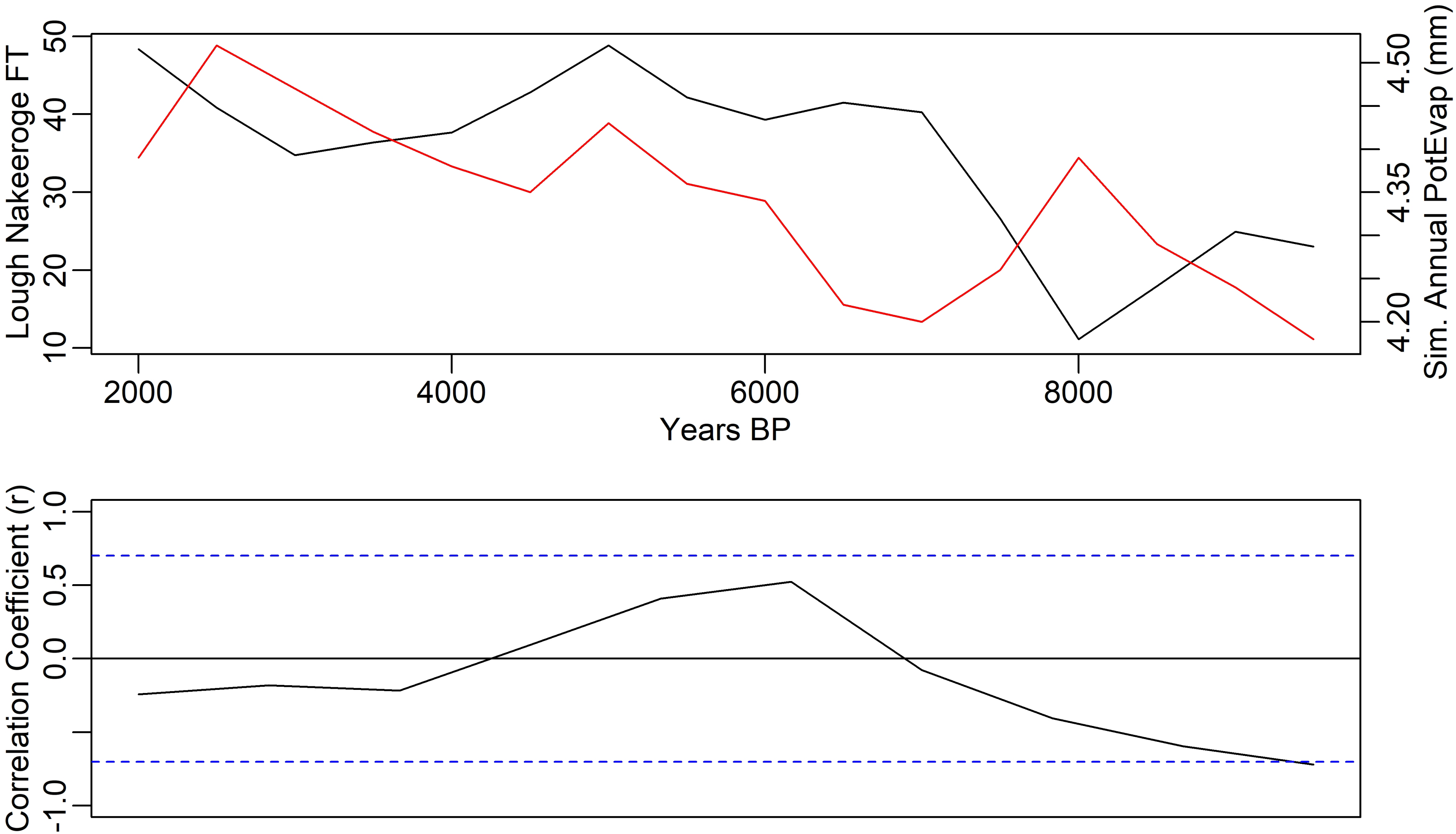

Lough Nakeeroge FT
Sim. Annual PotEvap (mm)
50
40
30
20
10
4.50
4.35
4.20
2000
4000
6000
8000
Years BP
Correlation Coefficient (r)
1.0
0.5
0.0
-1.0

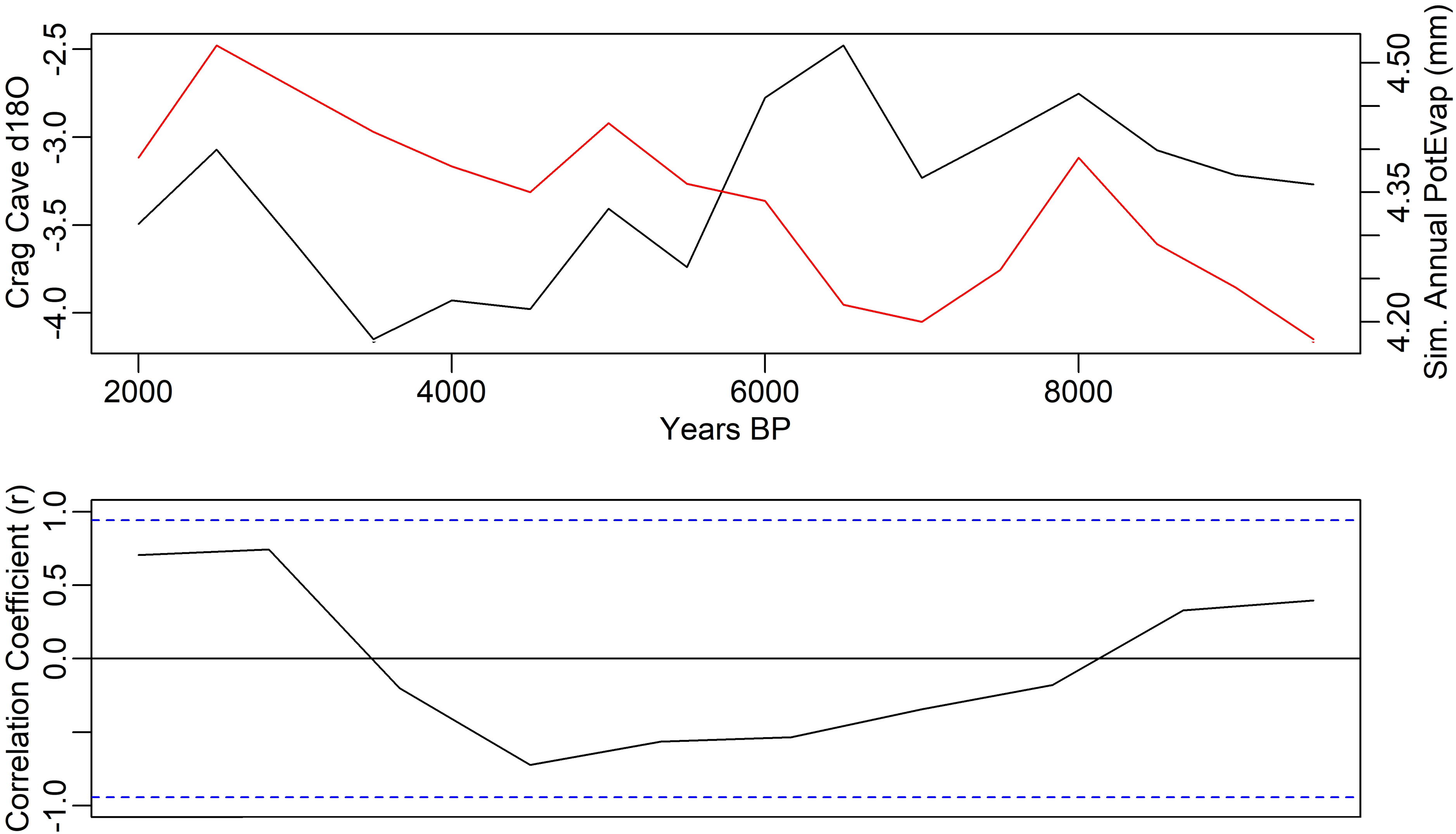

Crag Cave d18O
-2.5
-3.0
-3.5
-4.0
Sim. Annual PotEvap (mm)
4.50
4.35
4.20
2000
4000
6000
8000
Years BP
Correlation Coefficient (r)
1.0
0.5
0.0
-1.0

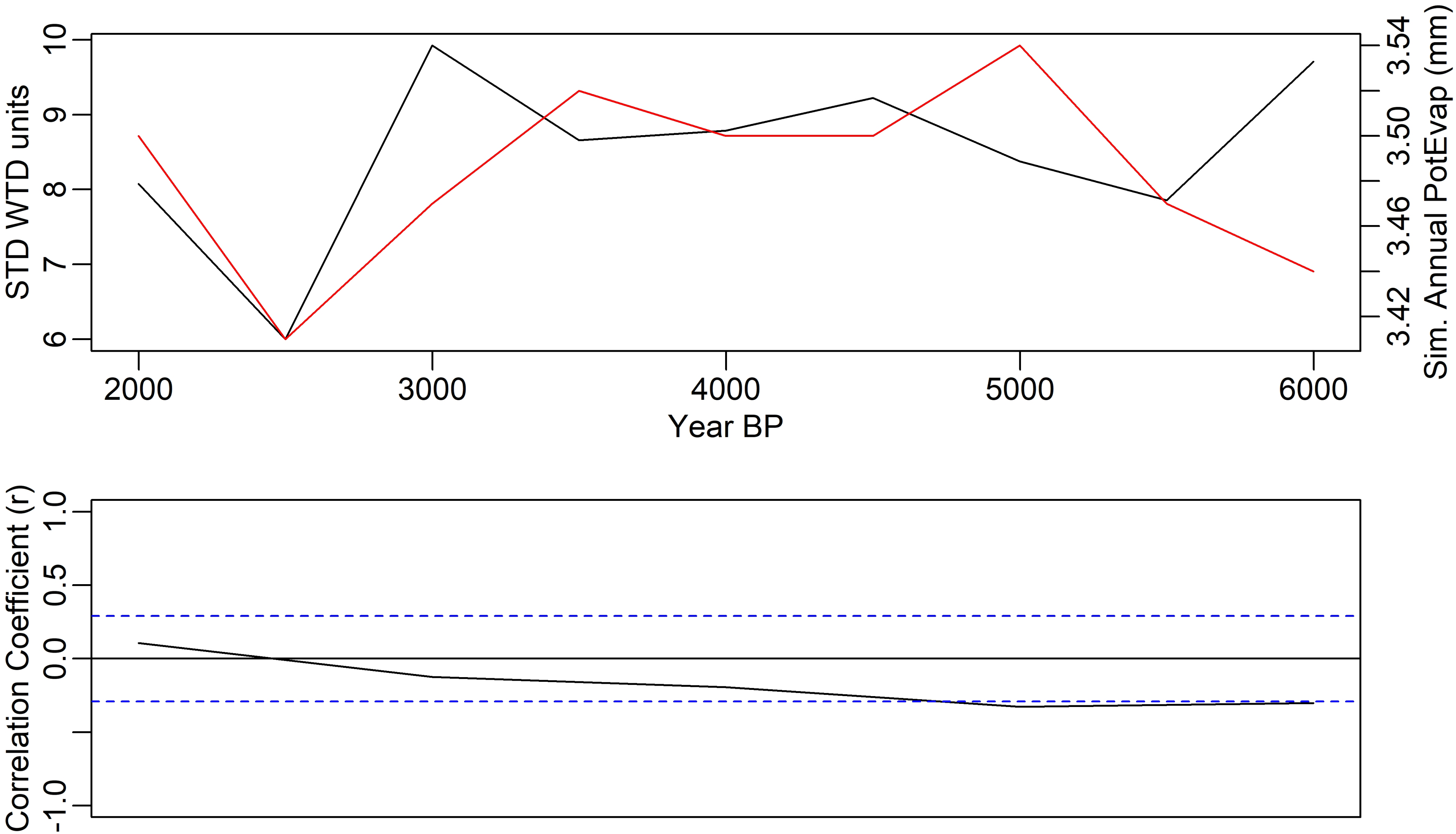

STD WTD units
Sim. Annual PotEvap (mm)
Year BP
Correlation Coefficient (r)

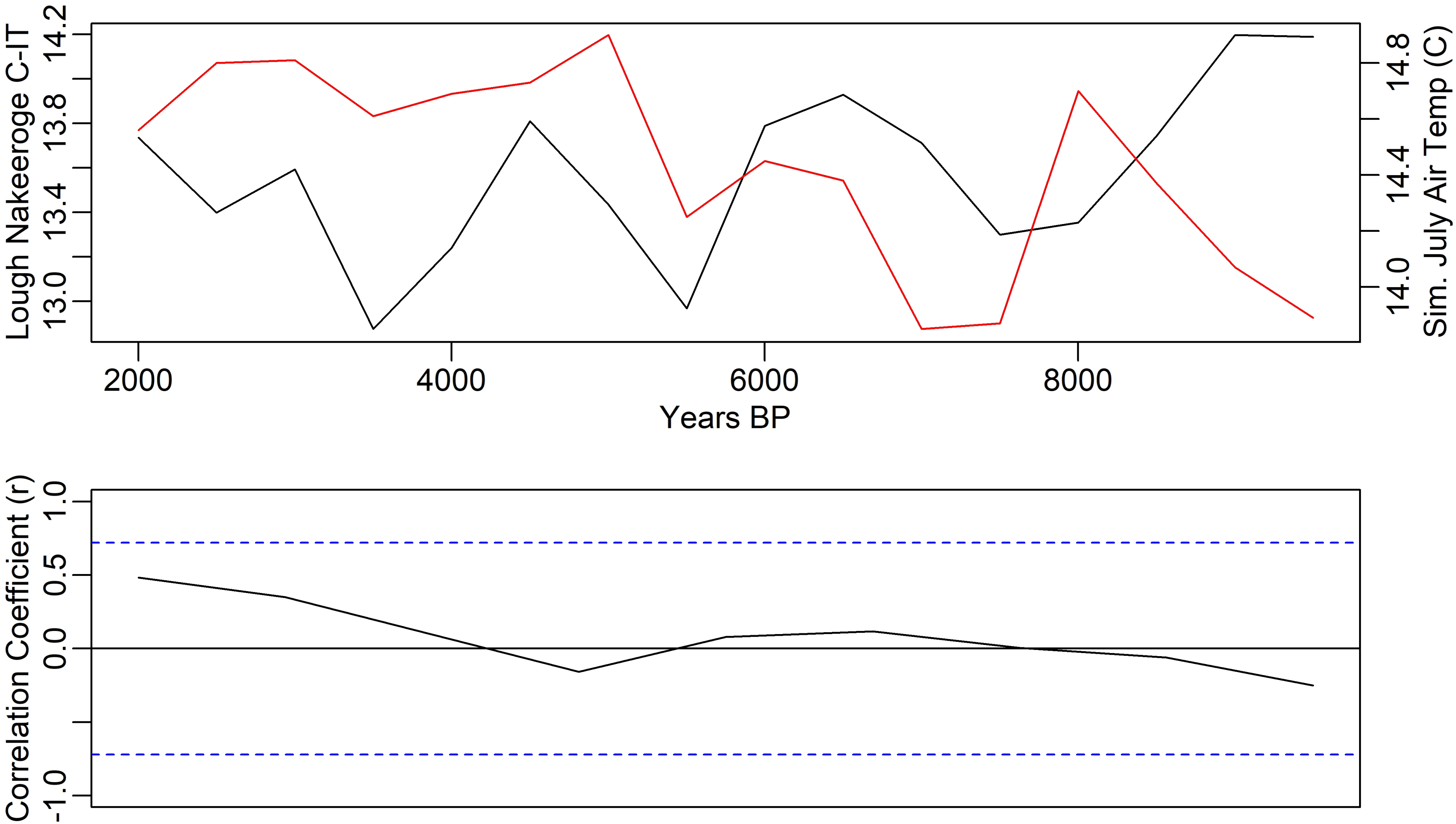
Lough Nakeeroge C-IT
13.0
13.4
13.8
14.2
Sim. July Air Temp (C)
14.0
14.4
14.8
2000
4000
6000
8000
Years BP
Correlation Coefficient (r)
-1.0
0.0
0.5
1.0

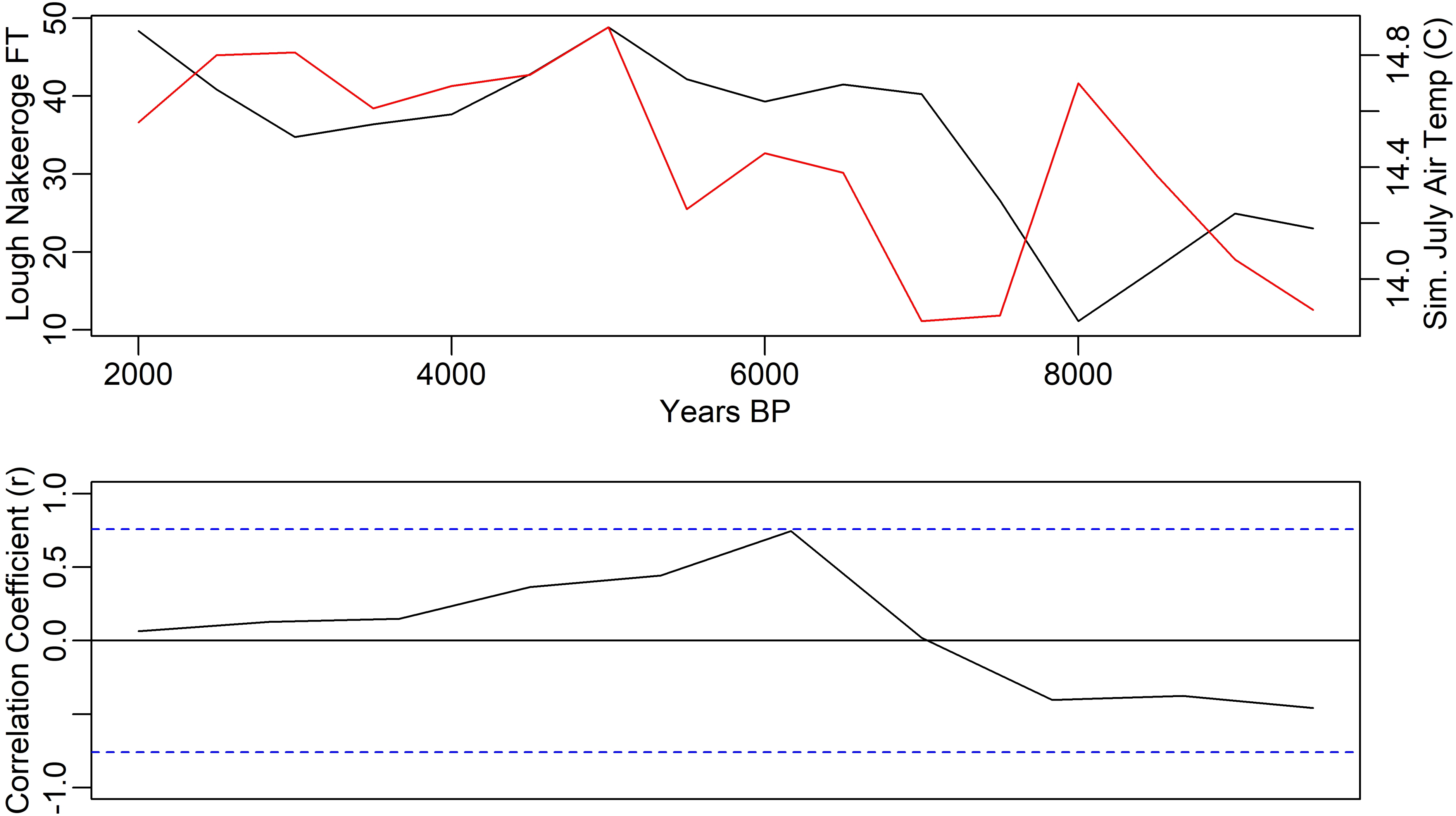

Lough Nakeeroge FT
10
20
30
40
50
Sim. July Air Temp (C)
14.0
14.4
14.8
2000
4000
6000
8000
Years BP
Correlation Coefficient (r)
-1.0
0.0
0.5
1.0

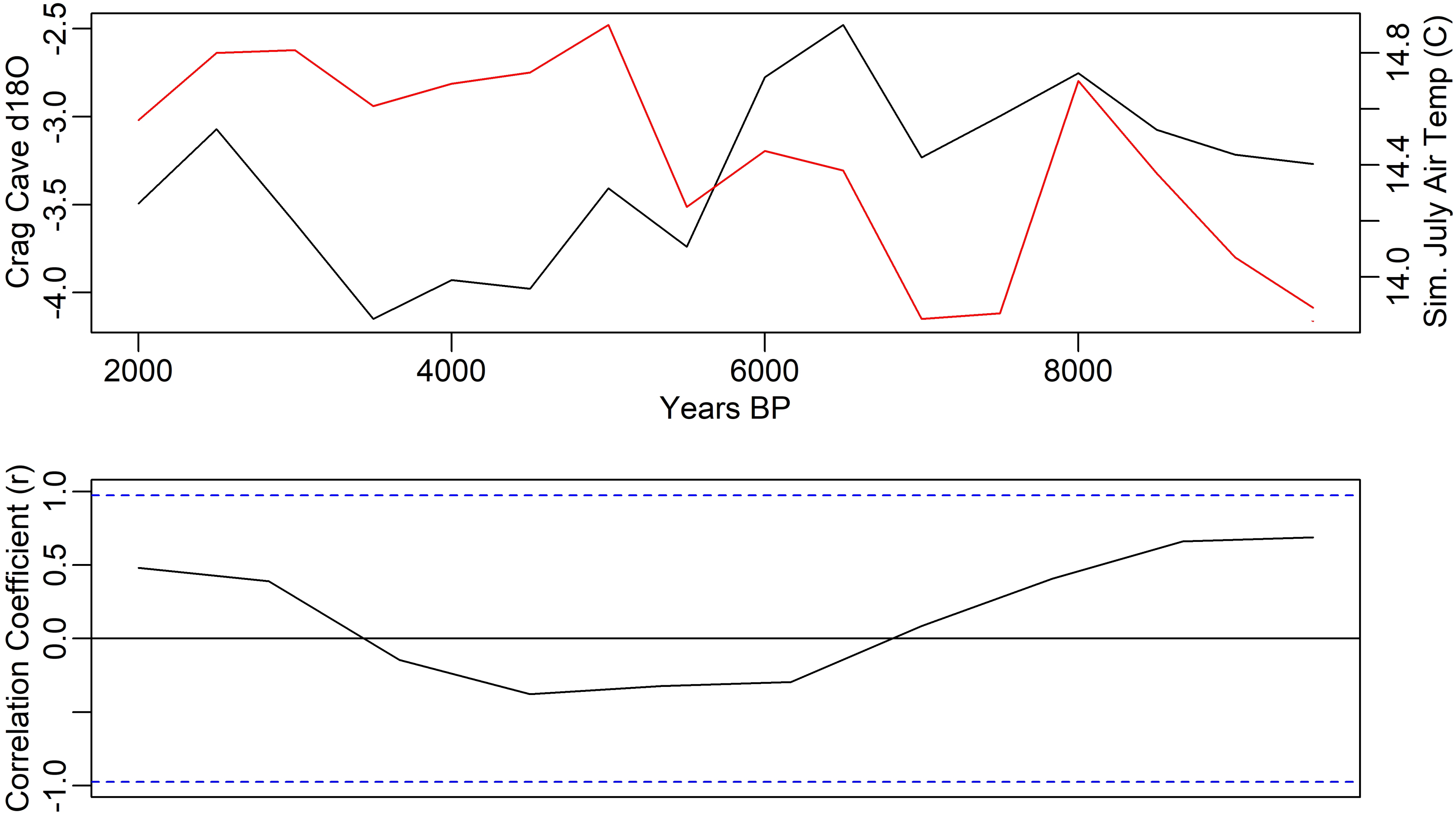

Crag Cave d18O
-2.5
-3.0
-3.5
-4.0
Sim. July Air Temp (C)
14.8
14.4
14.0
2000
4000
6000
8000
Years BP
Correlation Coefficient (r)
1.0
0.5
0.0
-1.0

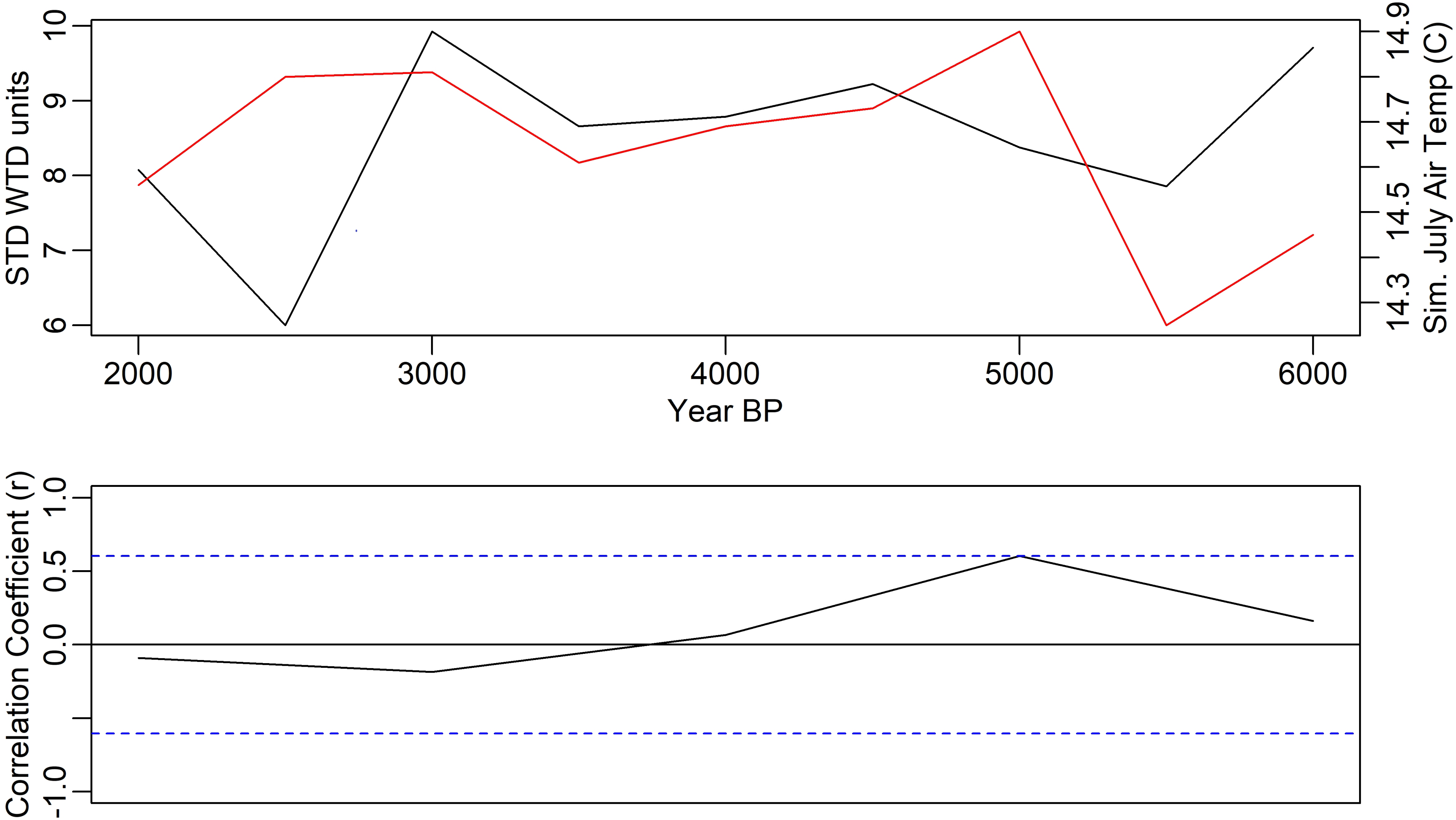

STD WTD units
Sim. July Air Temp (C)
10
9
8
7
6
14.9
14.7
14.5
14.3
2000
3000
4000
5000
6000
Year BP
Correlation Coefficient (r)
1.0
0.5
0.0
-1.0

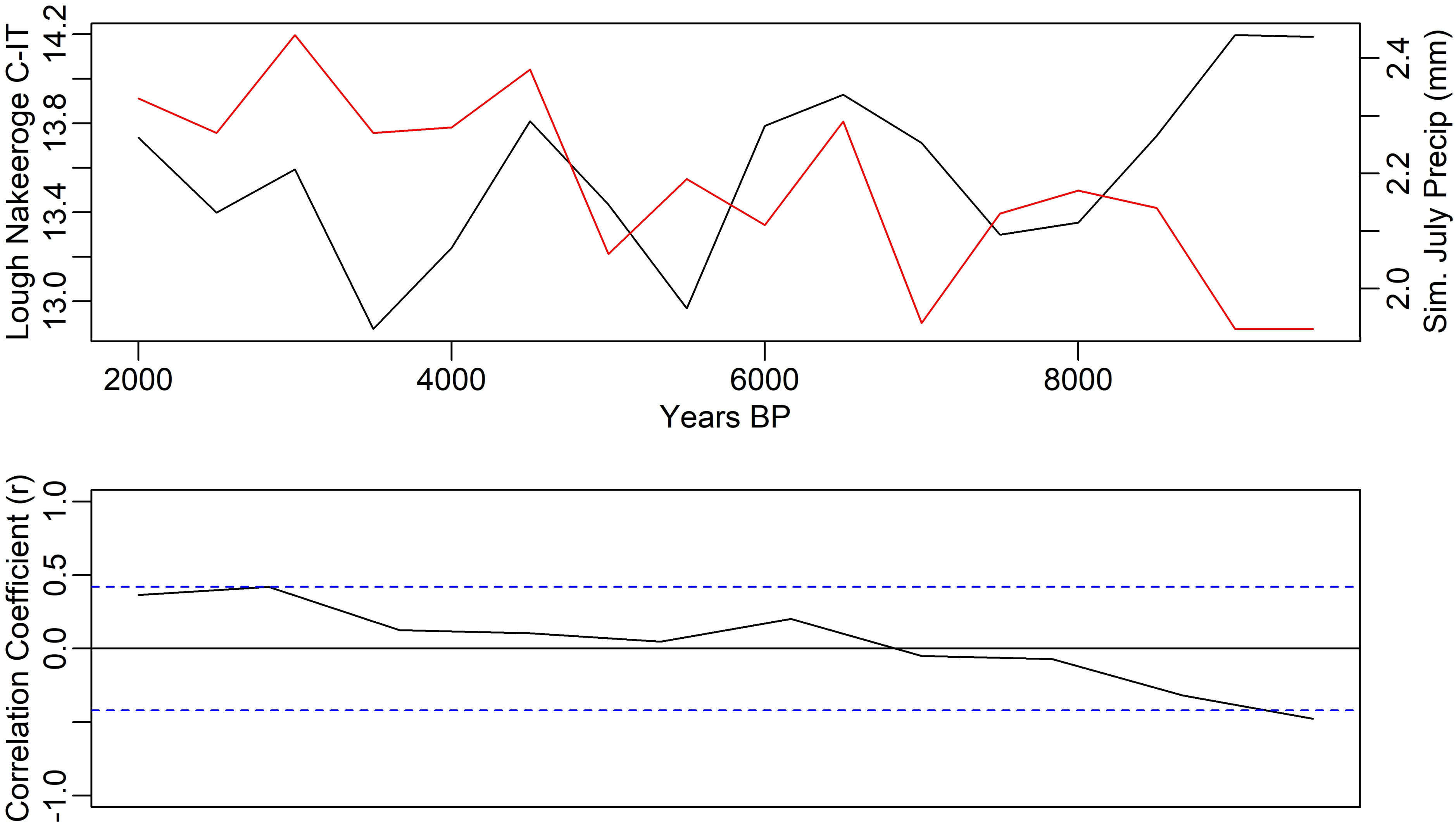

Lough Nakeeroge C-IT
13.0
13.4
13.8
14.2
Sim. July Precip (mm)
2.0
2.2
2.4
2000
4000
6000
8000
Years BP
Correlation Coefficient (r)
-1.0
0.0
0.5
1.0

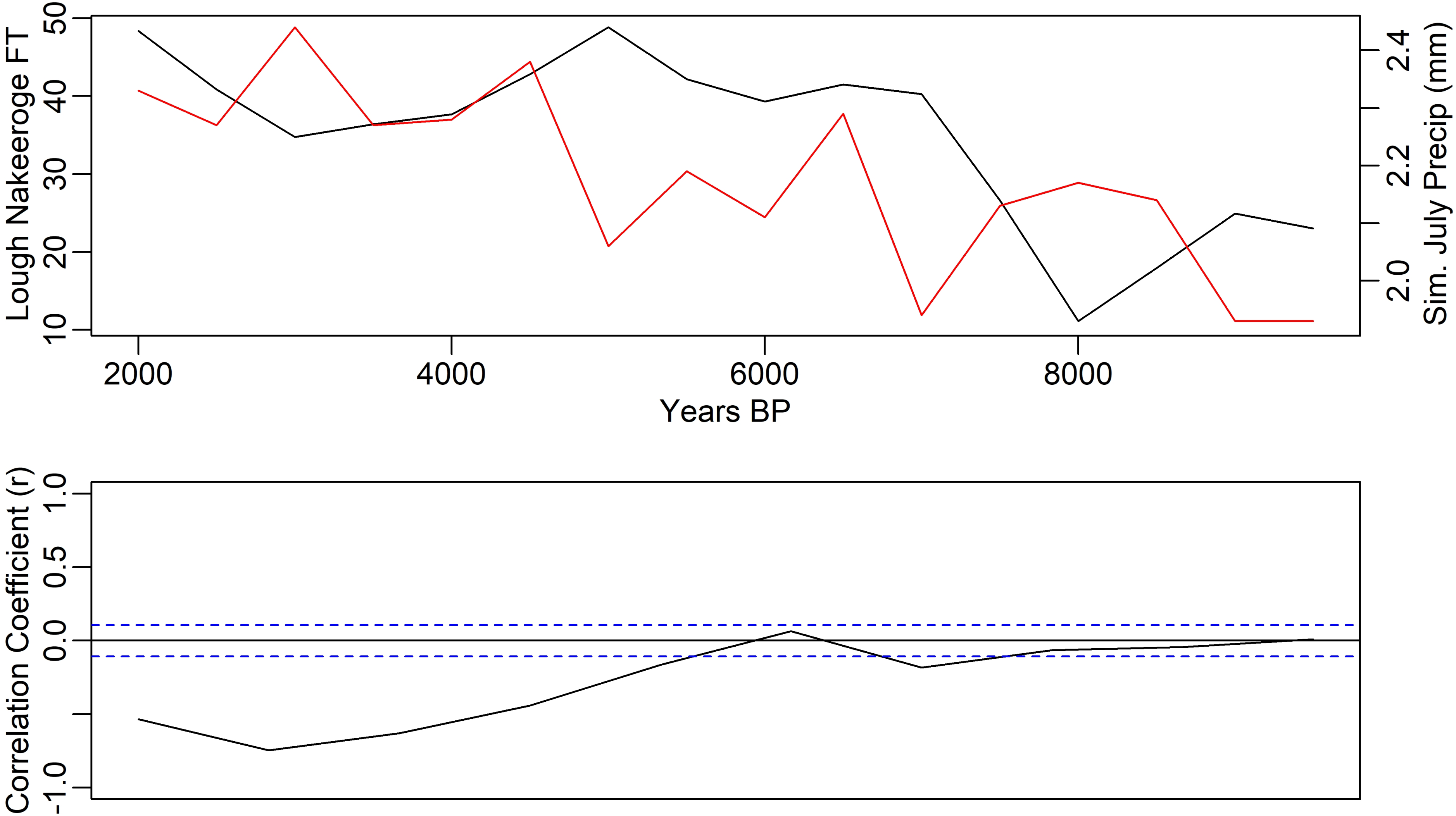

Lough Nakeeroge FT
10
20
30
40
50
Sim. July Precip (mm)
2.0
2.2
2.4
2000
4000
6000
8000
Years BP
Correlation Coefficient (r)
-1.0
0.0
0.5
1.0

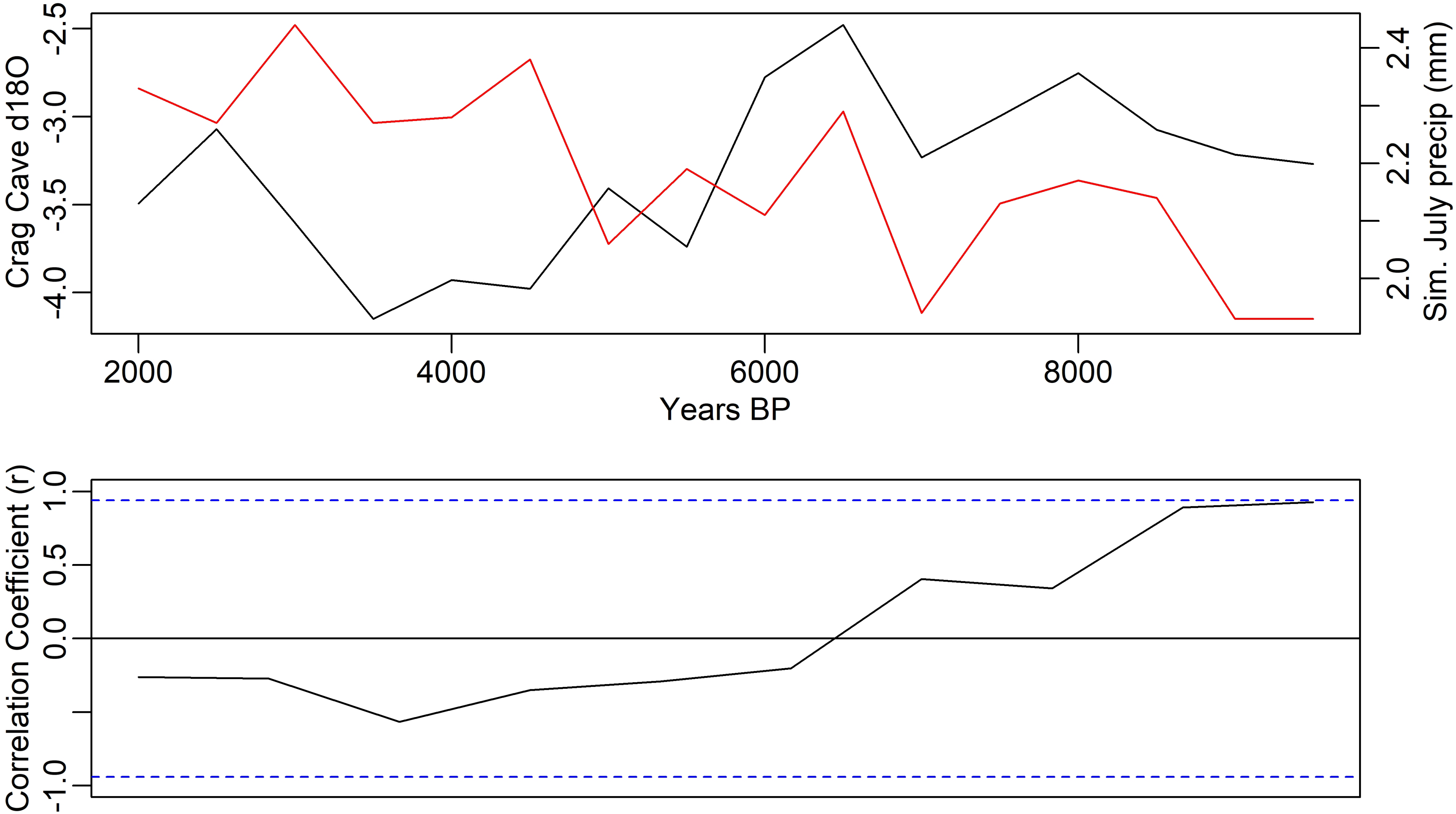
Crag Cave d18O
-2.5
-3.0
-3.5
-4.0
Sim. July precip (mm)
2.4
2.2
2.0
2000
4000
6000
8000
Years BP
Correlation Coefficient (r)
1.0
0.5
0.0
-1.0

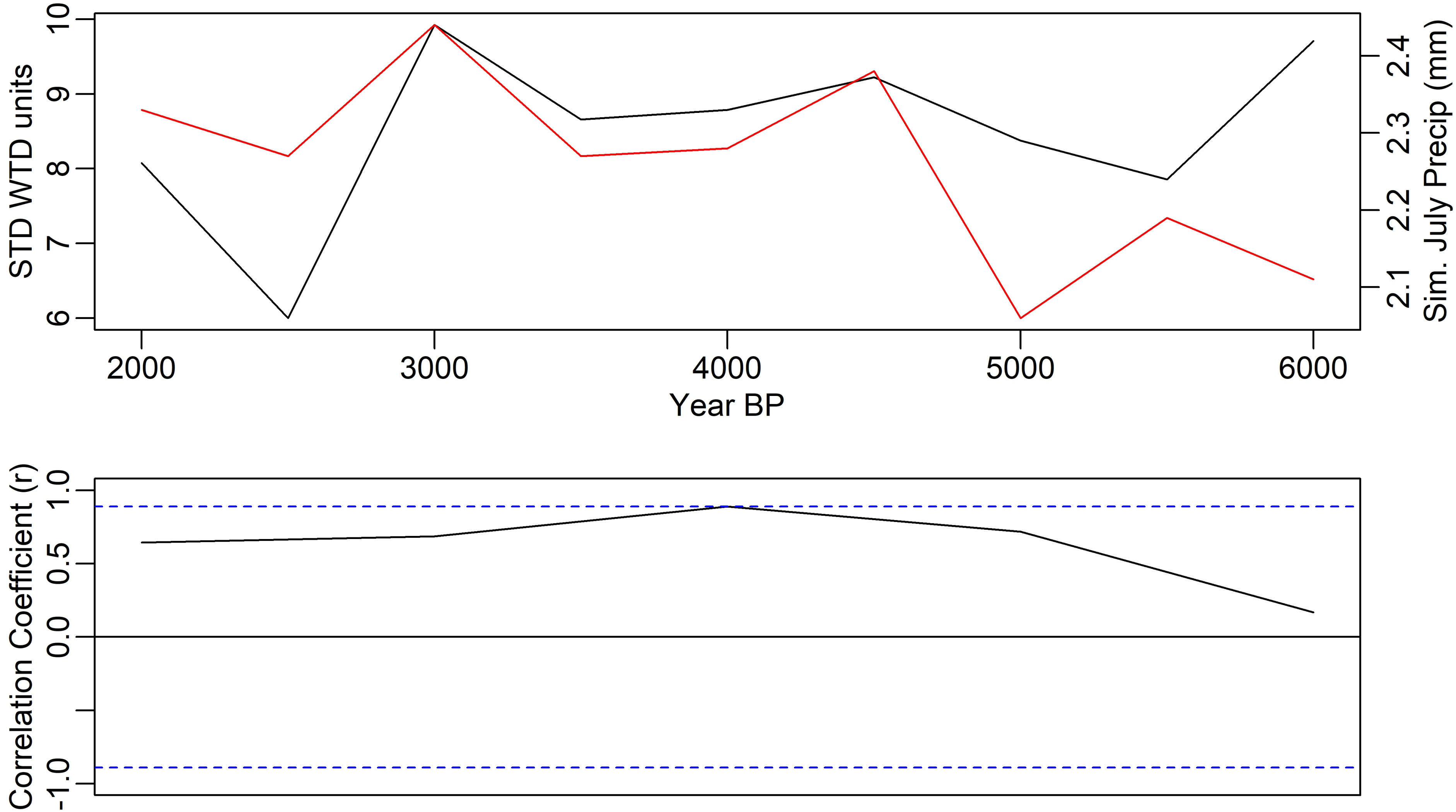

STD WTD units
10
9
8
7
6
Sim. July Precip (mm)
2.4
2.3
2.2
2.1
2000
3000
4000
5000
6000
Year BP
Correlation Coefficient (r)
1.0
0.5
0.0
-1.0

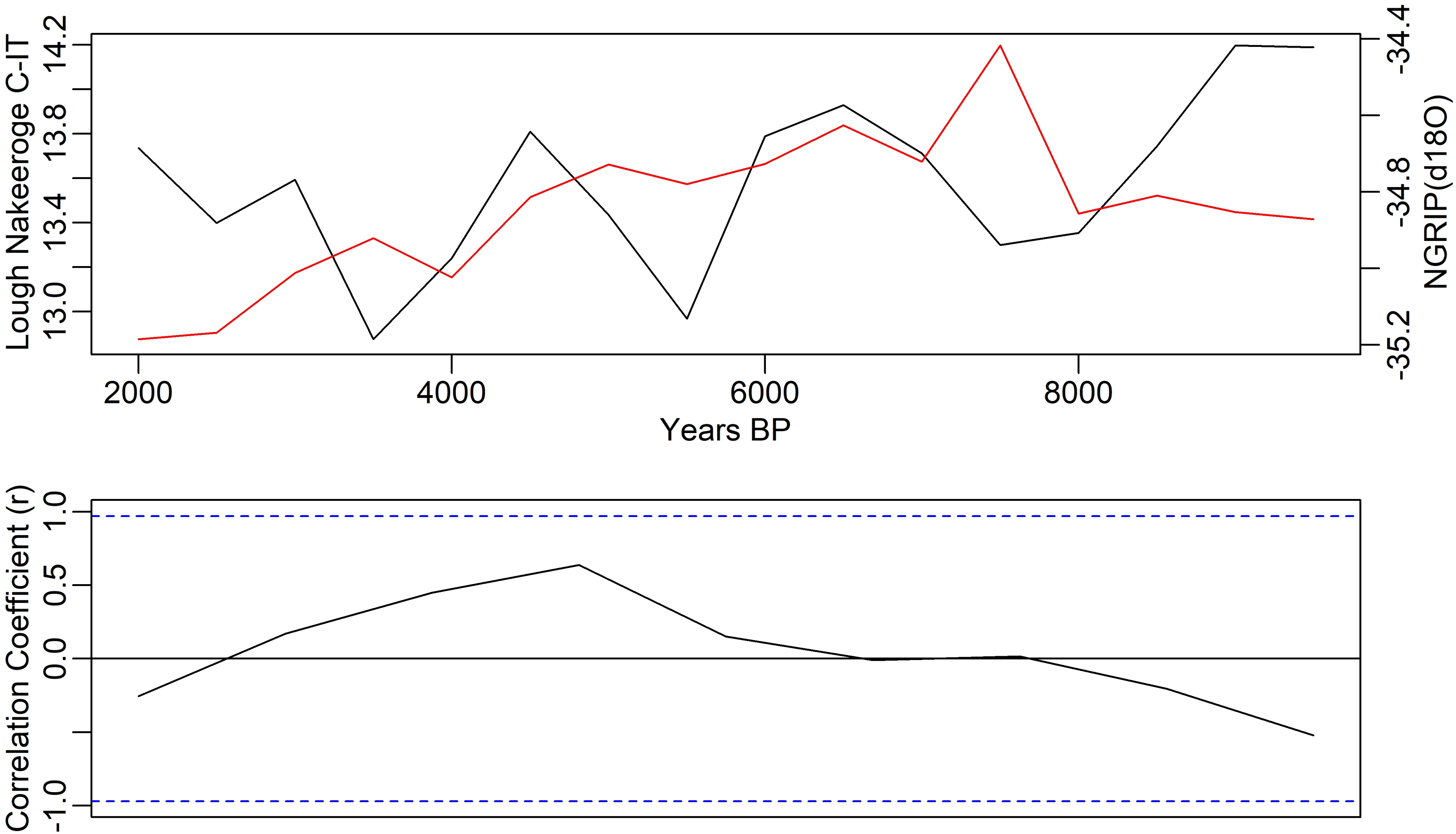

Lough Nakeeroge C-IT
13.0
13.4
13.8
14.2
NGRIP(d18O)
-35.2
-34.8
-34.4
2000
4000
6000
8000
Years BP
Correlation Coefficient (r)
-1.0
0.0
0.5
1.0

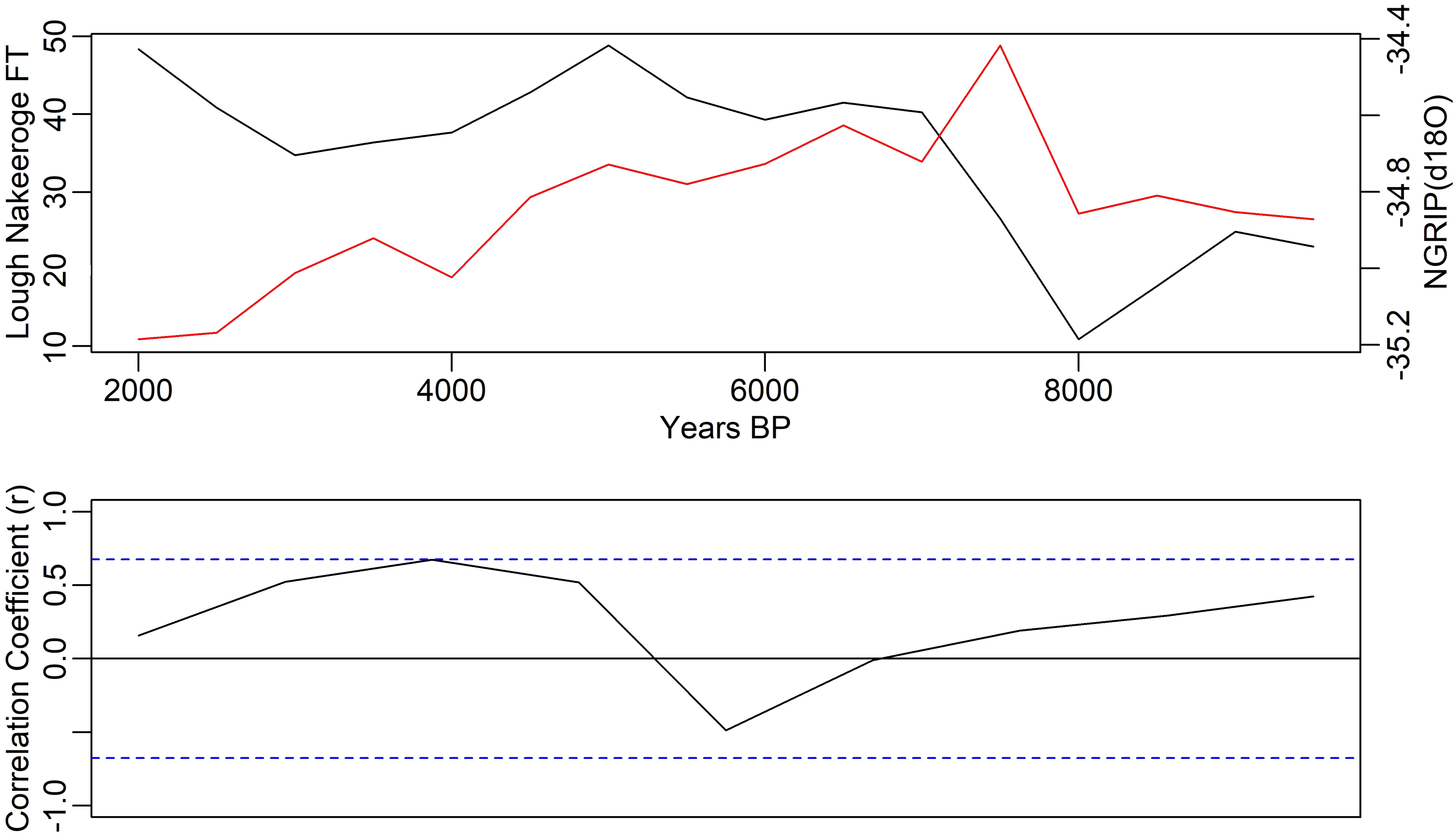
Lough Nakeeroge FT
10
20
30
40
50
-34.4
-34.8
-35.2
NGRIP(d18O)
2000
4000
6000
8000
Years BP
Correlation Coefficient (r)
-1.0
0.0
0.5
1.0

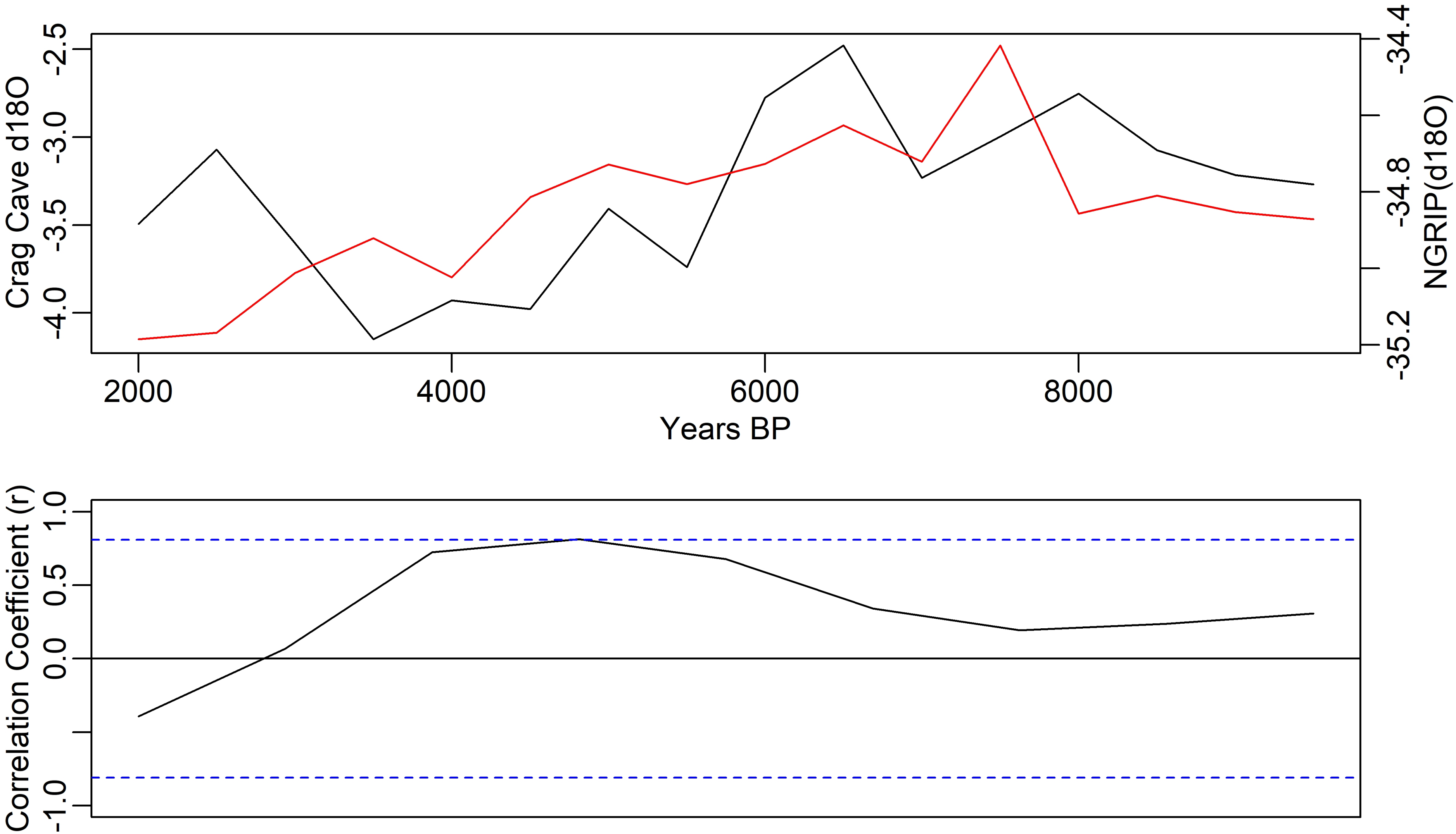

Crag Cave d18O
-2.5
-3.0
-3.5
-4.0
NGRIP(d18O)
-34.4
-34.8
-35.2
2000
4000
6000
8000
Years BP
Correlation Coefficient (r)
1.0
0.5
0.0
-1.0

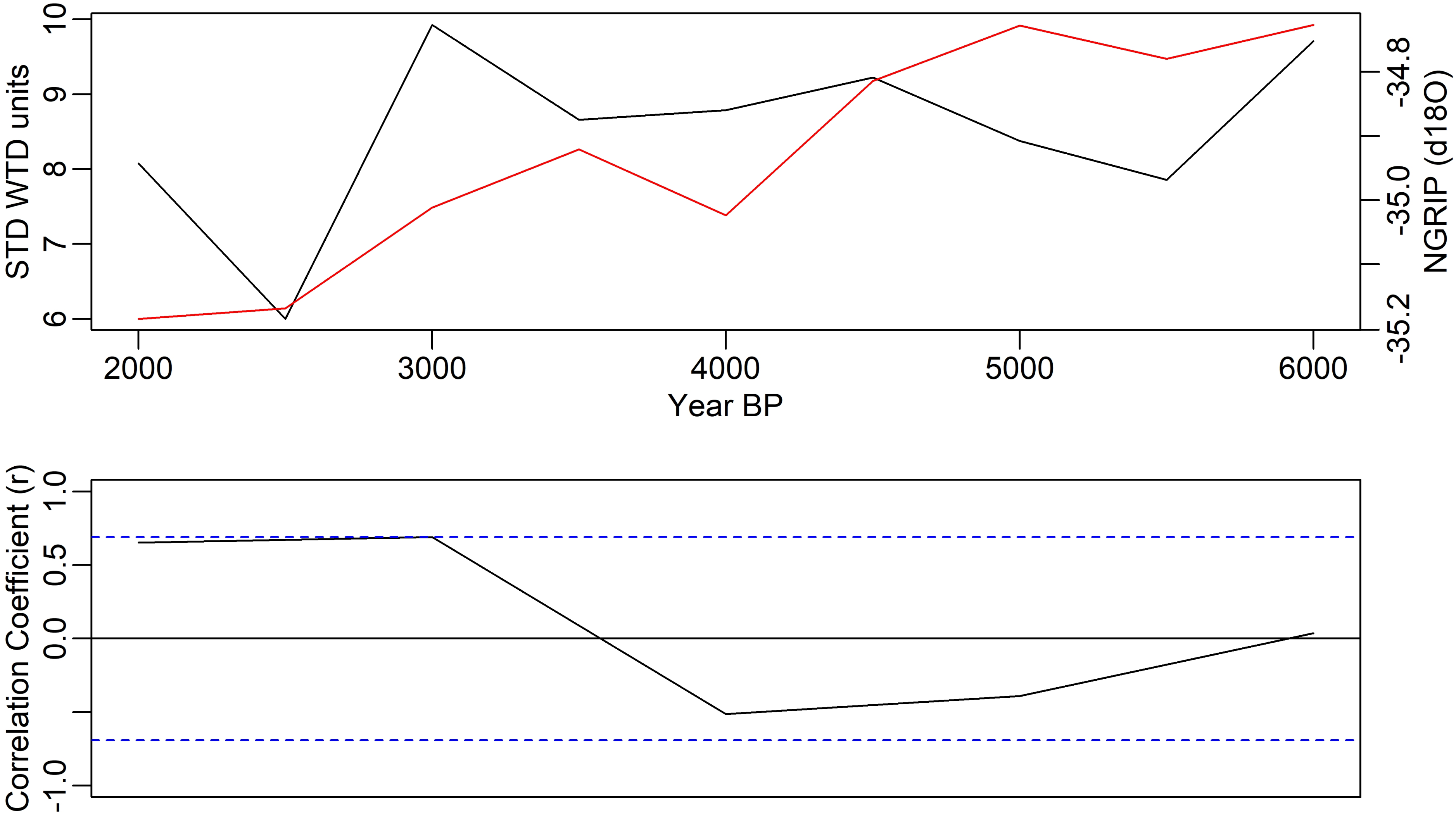

STD WTD units
10
9
8
7
6
NGRIP (d18O)
-34.8
-35.0
-35.2
2000
3000
4000
5000
6000
Year BP
Correlation Coefficient (r)
1.0
0.5
0.0
-1.0

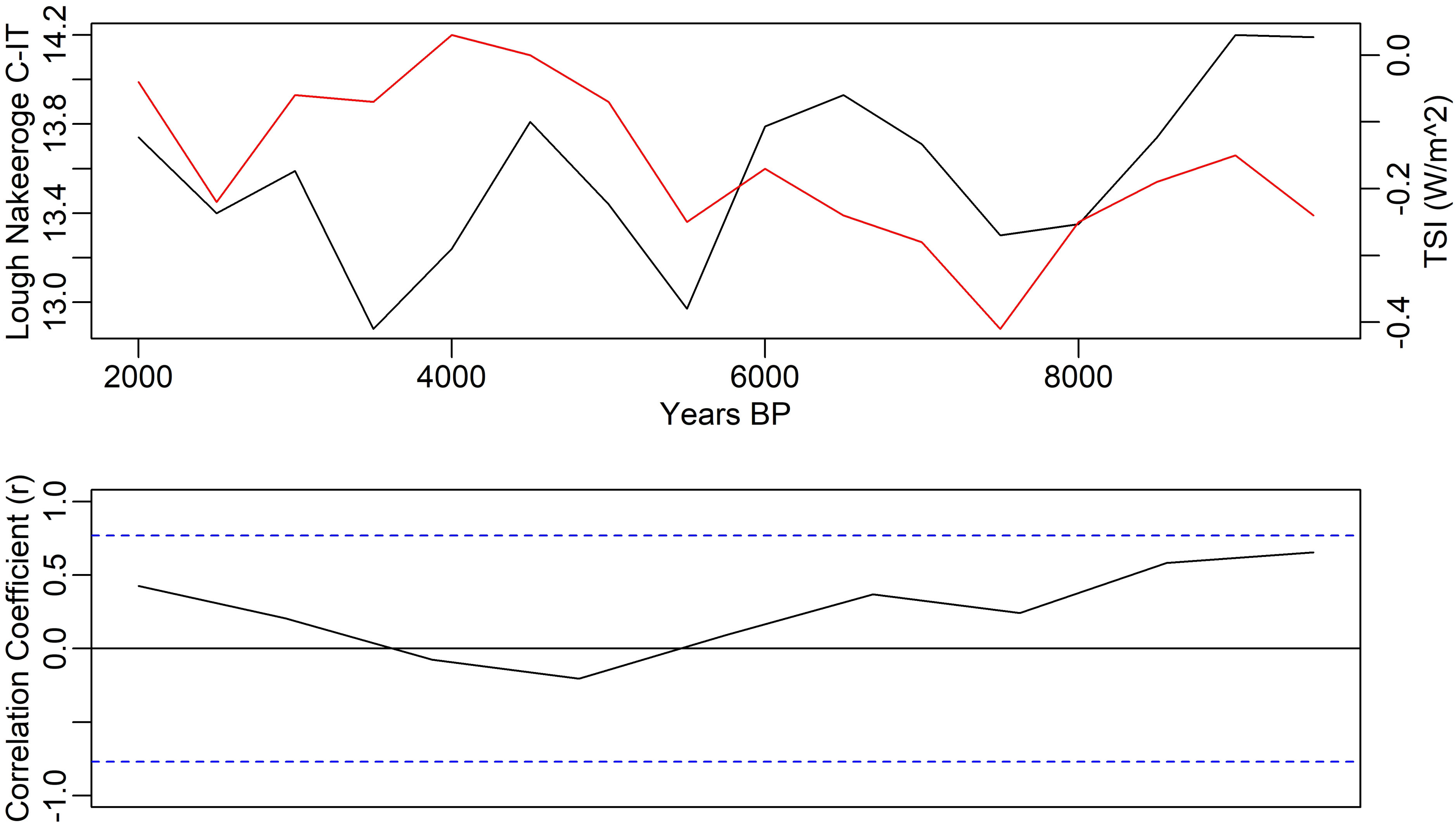

Lough Nakeeroge C-IT
13.0
13.4
13.8
14.2
TSI (W/m^2)
-0.4
-0.2
0.0
2000
4000
6000
8000
Years BP
Correlation Coefficient (r)
-1.0
0.0
0.5
1.0

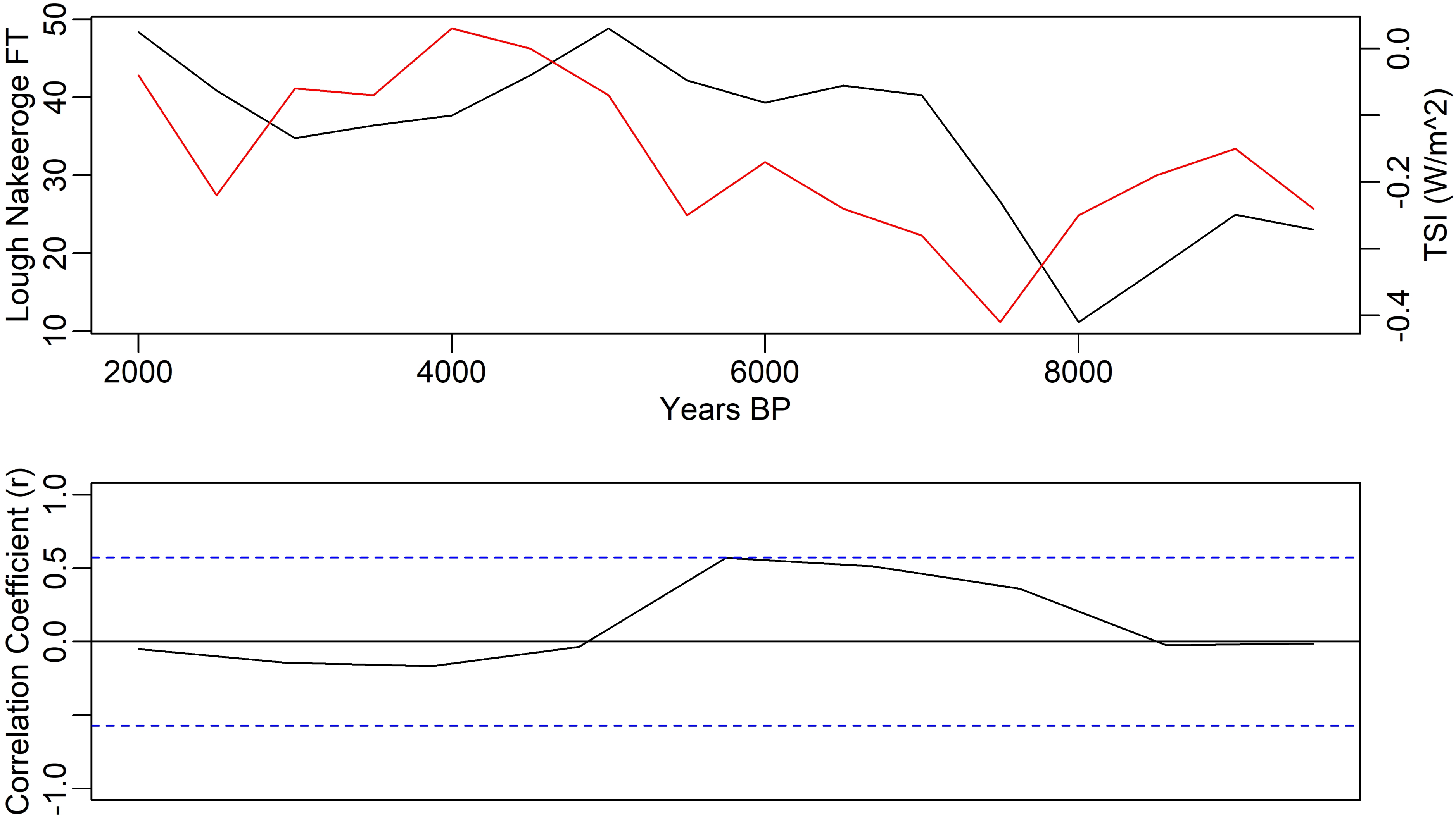

Lough Nakeeroge FT
10
20
30
40
50
TSI (W/m^2)
-0.4
-0.2
0.0
2000
4000
6000
8000
Years BP
Correlation Coefficient (r)
-1.0
0.0
0.5
1.0

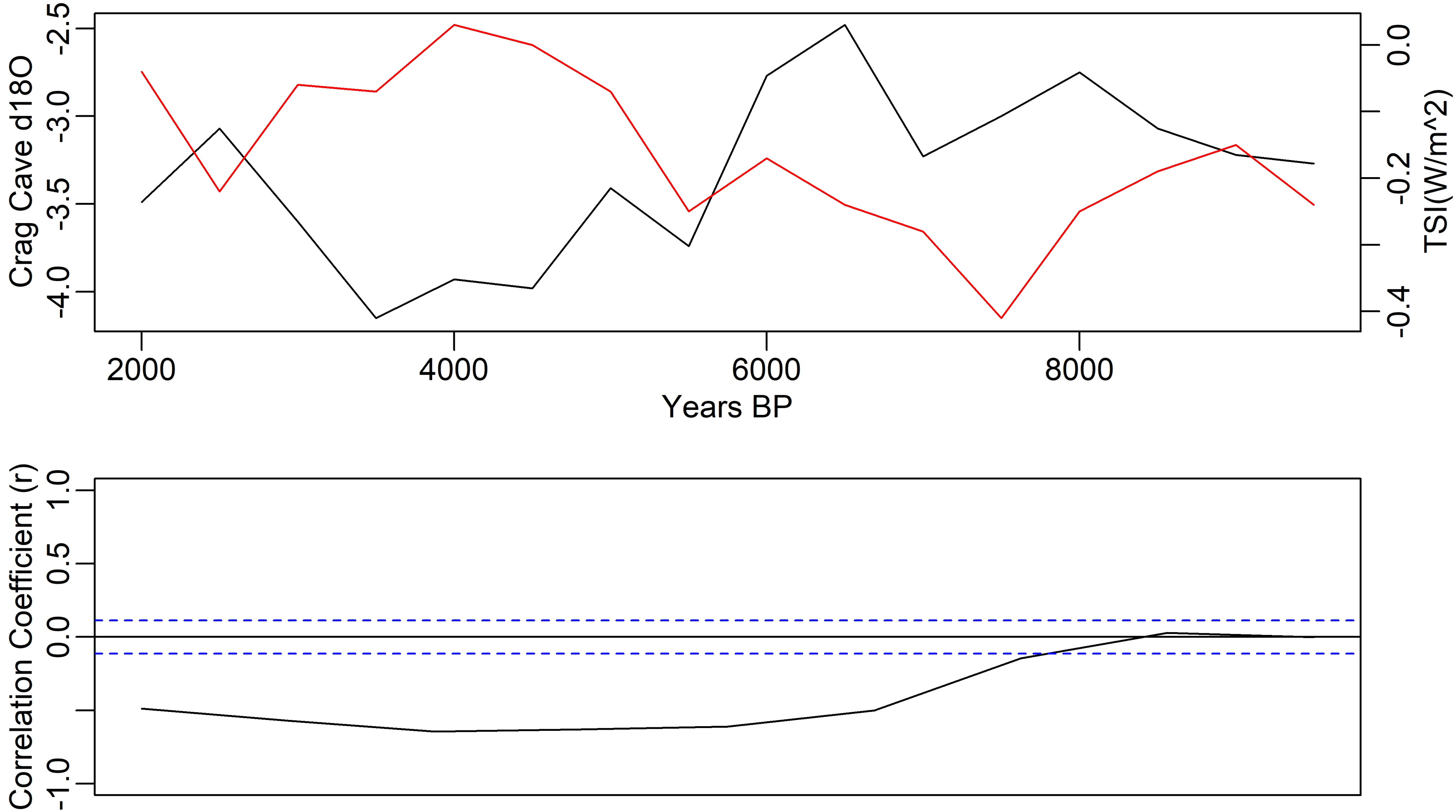

Crag Cave d18O
-2.5
-3.0
-3.5
-4.0
TSI(W/m^2)
0.0
-0.2
-0.4
2000
4000
6000
8000
Years BP
Correlation Coefficient (r)
1.0
0.5
0.0
-1.0

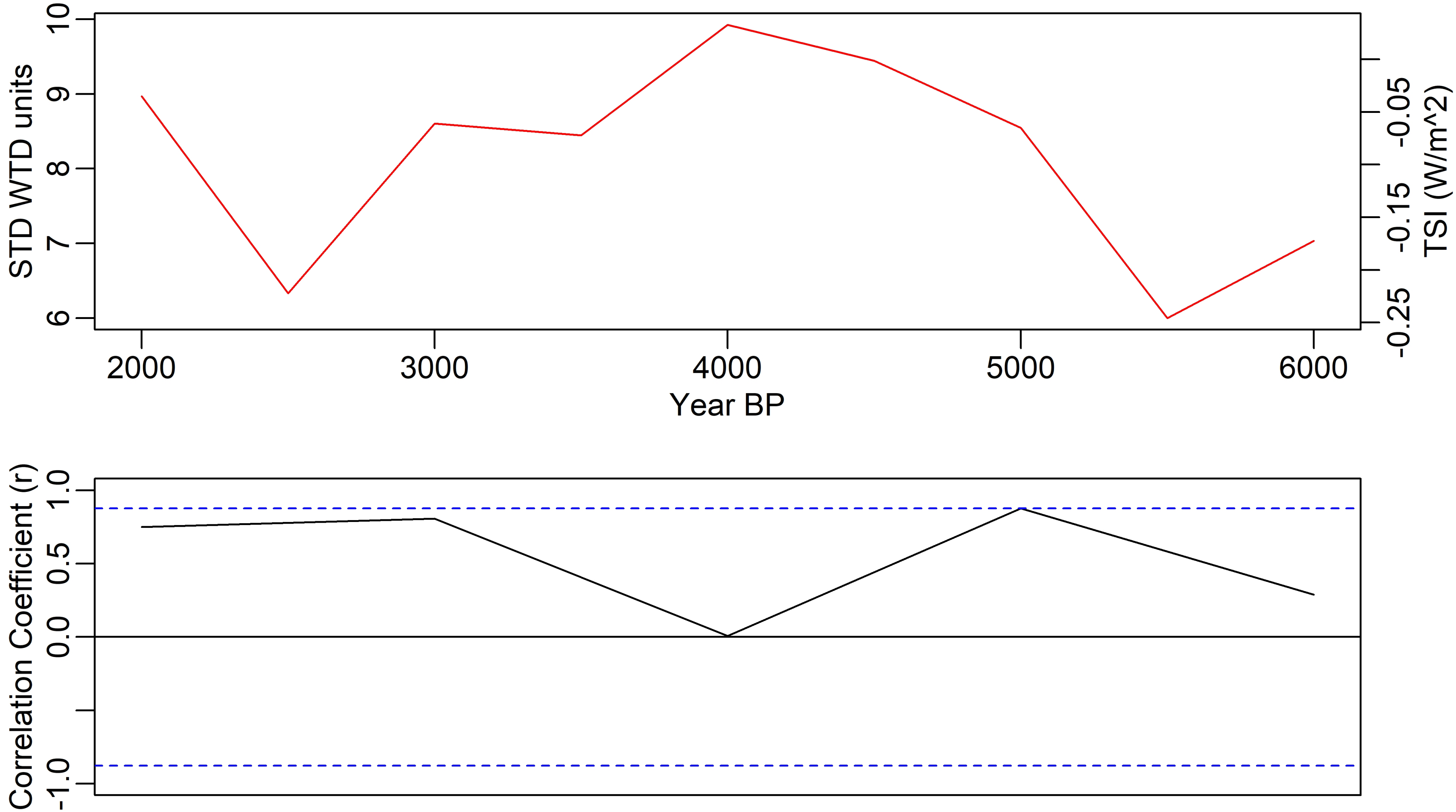
STD WTD units
10
9
8
7
6
TSI (W/m^2)
-0.05
-0.15
-0.25
2000
3000
4000
5000
6000
Year BP
Correlation Coefficient (r)
1.0
0.5
0.0
-1.0

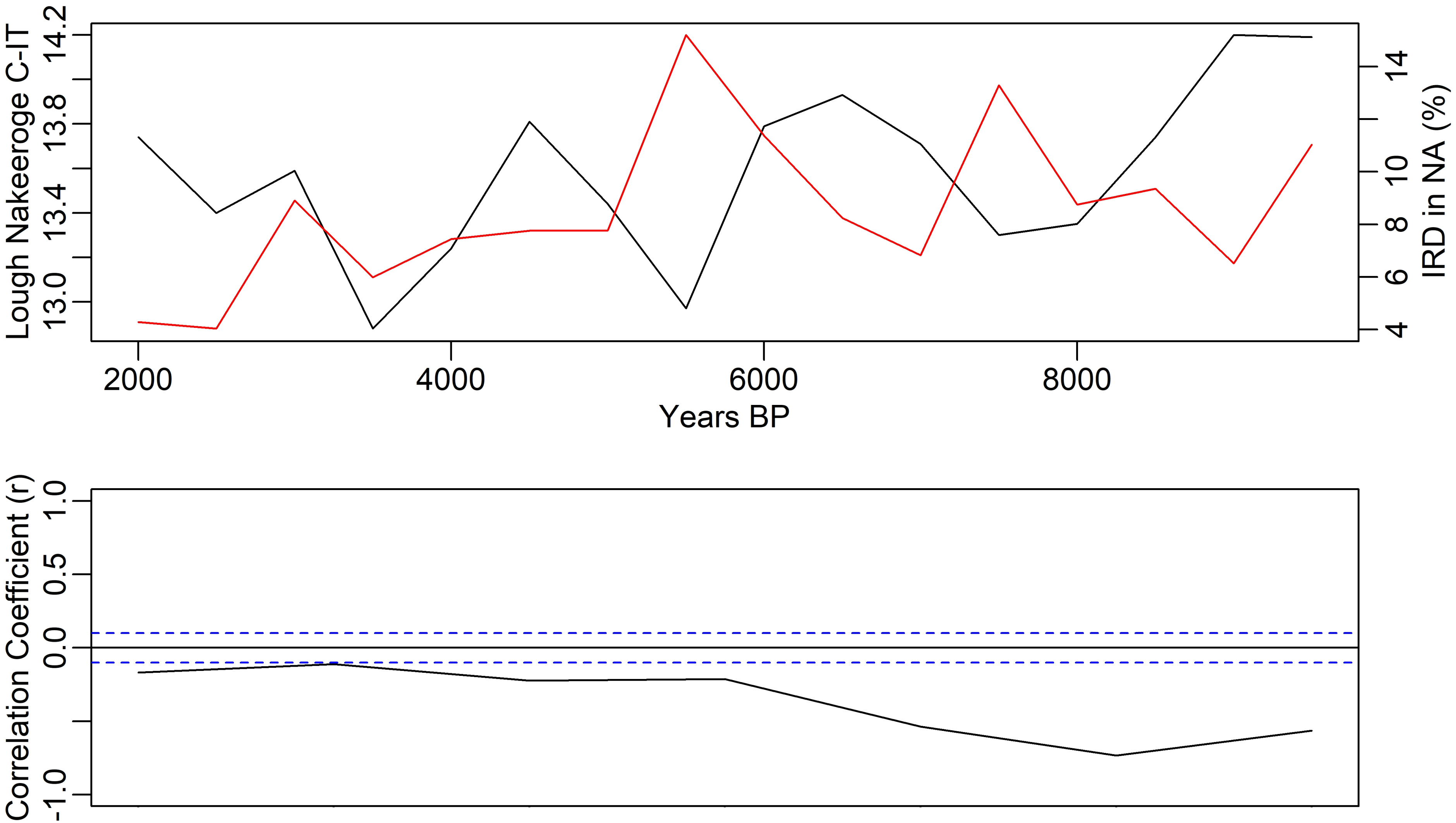

Lough Nakeeroge C-IT
14.2
13.8
13.4
13.0
IRD in NA (%)
14
10
8
6
4
2000
4000
6000
8000
Years BP
Correlation Coefficient (r)
1.0
0.5
0.0
-1.0

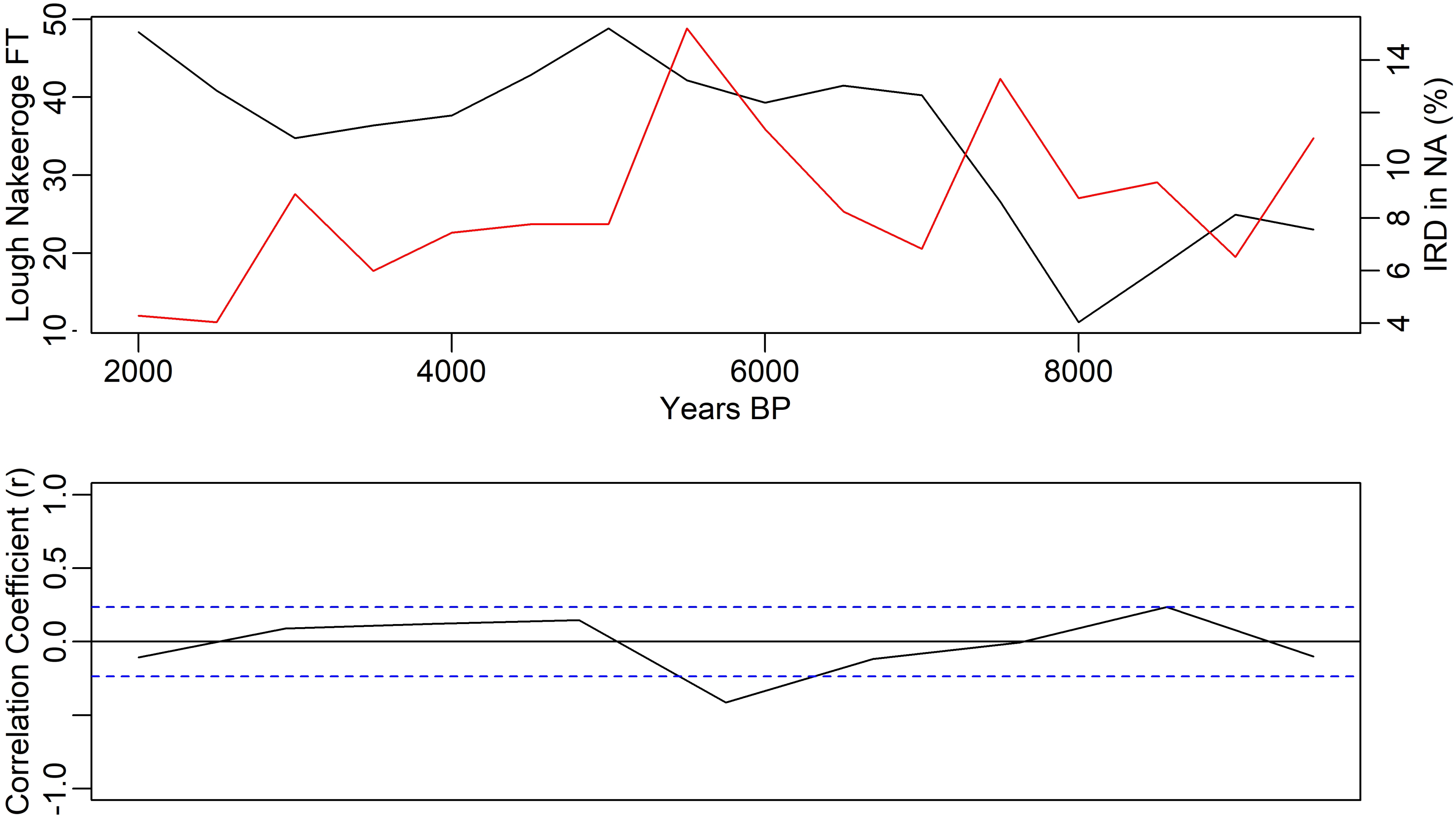
Lough Nakeeroge FT
IRD in NA (%)
Years BP
2000
4000
6000
8000
10
20
30
40
50
4
6
8
10
14
Correlation Coefficient (r)
-1.0
0.0
0.5
1.0

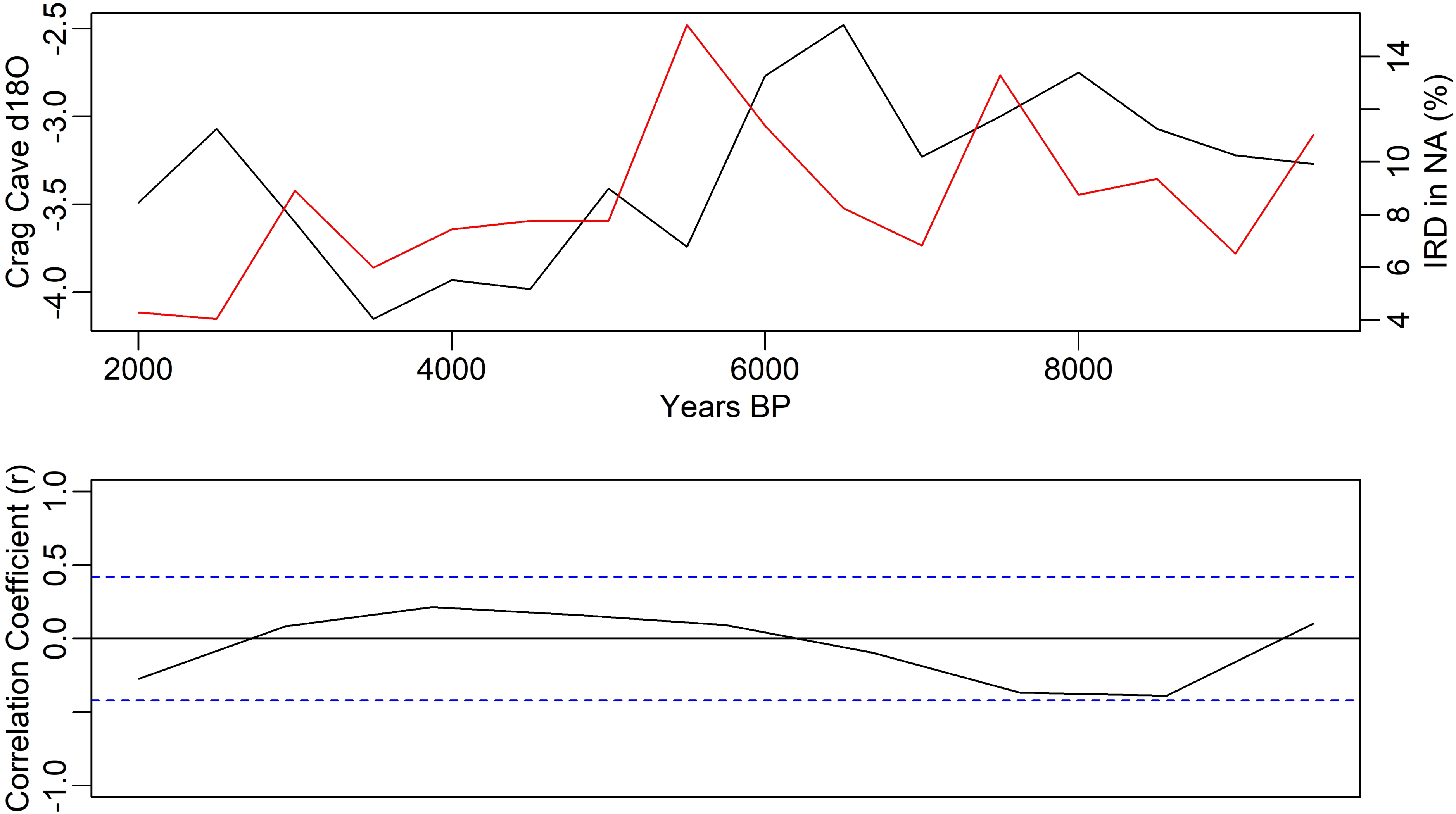
Crag Cave d18O
-2.5
-3.0
-3.5
-4.0
IRD in NA (%)
14
10
8
6
4
2000
4000
6000
8000
Years BP
Correlation Coefficient (r)
1.0
0.5
0.0
-1.0

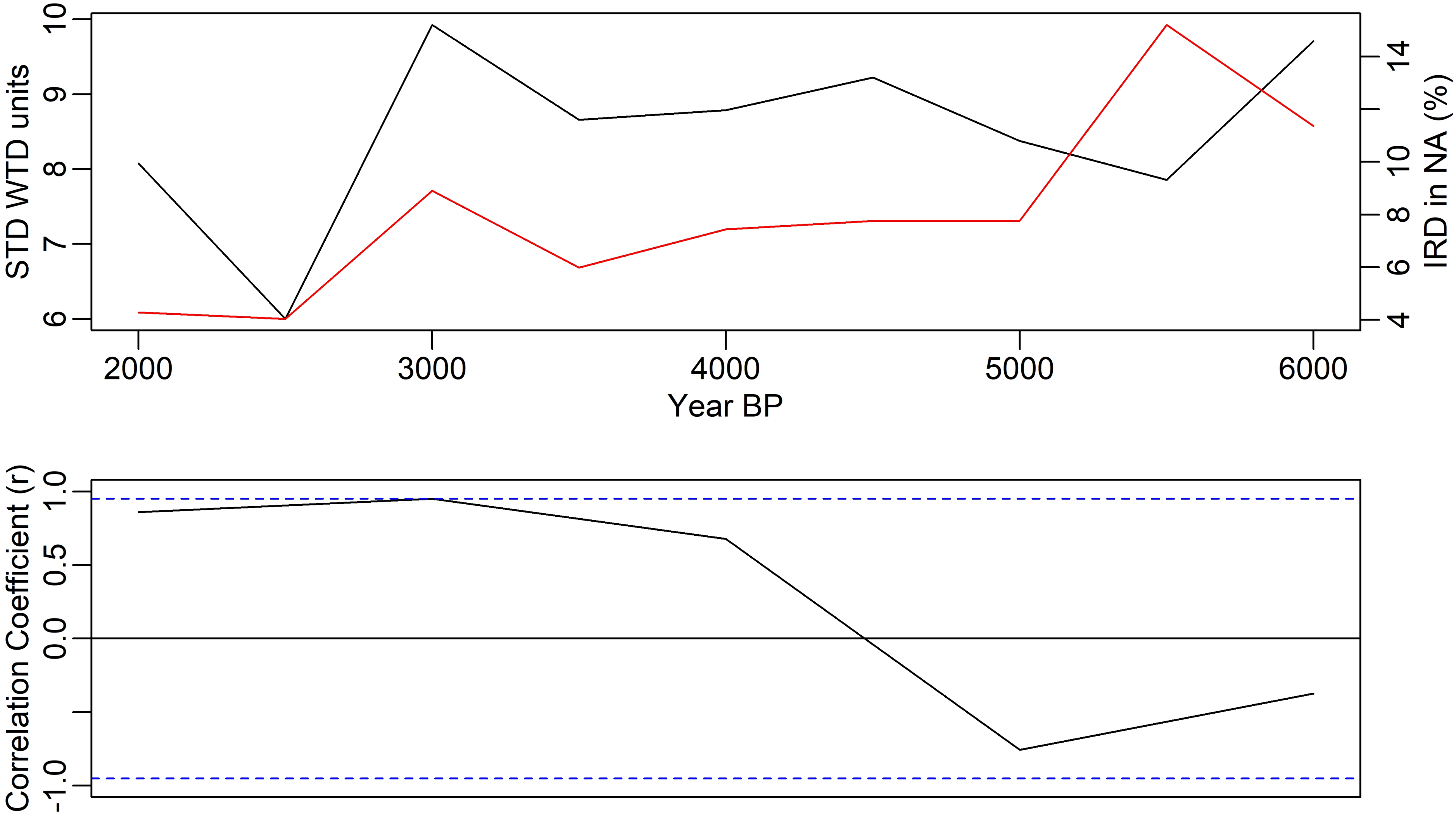
STD WTD units
IRD in NA (%)
Year BP
Correlation Coefficient (r)
10
9
8
7
6
14
10
8
6
4
2000
3000
4000
5000
6000
1.0
0.5
0.0
-1.0

Table 1 Calculated ages of the bulk sediment layers and the corresponding linear accumulation rates. Ages were calibrated using IntCal 13 (Reimer et al. 2013).

Depth (cm)	Core segment	Conventional radiocarbon age (years BP ± 1σ)	Calibrated 2σ age range	Mid-point 2σ age range
76-77	A	2068 ± 37	2254-1884	2027
168-169*	B	4349 ± 35	5328-4515	4932
180-181	A	3874 ± 38	4459-4102	4311
224-225	A	4835 ± 36	5721-5373	5577
279-280	B	6586 ± 40	7462-6838	7214
380-381	B	8993 ± 45	10170-9387	9832

*This date from the top of core B was discounted

Table 2. Pearson's correlations. C-IT = chironomid-inferred temperature, FT = chironomid collector-filterer guild, CC = Crag Cave $\delta^{18}0$, LM = An Loch Mor $CaCO_3$, DWT = Depth to Water table compiled and standardised from Irish peatland records, NGRIP = Greenland Ice NGRIP δ180, TSI = Total Solar Irradiance, IRD = Ice Rafted Debris in N. Atlantic.

	C-IT	FT	CC	LM	DWT	Ann Temp	Ann Precip	Ann PotEvap	July Temp	July Precip	NGRIP	TSI	IRD
C-IT		-0.16	0.43	-0.4	0.32	-0.55*	-0.54*	-0.58*	-0.34	-0.37	0.05	-0.03	-0.15
FT	-0.16		-0.36	0.42	-0.34	0.51*	0.31	0.31	0.32	0.34	-0.18	-0.42	-0.25
CC	0.43	-0.36		0.43	-0.18	-0.51*	-0.52*	-0.36	-0.28	0.33	0.38	-0.66*	0.14
LM	-0.4	0.42	0.43		0.07	0.06	<0.01	0.03	-0.04	0.1	0.33	-0.26	0.39
DWT	0.32	-0.34	-0.18	0.07		<-0.01	0.34	-0.51	-0.03	0.16	0.46	0.49	0.35
Ann Temp	-0.55*	0.51*	-0.51*	0.06	<-0.01						-0.39	0.55*	-0.30
Ann Precip	-0.54*	0.31	-0.52*	<0.01	0.34						-0.18	0.6*	-0.03
Ann PotEvap	-0.58*	0.31	-0.36	0.03	-0.51						-0.6*	0.48*	-0.33
July Temp	-0.34	0.32	-0.28	-0.04	-0.03						-0.53*	0.68*	-0.43
July Precip	-0.37	0.34	0.33	0.1	0.16						-0.4	0.49*	-0.21
NGRIP	0.05	-0.18	0.38	0.33	0.46	-0.39	-0.18	-0.6*	-0.53*	-0.4			
TSI	-0.03	-0.42	-0.66*	-0.26	0.49	0.55*	0.6*	0.48*	0.68*	0.49*			
IRD	-0.15	-0.25	0.14	0.39	0.35	-0.30	-0.03	-0.33	-0.43	-0.21			

**P* significance level for Monte Carlo permutation tests (999 unrestricted permutations). $P < 0.05$